

**Investigations on the Gas Phase Atmospheric
Chemistry of
Nitrophenols and Catechols**



Thesis submitted to the Faculty of Mathematics and Natural Sciences
Bergische Universität Wuppertal
for the Degree of Doctor of Natural Sciences
- Dr. rerum naturalium -

by
Iustinian Gabriel Bejan

November, 2006

Die Dissertation kann wie folgt zitiert werden:

urn:nbn:de:hbz:468-20070663

[<http://nbn-resolving.de/urn/resolver.pl?urn=urn%3Anbn%3Ade%3A468-20070663>]

The work described in this thesis was carried out in the Department of Physical Chemistry, Bergische Universität Wuppertal, under the scientific supervision of Prof. Dr. K.H. Becker, during the period of February, 2002 – November, 2006.

Referee: Prof. Dr. K.H. Becker

Co-referee: Prof. Dr. P. Wiesen

Soției mele, Dana

și

părinților mei

I would like to express my sincere thanks to Prof. Dr. Karl Heinz Becker for the opportunity of doing this Ph.D. in his research group and for the supervision of this work. I am also grateful for the chance to be your last Ph.D. student. I know that first and last students are most remembered.

I am very grateful to Prof. Dr. P. Wiesen for agreeing to co-referee the thesis and his many useful comments.

I would like to express my sincere thanks to Dr. Ian Barnes who not only helped me with his experience and guidance to understand at least a part of the atmospheric chemistry domain but also followed with particular care my scientific work during these years.

I am also indebted to PD Dr. Joerg Kleffmann for his guidance, fruitful discussions and suggestions and for his specialized help.

A special thanks to Prof. Dr. T. Benter for his appreciation and support.

I am very grateful to Prof. Dr. R. Mocanu for giving me the possibility to achieve such a work.

Special recognition to Dr. Romeo Olariu for initiating me in the "wonderland" of atmospheric chemistry and for his scientific discussions.

I especially appreciate the discussions with Dr. Cecilia Arsene. To Dr. Markus Spittler sincere thanks for his suggestions and advices. To Dr. Klaus Brockmann many thanks for his friendship and help.

My special thanks to Techn. Ang. Ronald Giese and Dipl. Ing. Willi Nelsen for their help in solving technical problems.

I wish to thank all my colleagues for their help, encouragement and pleasure to work in the "PC" group.

Very special thanks to my wife Dana for everything she has offered to me, for understanding my nights and weekends spent at the Uni. Thanks also to my mom for her unconditional support and encouragements and my father who unfortunately sees my achievement from the other world.

Abstract

The purpose of this work was to provide a scientific evaluation of the atmospheric fate of aromatic hydrocarbons, in particular, 1,2-dihydroxybenzenes and nitrophenols, which are important products in the oxidation of BTX. The data obtained within the present work will help to improve the knowledge on the atmospheric degradation of aromatic hydrocarbons.

The rate coefficients of the OH and NO₃ radical initiated oxidation of some nitro/hydroxy substituted monoaromatic hydrocarbons improve the kinetic data base required to model the degradation mechanisms of aromatic compounds and to develop structure reactivity relationships for OH and NO₃ radical with VOCs.

Relative rate coefficients have been measured for the first time for the reactions of NO₃ radicals with 1,2-dihydroxybenzene, 3-methyl-1,2-dihydroxybenzene and 4-methyl-1,2-dihydroxybenzene. The investigations were performed in two chambers: the 1080 l quartz glass reactor in Wuppertal and in the EUPHORE chambers in Valencia at 1000 mbar total pressure and 298 ± 3K. The following rate coefficients were obtained:

reactant	k_{NO_3} (cm ³ s ⁻¹)
1,2- dihydroxybenzene	$(9.80 \pm 5.0) \times 10^{-11}$
1,2-dihydroxy-3-methylbenzene	$(17.2 \pm 5.6) \times 10^{-11}$
1,2-dihydroxy-4-methylbenzene	$(14.7 \pm 6.5) \times 10^{-11}$

This work has provided rate coefficients for the gas phase reactions of the OH radical with a series of methylated 2-nitrophenols (2-nitrocresols). The following rate coefficients were obtained at 1000 mbar total pressure and 298 ± 3K in the 1080 l quartz glass reactor:

reactant	k_{OH} (cm ³ s ⁻¹)
3-methyl-2-nitrophenol	$(3.69 \pm 0.16) \times 10^{-12}$
4-methyl-2-nitrophenol	$(3.46 \pm 0.18) \times 10^{-12}$
5-methyl-2-nitrophenol	$(7.34 \pm 0.52) \times 10^{-12}$
6-methyl-2-nitrophenol	$(2.70 \pm 0.17) \times 10^{-12}$

Photolysis rates for the 2-nitrocresol isomers have also been determined. All the nitrocresols under investigation have a photolysis lifetime of less than 1 h. The results from this work have shown that photolysis will be the dominant gas-phase loss process for the 2-nitrocresols.

The photolysis of nitrophenols was found to be a new gas-phase source of HONO. Previously, no observations of nitrous acid formation from the gas-phase photolysis of nitrophenols had been reported in the literature. A series of detailed experiments were performed to ensure that the gas phase photolysis of the nitrophenols was the source of HONO, these included: variation of the S/V ratio of the reactors, variation of the light intensity, testing the influence of the buffer gas and tests for a possible mechanism involving reactions of gaseous NO₂. All the results were in line with gas-phase photolytic production of HONO from the nitrophenols.

Since a linear dependence of the HONO yield on the nitrophenol concentration was observed, the results obtained here have been extrapolated linearly to atmospheric concentrations. Based on the experimental data obtained for 3-methyl-2-nitrophenol a photolytic HONO formation rate in the atmosphere of 100 pptV h⁻¹ is estimated for a maximum J_(NO₂) value of 10⁻² s⁻¹ in the presence of 1 ppbV of nitrophenols. Based on the HONO formation yields, a general photolysis mechanism has been proposed.

The formation of secondary organic aerosol (SOA) from the photolysis of a series of nitrophenols was investigated for the first time. The effect of NO_x and the presence of an OH radical scavenger on the aerosol formation were also investigated. Significant aerosol formation was observed for the nitrophenols investigated. For 2-nitrophenol, the aerosol formation yield in the absence of an OH radical scavenger and NO_x varied between 18 - 24%. The gas-phase/aerosol partitioning was fitted assuming the presence of only one compound in both phases. A possible mechanism to explain the aerosol formation observed in the photolysis of nitrophenols is proposed.

Contents

1. Introduction	1
1.1 Aromatic hydrocarbons in the atmosphere	2
1.2 State of knowledge	5
1.2.1 Oxidation of aromatic hydrocarbons	5
1.2.2 Nitrophenols in the atmosphere	8
1.2.3 Nitrous acid (HONO) in the atmosphere	11
1.2.4 (Methylated) 1,2 dihydroxybenzene in the atmosphere	12
1.2.5 Secondary organic aerosol (SOA) formation in the atmospheric oxidation of aromatic hydrocarbons	14
1.3 Aim of the present work.....	15
2. Experimental section	17
2.1a Description of the 1080 I reaction chamber	17
2.1b Description of the EUPHORE chamber	19
2.2 Measurement procedure	21
2.2.1 Radical generation	21
NO ₃ radical generation	21
OH radical generation	22
2.2.2 Kinetic measurements	22
2.2.2.1 Relative rate method in kinetic data analysis	22
2.2.2.2 NO ₃ kinetic experiments on 1,2 dihydroxybenzenes	23
2.2.2.3 OH kinetic experiments on nitrocresols	26
2.2.3 Photolysis of nitrophenols. HONO formation	27
2.2.4 Photolysis of nitrophenols. Aerosol formation	31
3. Kinetic investigations of the gas-phase reaction of NO₃ and OH radicals with some nitro/hydroxy substituted monoaromatic hydrocarbons	35

3.1 Kinetics of the reaction of NO ₃ radicals with 1,2-benzenediol and methylated substitutes	35
3.1.1 Results	36
3.1.2 Discussion	42
3.1.3 Atmospheric implications	45
3.2 Photolysis rates and kinetics of the reaction of OH radicals with selected nitrocresols	46
3.2.1 Results	46
3.2.2 Remarks and conclusions	50
3.2.3 Atmospheric implications	54
4. Mechanistic investigations on the photolysis of nitrophenols: A new gas phase source of HONO formation	57
4.1 Results	57
4.2 Discussion	66
4.2.1 Internal rotation proton transfer between OH and NO ₂ groups positioned ortho to one another	66
4.2.2 Gas-phase process or surface chemistry?	68
4.2.3 Can impurities be responsible for HONO formation?	69
4.2.4 Is the HONO originating from a mechanism involving NO ₂ ?	70
4.2.5 Mechanistic investigations	70
4.3 Atmospheric implications	74
5. Secondary organic aerosol (SOA) formation from the photolysis of nitrophenols	77
5.1 Results	78
5.2 Discussion	83
5.2.1 OH radical influence on aerosol formation	83
5.2.2 NO _x influence on aerosol formation	84
5.2.3 Expression for SOA yield	85
5.2.4 Potential explanation of SOA formation in the photolysis of nitrophenols	86

6. Summary	91
Appendix I	95
Synthesis	95
I. 1. Synthesis of methyl nitrite (CH ₃ ONO)	95
I. 2. Synthesis of nitrogen pentoxide (N ₂ O ₅)	96
I. 3. Synthesis of nitrous acid (HONO)	96
Appendix II	98
Gas phase muconic acid infrared spectra	98
Appendix III	99
Origin and purity of the gases and chemicals used.....	99
III.1 Gases	99
III.2 Chemicals	99
Appendix IV	100
Gas/Particle partitioning and secondary organic aerosol yield.....	100
Appendix V	103
Gas-phase infrared absorption cross section.....	103
Appendix VI	105
Abbreviations	105
References	107

Chapter 1

1. Introduction

The atmosphere is a complex photochemical reactor, which contains a complex mixture of natural and anthropogenic compounds with diverse properties. Processes occurring within the atmosphere can have adverse effects on human health, ecosystems, visibility, climate and lead to ozone depletion. Since the industrial revolution, a strong anthropogenic influence on the tropospheric composition has taken place. Many volatile organic compounds (VOCs), originating entirely from anthropogenic sources, are detected at mixing ratios of the order of less than parts per million (ppmV); many of them are present in the atmosphere at parts per trillion (pptV) levels (Finlayson-Pitts and Pitts, 2000). Even at such low concentrations these “innocent molecules” may still have significant effects on the environment. Once emitted, species are converted at various rates into new substances generally characterized by higher chemical oxidation states than their parent substances (Atkinson, 1994). Some trace gases control or affect the Earth’s climate and habitability (Seinfeld, 1989). Increasing our understanding of the chemical behaviour and properties of these compounds and their physico-chemical processes is vital for properly assessing their role in pollution, climatic change and ultimately establishing effective control strategies (Seinfeld and Pandis, 1998).

VOCs sometimes referred to as non-methane organic compounds (NMOCs) or reactive organic gases (ROG) can react with hydroxyl radicals (OH) (Wang *et al.*, 1975; Barnes *et al.*, 1982; Atkinson, 1986, 1987, 1989), nitrate radicals (NO₃) (Carter *et al.*, 1981; Winer *et al.*, 1984; Atkinson *et al.*, 1984; 1988; Atkinson, 1991; Platt and Heintz, 1994), ozone (O₃) (Logan, 1985), ground-state oxygen atoms (O³P) (Boocock and Cvetanovic, 1961; Jones and Cvetanovic, 1961) and different other reactive species. In particular, reactions of VOCs with nitrogen oxides (NO_x) in the presence of sunlight can lead to the formation of ozone, other oxidants, and particulate matter (PM), commonly referred to as “smog” (Warneck, 1988; Derwent *et al.*, 1996, 1998; Seinfeld and Pandis, 1998; Finlayson-Pitts and Pitts, 2000, Calvert *et al.*, 2002). In marine coastal areas the chlorine (Cl) atom can be an important reactive species for NMOCs (Fantechi *et al.*, 1998).

1.1 Aromatic hydrocarbons in the atmosphere

Aromatic hydrocarbons are an important class of volatile organic compounds (VOC) emitted into the atmosphere (Calvert *et al.*, 2002). The importance of aromatic hydrocarbons has increased since the sixties when the formation of photooxidants was discovered to be linked with the presence of aromatic/NO_x/light-mixtures (Altshuller *et al.*, 1962). The presence of aromatic hydrocarbons in the environment was first detected in 1968 by Lonnemann *et al.* (1968). In the initial studies the main hydrocarbon degradation pathway in the gas-phase was considered to be reaction with ozone, however, it was later proposed that the degradation of most aromatic hydrocarbons (benzene, toluene, o-, m- and p-xylene, etc.) is initiated by reaction with OH radicals (Weinstock, 1969; Levy, 1971; Atkinson *et al.*, 1989; Atkinson, 1994; Calvert *et al.*, 2002). Although reaction of aromatic hydrocarbons with OH radicals is a major atmospheric loss pathway for these compounds, reaction with NO₃ radicals is also important for some aromatics such as hydroxylated benzenes (Carter *et al.*, 1981). While the reaction of NO₃ radicals with benzene is quite slow (rate constant of the order of 10⁻¹⁷ cm³ s⁻¹), OH-substituted phenol-type compounds react fast, with reaction rate constants of the order of 10⁻¹² cm³ s⁻¹ (phenol) to 10⁻¹¹ cm³ s⁻¹ (cresols) (Calvert *et al.*, 2002). Ten times faster rates have been obtained for the reaction of NO₃ radicals with di-

hydroxy-substituted-benzenes as will be presented in a section of this work (Bejan *et al.*, 2002; Olariu *et al.*, 2004b).

The presence of aromatic hydrocarbons in the troposphere is mainly related to anthropogenic activities (Calvert *et al.*, 2002) such as solvent use, fossil fuel combustion, gasoline emissions, and industrial processing. However, the presence of aromatic hydrocarbons in the troposphere is not restricted only to emissions from anthropogenic activities, natural emissions of aromatics to the atmosphere occur from biomass burning (Eyde and Richards, 1991; Blake *et al.*, 1994), eruption of volcanoes (Isidorov *et al.*, 1990) and lakes (Juettner and Henatsch, 1986). Plants are also known to emit aromatic hydrocarbons under conditions of environmental stress (Heiden *et al.*, 1999). Estimations of the global emissions of aromatic hydrocarbons suggest that they comprise between 17-25% of the total anthropogenic NMVOC emissions (Calvert *et al.*, 2002).

Benzene, toluene and the xylenes isomers (BTX) are the main aromatic hydrocarbons present in the urban atmosphere (see Table 1.1). Recent field measurements (1995-2003) presented in Table 1.1 show the high abundance of aromatic hydrocarbons in urban air. As can be seen in Table 1.1, the concentrations in east European cities are twice as high as those measured in other world cities. This reflects the high permissive legislation on the control of urban pollution in Eastern Europe. In Germany, the overall hydrocarbon emissions have been greatly reduced in the last years (Kurtenbach, 2005).

The modelling of the atmospheric chemistry of aromatic hydrocarbons and the determining the influence of these hydrocarbons on the urban atmosphere is an especially challenging task, since many of the details of the complex reactions that occur are presently unknown (Calvert *et al.*, 2002). Many developments have occurred in computer modelling studies of aromatic hydrocarbon photooxidation over the last decade (Jenkin *et al.*, 2003; Bloss *et al.*, 2005a, 2005b). Based on the presently accepted but inadequate mechanism for the atmospheric degradation of aromatic hydrocarbons, it has been calculated that this class of VOC could account for up to 30% of the photooxidant formation in urban areas (Derwent *et al.*, 1996; 1998). In order to provide relevant data for modelling studies, kinetic information concerning atmospheric loss processes for aromatic hydrocarbons, e.g. reaction

with ozone, OH and NO₃ radicals have been intensively studied during the last years (Atkinson *et al.*, 1984, 1988, 1992b, 1997; Atkinson, 1989).

Table 1.1 Urban median mixing ratios compared to traffic median mixing ratios in different world cities.

Mixing ratios (ppbV)	Benzene	Toluene	o-, m-. p-xylene
Berlin [traffic] ^a	2.09 [10.30]	3.84 [23.00]	2.72[12.49]
Bucharest [traffic] ^a	1.75 [32.00]	3.83 [50.60]	2.03 [56.70]
Dresden ^a	0.74	1.15	0.79
Krakow [traffic] ^a	2.43[31.7]	2.76 [83.80]	1.71 [54.70]
Prague [traffic] ^a	2.46 [62.7]	3.49 [98.10]	1.72 [100.5]
Vienna [traffic] ^a	0.99 [13.3]	1.17 [21.90]	0.97 [19.22]
Warsaw ^a	0.75	0.96	0.67
Zagreb ^a	3.12	6.85	2.50
London [traffic] ^a	0.8 [22]	2.01 [36.50]	1.34 [26.74]
Paris 96 [traffic 98] ^a	0.68 [34.4]	2.36 [65.70]	1.11 [36.11]
Rome [traffic] ^a	3.62 [8.2]	9.28 [21.40]	7.39 [20.45]
Rome [traffic] ^b	[14.00]	[35.00]	-
Taipei ^a	0.52	1.49	0.73
Hong Kong ^a	1.64	4.45	1.26
Mexico City ^c	1.7-3.7	7.50-17.60	-
Wuppertal City ^d	11.70	18.50	3.10
Kiesberg tunnel ^d	15.80	24.90	12.60
München ^e	3.60	7.00	5.30
New York (1990-2003) ^f	1.60-32.00		
New York (2001-2003) ^f	0.70-4.40		

data from: (^a) Monod *et al.*, 2001; (^b) Brocco *et al.*, 1997; (^c) Bravo *et al.*, 2002; (^d) Kurtenbach *et al.*, 2002; (^e) Rappenglück and Fabian, 1999; (^f) Aleksic *et al.*, 2005.

An important aspect of the atmospheric behaviour of aromatic hydrocarbon is their impact on human health (Pitts *et al.*, 1978; Shepson *et al.*, 1985; Dumdei *et al.*, 1988; Grosjean, 1991; Finlayson-Pitts and Pitts, 1997; Cocheo *et al.*, 2000).

Over the past decade, there has been intense interest concerning the role of aerosols in climate and atmospheric chemistry (Andreae and Crutzen, 1997; Seinfeld and Pandis, 1998; Finlayson-Pitts and Pitts, 2000; McMurry, 2000).

Particles in the atmosphere have different properties compared to their gaseous precursors. They scatter, absorb, or reflect the solar radiation and additionally, they can play an important role in cloud droplet formation (Ravishankara, 1997). Therefore, the study of particles and their formation pathways are of great interest. The formation of particles and their size distribution are dependent on the chemical composition of the surrounding air. Accordingly, industrial plumes or other gaseous components have an effect on the aerosols (Kulmala, 2003).

Besides photooxidant formation, aromatic hydrocarbons are also assumed to make a significant contribution to secondary organic aerosol (SOA) formation in urban areas (Odum *et al.*, 1996, 1997b; Forstner *et al.*, 1997; Hurley *et al.*, 2001; Kleindienst *et al.*, 2004). These facts make aromatic hydrocarbon one of the most important classes of hydrocarbons emitted into the urban atmosphere. SOA is generally formed only from the oxidation of organic molecules sufficiently large to lead to products that have vapour pressures low enough to enable them to condense into the aerosol phase.

What is particularly interesting from a chemical point of view is that a relationship exists between mortality and aerosols; a well known example is the London pollution episode in 1952 when the number of deaths increased by 4000 persons over the average because of the sulphate aerosol accumulation caused by the large emissions of SO₂. It is suggested that in cities with major particle sources there is a general inflammatory response to the inhalation of particles. The respiratory tract inflammation does not appear to depend too much on the specific chemical composition (Finlayson-Pitts and Pitts, 1997).

1.2 State of knowledge

1.2.1 Oxidation of aromatic hydrocarbons

Aromatic hydrocarbons contribute significantly to the chemistry of urban air (Atkinson and Aschmann, 1994; Odum *et al.*, 1997a; Calvert *et al.*, 2002). Despite many years of intensive research on the atmospheric chemistry of aromatic hydrocarbons, our understanding of the oxidation mechanisms is still poor and is mainly limited to the principal oxidation steps.

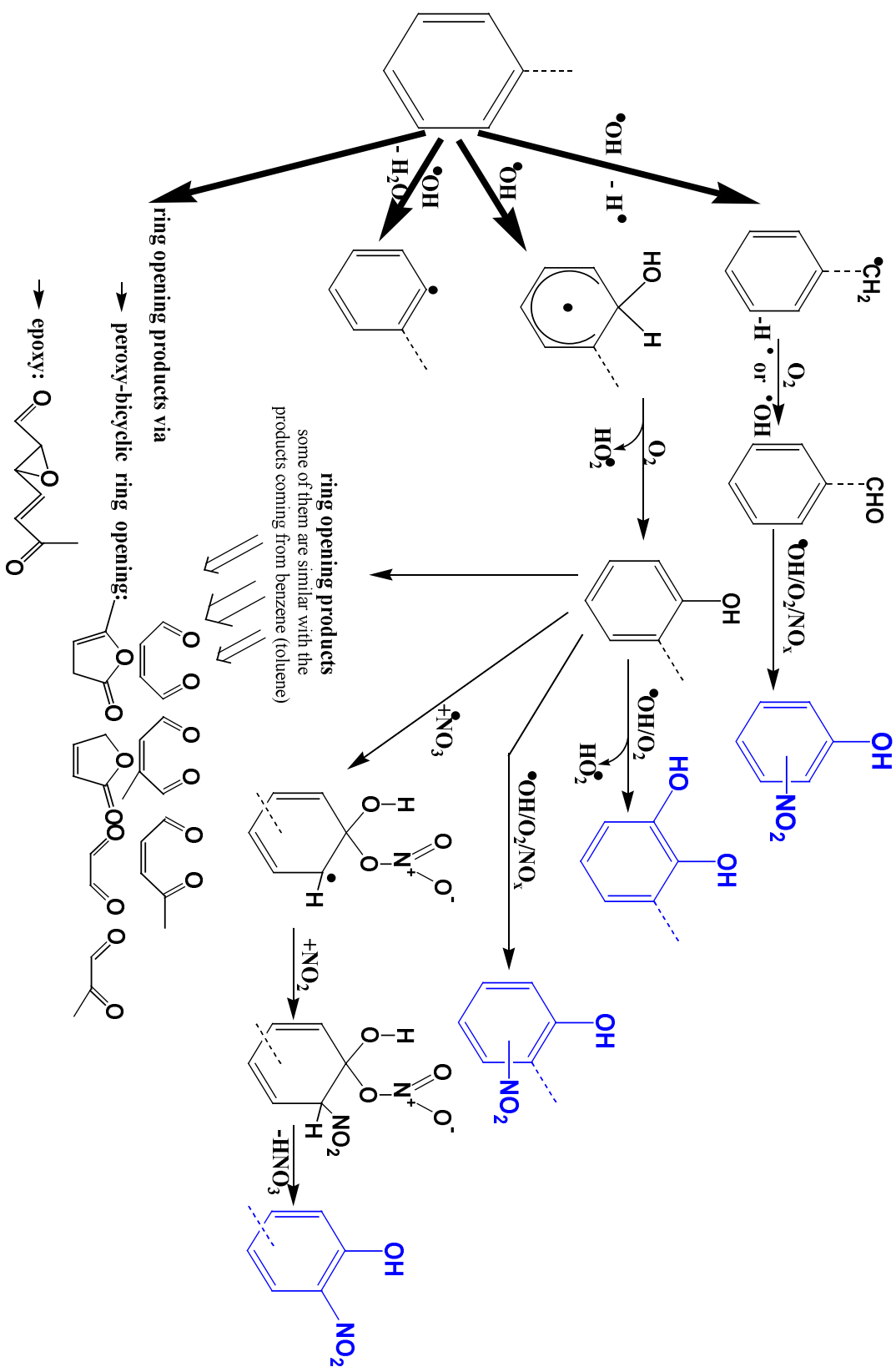


Figure 1.1 The main pathways of benzene (toluene) oxidation. Processes leading to the formation of nitrophenols and 1,2-dihydroxybenzenes from benzene (toluene) via benzaldehyde and phenol, in gas-phase under conditions of OH and NO_3 oxidation (Atkinson et al., 1989; Bolzacchini et al., 2001; Calvert et al., 2002; Olariu et al., 2002; Volkamer et al., 2002; Bloss et al., 2005a, 2005b).

Benzene, toluene (xylenes) and phenol (alkylphenols) have been studied intensively by different groups and the results, implemented into different detailed mechanisms. A simplified representation of the important identified pathways in the oxidation of benzene and toluene leading to the main oxidation products, with focus on the ring-retaining products, is given in Figure 1.1 (Atkinson *et al.*, 1989; Seuwen and Warneck, 1996; Klotz *et al.*, 1997; 1998; Calvert *et al.*, 2002; Volkamer *et al.*, 2002; Bloss *et al.*, 2005a, 2005b).

The degradation of aromatic hydrocarbons is mainly initiated during the day by reaction with the hydroxyl radical (OH). Reactions with NO₃ radicals are important only for the OH-substituted aromatic compounds; for BTX the reactions are too slow to be of significance (Atkinson *et al.*, 1988, 1992a; Olariu *et al.*, 2004b).

Monocyclic aromatic hydrocarbons absorb very little of the sunlight present in the troposphere. However, for oxygenated nitroaromatic compounds photodissociation may be very important and could be contributing to the generation of precursors of photooxidants in the troposphere (Bejan *et al.*, 2006).

For the atmospherically important emitted monocyclic aromatic hydrocarbons, i.e. BTX, the rate constants for their reactions with the active species OH, NO₃ and O₃ are fairly well established (Calvert *et al.*, 2002). However, rate constants for the reactions of these species with substituted (alkyl)aromatic hydrocarbons of atmospheric relevance are either unknown, have been determined only from a single study or are associated with very large uncertainty factors.

Product studies reported in the literature have been mainly focused on the analysis of the OH-radical initiated photooxidation of benzene and toluene. It is well established that the reaction of benzene (toluene) with OH radicals proceeds mainly by addition (~90%) to the aromatic ring forming an (methylated)hydroxycyclohexadienyl radical (OH-aromatic adduct); see Figure 1.1. Adduct formation is an intermediate step in the reaction pathway leading to phenol (cresol) formation (Atkinson *et al.*, 1989; Seuwen and Warneck, 1996; Calvert *et al.*, 2002; Volkamer *et al.*, 2002). An interesting additional pathway of the OH-aromatic adduct reaction to form benzene oxide/oxepin was proposed by Klotz *et al.* (1997), however, this pathway is now considered to be of negligible importance.

The H-atom abstraction channel for the reaction of OH with benzene is of minor importance (~5%) under atmospheric conditions (Calvert *et al.*, 2002). The abstraction pathway for toluene, leads eventually to the formation of benzaldehyde with a yield of less than 10% (Bandow and Washida, 1985; Finlayson-Pitts and Pitts, 2000; Calvert *et al.*, 2002). Further oxidation of benzaldehyde in the atmosphere results initially in formation of the C₆H₅CO radical via an aldehydic hydrogen abstraction channel. In the presence of NO_x formation of 2-nitrophenol in substantial yield has been observed as a final oxidation product as shown in Figure 1.1 (Calvert *et al.*, 2002).

1.2.2 Nitrophenols in the atmosphere

Among the various types of aromatic hydrocarbons, nitroaromatics are of particular interest. Nojima *et al.* (1975) were the first to detect nitrophenols in the environment and reported the presence of several nitrophenols in rainwater. The initial impetus to study the atmospheric behaviour of nitroaromatics stems from interest in the possible contribution of these compounds to forest decline (Rippen *et al.*, 1987) and their phytotoxic properties (Kawai *et al.*, 1987; Grosjean, 1991; Behnke *et al.*, 1998). Nitrophenols have been identified in air (Grosjean, 1991; Tremp *et al.*, 1993; Belloli *et al.*, 1999; Harrison *et al.*, 2005), clouds (Lüttke and Levsen, 1997), water (Geissler and Schöler, 1994), rain (Schüssler and Nitschke, 2001), soil (Voznakova *et al.*, 1996), fog (Herterich, 1991) and snow (Kawamura and Kaplan, 1986).

The phytotoxicity of nitro- and dinitrophenols is well known (Howe *et al.*, 1994; Isayev *et al.*, 2006). The toxicity of mononitrophenols to mammals is low and in the case of dinitrophenols it is strongly dependent on the position of the nitro groups (Barleta *et al.*, 1998, 1999).

Nitroaromatics are directly emitted to the atmosphere and are also formed *in situ* in the atmosphere by secondary chemical processes. Nitrophenols and nitrocresols are known to be formed in internal combustion engines (Tremp *et al.*, 1993). Other primary sources may be the combustion of coal and wood, and the manufacture of phenol-formaldehyde resins, pharmaceuticals disinfectants, dyes and explosives (Harrison *et al.*, 2005).

Studies in Wuppertal and other laboratories have shown that an additional important source of these compounds in the atmosphere (see Figure 1.1) could be the gas-phase OH-radical initiated photooxidation of aromatic hydrocarbons such as benzene, toluene, phenol, cresols and dihydroxybenzenes in the presence of NO_x during the daytime as well as the reaction of NO₃ radicals with these aromatics during the night time (Grosjean, 1985; Atkinson *et al.*, 1992a; Bolzacchini *et al.*, 2001; Olariu *et al.*, 2002). Once released to or produced in the troposphere, these compounds will undergo further oxidation and are also expected to partition between the gas and aerosol phases.

Quantification of nitrophenol formation in the gas phase reactions of OH or NO₃ radicals with phenols has been reported in only a few studies. Table 1.2 gives an overview of the published nitrophenol product yields from studies on the OH- and NO₃-radical initiated oxidation of several aromatic precursors.

Olariu *et al.* (2002), reported the formation of *ortho*-nitro methyl substituted phenols in the gas phase OH-radical initiated photooxidation of phenolic compounds in the presence of NO_x. These studies confirmed the yields reported for similar oxidation systems by Atkinson (1992). *para*-Nitrophenol formation from the photooxidation of phenols/OH/NO_x has also been reported by Olariu *et al.* (2002).

Berndt and Böge (2003) have studied the gas phase reaction of OH radicals with phenol and reported a 4% formation yield of nitrophenol. In the study they tested the influence of the oxygen, NO and NO₂ concentrations on the nitrophenol formation yield. No affect on the yield was observed on changing the NO concentration. Increasing the NO₂ concentration led to increase in the 2-nitrophenol yields, which were significant for NO₂ concentrations of 10 ppmV or more.

The NO₃-radical initiated oxidation of phenol leads to formation of 2-nitrophenol and 4-nitrophenol as main ring-retaining products (Atkinson *et al.*, 1992a; Olariu, 2001; Bolzacchini *et al.*, 2001). The mechanism involves the initial formation of an NO₃ "ipso" adduct which decomposes (decomposition rate of $\sim 5 \times 10^8 \text{ s}^{-1}$ at 298 K) via H-atom abstraction to form HNO₃ and phenoxy radicals;

further interactions of the phenoxy radicals with NO₂ result in nitrophenol formation (Atkinson, 1991).

Table 1.2 Molar product yields for the nitrophenols formed in the gas phase OH- and NO₃-radical initiated oxidation of aromatic precursors.

reactant	product	yield (%)		reference
		OH reaction	NO ₃ reaction	
phenol	2-NP	6.7 ± 1.5	25.1 ± 5.1	Atkinson <i>et al.</i> , 1992a
	2-NP	5.8 ± 1.0	~ 22.7	Olariu, 2001
	2-NP	4 - 9	-	Berndt and Böge, 2003
	2-NP	-	58.8 ± 9.4	Bolzacchini <i>et al.</i> , 2001
	4-NP	-	~ 50.0	Olariu, 2001
	4-NP	-	27.6 ± 7.9	Bolzacchini <i>et al.</i> , 2001
ortho-cresol	NC	4.9 ± 11.0	~ 22.7	Grosjean, 1985
	6M2NP	6.8 ± 1.5	~ 11.5	Olariu, 2001
	6M2NP	-	12.8 ± 2.8	Atkinson <i>et al.</i> , 1992a
meta-cresol	3M2NP	1.6 ± 1.0	16.8 ± 2.9	Atkinson <i>et al.</i> , 1992a
	5M2NP	1.6 ± 1.0	19.6 ± 3.6	Atkinson <i>et al.</i> , 1992a
	3M2NP	4.3 ± 1.6	~ 22.0	Olariu, 2001
	5M2NP	4.4 ± 1.5	~ 23.0	Olariu, 2001
	3M4NP	-	~ 22.0	Olariu, 2001
para-cresol	4M2NP	10.0 ± 4.0	~ 74.0	Atkinson <i>et al.</i> , 1992a
	4M2NP	7.6 ± 2.2	~ 43.0	Olariu, 2001

In contrast to the liquid phase (Ishag and Moseley, 1977; Alif *et al.*, 1987; Alif *et al.*, 1990, 1991; Chen *et al.*, 2005; Harrison *et al.*, 2005), the photochemistry of nitrophenols in the gas phase (Bejan *et al.*, 2004, 2005b, 2006) has received virtually no attention.

Nitrophenols absorb strongly in the atmospherically relevant UV range 300-400 nm, (Ishag and Moseley, 1977; Alif *et al.*, 1991; Chen *et al.*, 2005; Harrison *et al.*, 2005) corresponding to the S₁ → S₀ transition as reported for the liquid phase (Ishag and Moseley, 1977). Thus, the photochemistry of nitrophenols might be of importance for the atmosphere. In the liquid phase, photolysis of nitrophenols leads to the formation of catechol, cyclopentadiene carboxylic acid, nitrohydroquinone, 3-nitrocatechol, 2-nitrosophenol and 2-aminophenoxazone (Alif *et al.*, 1991). The

formation of nitrous acid (HONO)/nitrite has been observed during the photolysis of nitrophenols in the liquid phase (Ishag and Moseley, 1977; Alif *et al.*, 1991).

Photochemical transformation of nitrophenols on ice surfaces has been studied and similar product compounds to those seen in the aqueous solution photolysis studies have been observed (Dubowski and Hoffmann, 2000; Baitinger *et al.*, 1964; Schreiber, 1989; Borisenko and Hargittai, 1996; Chen *et al.*, 1998; Kovács *et al.*, 1998; 2000).

1.2.3 Nitrous acid (HONO) in the atmosphere

Nitrous acid (HONO) was detected for the first time in ambient air by Perner and Platt in 1979, and numerous subsequent laboratory, field, and modelling studies have since been conducted to explain the observed atmospheric concentration.

Nitrous acid is of considerable atmospheric interest since its photolysis



leads to the formation of OH radicals (Stockwell and Calvert, 1978), the key atmospheric oxidant in the degradation of most air pollutants. HONO is a crucial intermediate in the formation of photochemical smog in the troposphere (Platt *et al.*, 1980). Despite the other important sources for OH radical formation such as the photolysis of ozone and formaldehyde and the ozonolysis of VOCs, field and modelling studies have demonstrated that HONO photolysis can contribute considerably to the daily OH production with an integrated contribution of up to 60% (Neftel *et al.*, 1996; Staffelbach *et al.*, 1997a, 1997b; Zhou *et al.*, 2002a; Alicke *et al.*, 2002, 2003; Kleffmann *et al.*, 2003; Vogel *et al.*, 2003; Kleffmann *et al.*, 2005; Acker *et al.*, 2006). Night-time HONO mixing ratios up to 15 ppbV have been observed in field measurements. HONO is a dominant source for OH radicals in the early morning being responsible for up to 80% of the OH concentration at this time of the day (Alicke, 2000; Alicke *et al.*, 2003). While the night time formation of HONO in the atmosphere is reasonably well explained by direct

emissions and different heterogeneous conversion processes of NO₂ (Gutzwiller *et al.*, 2002; Finlayson-Pitts *et al.*, 2003; Ammann *et al.*, 2005) on ground surfaces (Vogel *et al.*, 2003), recent measurements have shown unexpectedly high HONO concentrations during the daytime (Neftel *et al.*, 1996; Zhou *et al.*, 2001, 2002a; Kleffmann *et al.*, 2002; 2003; 2005). The measured HONO levels were significantly higher than the values predicted on the basis of the available knowledge about daytime sources and sinks of HONO. The experiments revealed the existence of a strong unknown daytime source of HONO up to 60 times higher than the night time sources (Kleffmann *et al.*, 2005). The results from the field studies imply that this source can contribute up to 60% to the direct OH radical sources (Ren *et al.*, 2003), which were suggested to arise from the photolysis of adsorbed HNO₃/nitrate (Zhou *et al.*, 2001; 2002a, 2002b, 2003; Ramazan *et al.*, 2004) or by heterogeneous photochemistry of NO₂ on organic substrates (George *et al.*, 2005; Stemmler *et al.*, 2005; 2006).

1.2.4 (Methylated) 1,2 dihydroxybenzene in the atmosphere

Catechols are used widely in industry in dye and drug production, in the production of antioxidants, in rubber and oil industries, in photographic processes and in special types of ink (Flickinger, 1976). Significant amounts of catechols have been found in the particulate phase from both the wounding and burning of wood (Hawthorne *et al.*, 1992; Fine *et al.*, 2002). Catechols are common contaminants of smoked products (Waltz *et al.*, 1965; Eskinja *et al.*, 1995). Catechols are strongly mutagenic and carcinogenic aromatic compounds (Stohs *et al.*, 1997; Li *et al.*, 1997; Tsutsui *et al.*, 1997; Silva *et al.*, 2003).

It is now known that catechols can be produced in the atmosphere by the photooxidation of phenols. Phenols are produced in substantial yields in atmosphere in the reactions of OH with BTX (benzene, toluene, xylene isomers), benzene producing phenol (Atkinson, 1994; Calvert *et al.*, 2002; Volkamer *et al.*, 2002), toluene a mixture of *o*-, *m*- and *p*-cresols (Atkinson *et al.*, 1989; Klotz *et al.*, 1998; Smith *et al.*, 1998) and the xylene isomers a series of hydroxydimethylbenzenes (Smith *et al.*, 1999).

The strongly ortho directing effect of the OH group in phenols leads to the formation of catechols as main products in the OH radical initiated photooxidation of these compounds. Olariu *et al.* (2002) have quantified the catechol yields in the OH-initiated oxidation of several phenols and cresols. Catechol yields of more than 80 % were observed in some cases. Berndt and Böge (2003) have confirmed the data of Olariu *et al.* (2002) for the OH-initiated oxidation of phenol. In the studies of both Olariu *et al.* and Berndt and Böge the level of NO in the reaction system had no influence on the catechol yield, however, the yield was found to vary slightly with the NO₂ concentration; decreasing with increasing NO₂ concentration. A strong influence of temperature on the catechol yield in the reaction of OH with phenol has been observed by Berndt and Böge (2003) with the catechol yield increasing from 37% at 266 K to 87% at 364 K.

An unexpected low yield of catechol (23.9%) for a phenol/OH/NO_x reaction system has been reported by Sommariva (2000). Sommariva used PTR-MS (Proton Transfer Reaction Mass Spectrometry) in order to quantify the products of a phenol/OH/NO_x reaction system. At present the reason for the 4 times lower yield obtained by Sommariva compared to the other studies is not known.

Table 1.3 Rate coefficients for the reactions of OH, O₃ and NO₃ with 1,2-dihydroxybenzenes (Olariu *et al.*, 2000; Bejan *et al.*, 2002; Olariu *et al.*, 2004b; Tomas *et al.*, 2003).

compound	$k(\text{OH}) \times 10^{11}$ (cm ³ s ⁻¹)	$k(\text{O}_3) \times 10^{17}$ (cm ³ s ⁻¹)	$k(\text{NO}_3) \times 10^{10}$ (cm ³ s ⁻¹)
1,2-dihydroxybenzene	10.4 ± 2.1	0.96 ± 0.11	0.98 ± 0.5
1,2-dihydroxy-3-methylbenzene	20.5 ± 4.3	2.81 ± 0.23	1.72 ± 0.56
1,2-dihydroxy-4-methylbenzene	15.6 ± 3.3	2.63 ± 0.34	1.47 ± 0.65

Benzenediols have been shown to react rapidly with OH radicals (Olariu *et al.*, 2000). Reaction of benzenediols with NO₃ radicals is also very fast (Bejan *et al.*, 2002; Olariu *et al.*, 2004b). OH and NO₃ radicals compete for the decay of catechols even during the day and under certain conditions their contributions to

the decay are almost equal. Benzenediols have also been shown to react reasonably fast with O₃ (Tomas *et al.*, 2003). The reported rate coefficients for the reaction of catechols with OH, O₃ and NO₃ are summarized in Table 1.3. A very fast reaction of catechol with chlorine (Cl) atoms has also been reported (Bejan *et al.*, 2005a).

1.2.5 Secondary organic aerosol (SOA) formation in the atmospheric oxidation of aromatic hydrocarbons

Atmospheric aerosols are present in virtually all areas of the troposphere, and, in particular, in urban areas (Seinfeld and Pandis, 1998; Finlayson-Pitts and Pitts, 2000; Calvert *et al.*, 2002). Aerosols affect the global budget of O₃, OH and VOCs (mainly CH₄) through their alteration of photolysis rates and through their direct chemical interaction with gases (Reuder and Schwander, 1999; Bian *et al.*, 2003; Tie *et al.*, 2005; Kanakidou *et al.*, 2005).

Secondary organic aerosols (SOAs) result from the atmospheric oxidation of primary organic compounds, which lead to products that have vapour pressures low enough to enable them to condense into the particle phase.

Aromatic hydrocarbon photooxidation is alleged to make a significant contribution to secondary organic aerosol (SOA) formation in urban air (Leone *et al.*, 1985; Stern *et al.*, 1987; Izumi and Fukuyama, 1990; Odum *et al.*, 1996, 1997a; 1997b; Kleindienst *et al.*, 1999; Johnson *et al.*, 2005; Martin-Reviejo and Wirtz, 2005).

Studies on the aromatic SOA molecular composition have been focused on benzene and methylated benzene (Forstner *et al.*, 1997; Kleindienst *et al.*, 1999; Cocker *et al.*, 2001; Jang and Kamens, 2001; Hurley *et al.*, 2001). Based on the relationship between vapour pressure and the changes in molecular structure ring-retaining products should have an important role in SOA formation as the oxidation process of the aromatic proceeds. Large decreases in vapour pressure occur when –OH and –NO₂ groups are added to the aromatic ring structure (Yaws, 1999). Studies have been performed recently in the Wuppertal laboratories in order to investigate the SOA formation from phenol, catechols and nitrophenols (Olariu *et al.*, 2003, 2004; Bejan *et al.*, 2004).

While it has been known for some time that the oxidation of aromatic hydrocarbons leads to aerosol formation, the exact mechanism by which particles are formed is still unclear. In the last decade, a gas/particle absorption model has been developed in order to explain SOA yield data (see Annex IV) (Pankow, 1994a, 1994b; Odum *et al.*, 1996, 1997a, 1997b).

1.3 Aim of the present work

The atmospheric chemistry of aromatic hydrocarbons is complex and presently not well understood. Much research is required to elucidate the rates and mechanisms involved in the gas-phase initiated oxidation of aromatic hydrocarbons by reactive species such as OH, NO₃ and O₃. The detailed product analyses necessary in conjunction with the experimental rate measurements are extremely challenging.

At present our understanding of secondary organic aerosol (SOA) formation, composition, physical and chemical properties, sources, and transformation characteristics are very limited, and estimates of the actual environmental effects of SOA are highly uncertain.

The purpose of this work was to provide a scientific evaluation of the atmospheric fate of the following aromatic compounds, which are important products in the oxidation of BTX: 1,2-dihydroxybenzene, 3-methyl-1,2-dihydroxybenzene, 4-methyl-1,2-dihydroxybenzene, 2-nitrophenol, 3-methyl-2-nitrophenol, 4-methyl-2-nitrophenol, 5-methyl-2-nitrophenol, 6-methyl-2-nitrophenol. The following investigations were performed:

- Laboratory chamber experiments were performed at Wuppertal and at the EUPHORE outdoor chamber facilities Valencia/Spain in order to determine rate coefficients for the reactions of NO₃ radicals with the dihydroxybenzenes (no literature data are available).
- Kinetic experiments were carried out on the reactions of OH radicals with nitrocresols, which are important photooxidation products of cresols (only a computer estimation of the rates

based on the structure-activity relationship (SARs) is available in the literature).

- The photolysis of several nitroresols was investigated with respect to establishing
 - i) their importance as an atmospheric source of HONO (no literature data are available).
 - ii) the potential of the photolysis of these compounds to form secondary organic aerosols (only very limited literature data are available).

Chapter 2

2. Experimental section

The kinetic investigations were carried out in a 1080 l quartz glass reactor at the Bergische University Wuppertal, Germany, and in the EUPHORE photoreactor chamber at the Centro des Estudios Ambientales (CEAM), Valencia, Spain. The experiments in EUPHORE, a large volume simulation smog chamber, were performed under conditions of natural sunlight irradiation.

Aerosol formation studies were carried out in the 1080 l quartz glass reactor noted above while the mechanistic investigations on the photolysis of nitrophenols were performed in a specially designed glass flow photoreactor.

2.1a Description of the 1080 l reaction chamber

A schematic outline of the 1080 l reactor is shown in Figure 2.1 and a detailed description can be found in the literature (Barnes *et al.*, 1994).

The reactor consists of two quartz glass tubes with an inner diameter of 47 cm and a wall thickness of 5 mm. The reactor has a total length of 6.2 m. Silicone rubber rings are used for all the glass-metal connections as well as for metal-metal connections. The tubes are joined together by an enamelled flange ring and the ends are capped with two enamelled aluminium flanges. The reactor is connected

to a turbo molecular pump system via the central flange ring (Leybold-Heraeus PT 450 C). With the pumping system an end vacuum of 10^{-3} mbar can be achieved. Also connected to this central ring is a temperature sensor PT-100, a Teflon mixing fan and two steel sampling lines. The sampling lines are connected to aerosol measurement and gas-chromatography analytical instruments. A total of three fans are used for homogeneous mixing of compounds within the reactor. Different types of inlets are mounted on the end flanges for the introduction of chemicals and bath gases and for pressure measurement. Optionally, the inlets can be heated to facilitate the addition of solid compounds into the chamber. A gas flow controller can be used for the compensation of total pressure within the reactor when using analytical instrumentation that requires high volume gas samples.

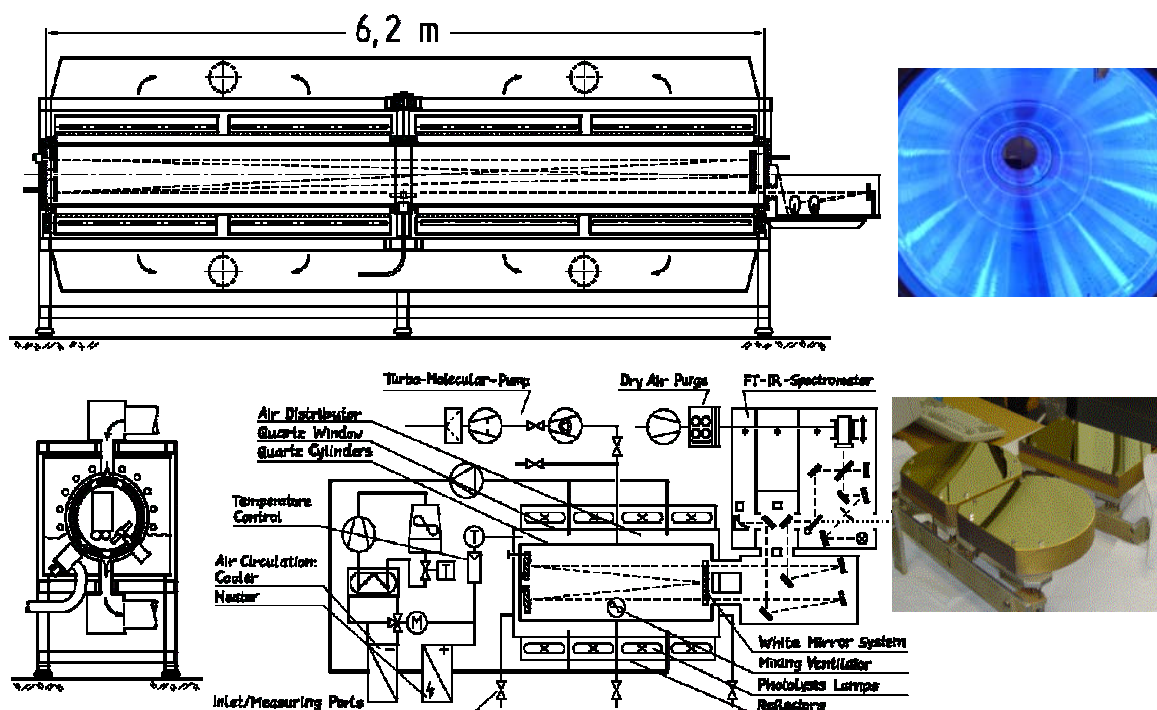


Figure 2.1 Schematic representation of the 1080 l reactor with details of the quartz tube and gold-coated mirrors.

The beam from an externally situated FT-IR (Fourier Transform Infrared) spectrometer is coupled, via a mirror system, into the reactor through KBr windows located in one of the end flanges. A White-type mirror system (base path length (5.91 ± 0.01) m), mounted inside the reactor, is used for multiple-reflection of the infrared beam within the reactor volume before it reaches the detector. Reactants

and products were monitored *in situ* in the reactor in the infrared using 82 traverses of the beam, which is equivalent to a total optical path length of (484.7 ± 0.8) m. All of the spectra in the experimental part of this work were recorded with a spectral resolution of 1 cm^{-1} .

The FT-IR spectrometers (BRUCKER IFS 88 and NICOLET NEXUS) used in this work are equipped with liquid nitrogen cooled (77 K) mercury-cadmium-tellurium (MCT) detectors. A Globar was used as the source of IR light. All the mirrors are gold coated to increase the reflectivity efficiency.

Two different types of lamps (32 each) are installed around the reactor. They are mounted alternatively around the reactor to ensure homogeneity of the light intensity within the reactor. The first type, Philips TL05 – 40W superactinic lamps, emit in the range 320 – 480 nm and have a maximum intensity at 360 nm. These lamps will be named VIS lamps in this work. The second type, low-pressure mercury lamps, Philips TUV – 40W, have an emission maximum at 254 nm and will be termed UV lamps in this work. The experiments can be performed at different temperatures within the range 283-313 K with a precision of ± 1 K.

2.1b Description of the EUPHORE chamber

The outdoor European Photo-Reactor (EUPHORE) is part of the Centro de Estudios Ambientales del Mediterraneo (CEAM), located near Valencia, Spain (Becker, 1996). A schematic diagram of the chamber together with a photographic panoramic view is presented in Figure 2.2.

Detailed descriptions of the chambers can be found in EUPHORE reports (Becker, 1996; Barnes and Brockmann, 2001). The two hemispherical chambers are made from FEP (fluorine-ethene-propene) foil with a thickness of 0.127 mm. This foil has a transmission of more than 80% in the wavelength range between 280 and 640 nm. The flat aluminium floor panels of the chambers are covered with FEP foil and can be cooled with water to avoid heating of the chambers during sun exposure. The chambers are protected against wind and rain by steel housings, which can be opened and closed hydraulically. In the closed position, experiments can also be performed in the dark on O_3 and NO_3 reactions.

The chambers are filled with air from a separate air purification system. With the help of a special charcoal absorber, NO_x is eliminated and oil vapour and non-methane hydrocarbons are reduced to $\leq 0.3 \mu\text{g m}^{-3}$. In order to avoid the collapse of the foil hemisphere an overpressure is necessary. A magnetic valve controls the addition of air into the chamber. More details can be found in Becker (1996).

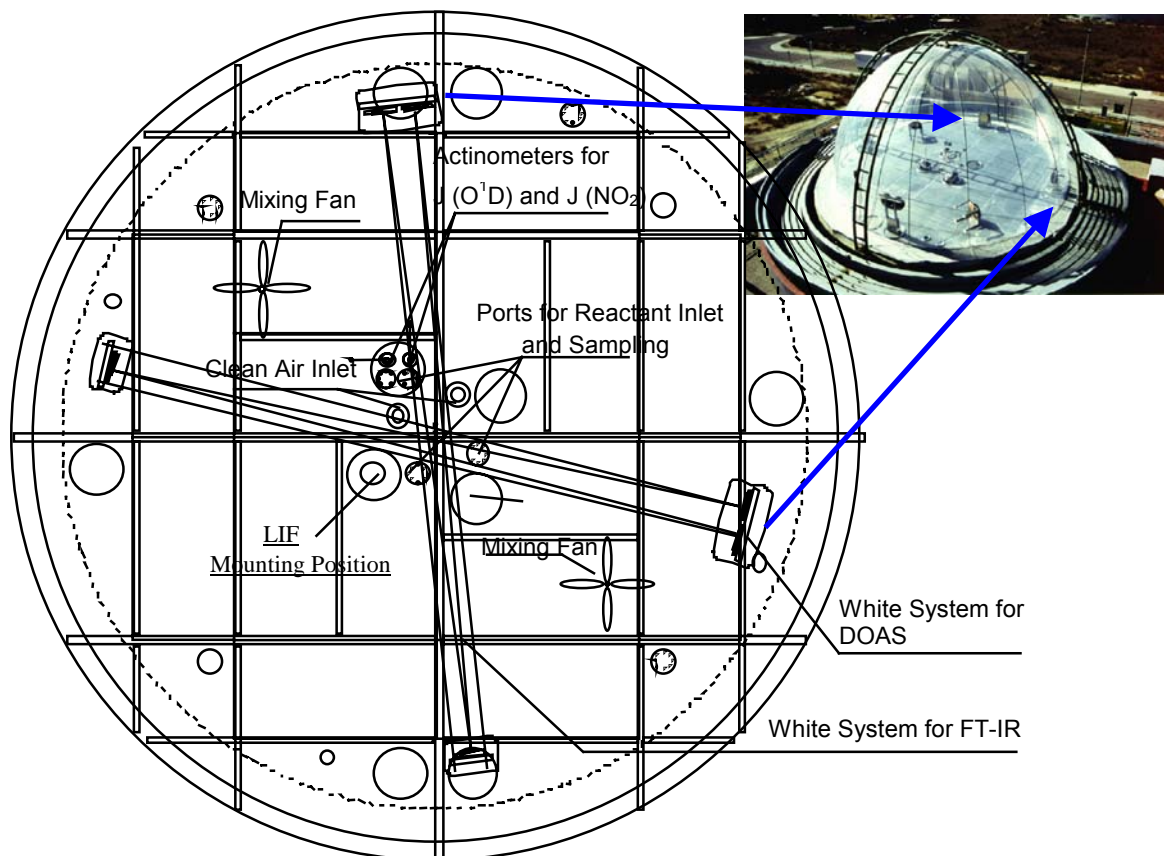


Figure 2.2 Top view of the EUPHORE “chamber A” which was used in this study.

The air inlets are located in the centre of the chamber floor. Outlets for the different analytical instruments used for monitoring of reactants and products are also integrated in the floor. Besides the conventional analytical instrumentation (GC-FID, GC-ECD, GC-PID, GC-MS, HPLC, monitors (O_3 , NO_x , NO_y), $\text{J}(\text{O}^1\text{D})$ actinometer, $\text{J}_{(\text{NO}_2)}$ actinometer, the chambers are equipped with *in situ* measurement techniques: DOAS – **D**ifferential **O**ptical **A**bsorption **S**pectroscopy, FT-IR – **F**ourier **T**ransform **I**nfra**R**ed Spectroscopy, TDL – **T**uneable **D**iode **L**aser. A **S**canning **M**obility **P**article **S**izer (SMPS) is used for monitoring the aerosol

distribution. Two White-type multiple-reflection mirrors are mounted inside this chamber, one coupled to a FT-IR spectrometer and one to a DOAS system.

The FT-IR spectrometer, a NICOLET MAGNA 550, was operated with a resolution of 1 cm^{-1} . The White mirror arrangement in chamber A, used in this study, had a total optical path length of 326.8 m and a base path length of 8.17 m.

2.2 Measurement procedure

Kinetic experiments were performed in the 1080 l quartz glass reactor. The aerosol formation resulting from the photolysis of nitrophenols was also studied in this reaction chamber.

Studies on the products produced by the photolysis of nitrophenols were performed in a specially constructed photolysis box connected to a small reactor, which was used for monitoring the nitrophenols by FT-IR. Also connected to the reactor was a LOPAP (**L**ong **P**ath **A**bsorption **P**hotometer) instrument for measuring HONO (nitrous acid) formation. More details can be found in Kleffmann *et al.* (2002).

2.2.1 Radical generation

NO₃ radical generation

In the 1080 l reaction chamber, NO₃ radicals were generated by the thermal decomposition of N₂O₅.



N₂O₅ was synthesised according to the procedure given in Appendix I.

In the EUPHORE photoreactor, the reaction of O₃ with NO₂ was used to produce NO₃ radicals.



O₃ was produced by a corona discharge in O₂ using a commercial ozone generator.

OH radical generation

The photolysis of CH₃ONO (methyl nitrite) with 32 superactinic fluorescent lamps (Philips TL05/40 W; 320 nm < λ < 480 nm, with λ_{max} = 360 nm) in the presence of NO was used as the OH radical source (equations 2.4 – 2.6). With this method steady-state OH radical concentrations of around 5 x 10⁷ cm⁻³ can be generated. Methyl nitrite was synthesised by the procedure described in Appendix I. Methyl nitrite was stored at -78°C.



2.2.2 Kinetic measurements

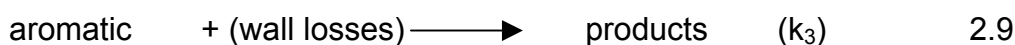
Two sets of experiments were performed to determine the rate coefficients for the reactions of NO₃ radicals with 1,2-dihydroxybenzenes and OH radicals with nitrocresols. A relative kinetic rate method was used for the rate coefficient determinations.

2.2.2.1 Relative rate method in kinetic data analysis

In the relative rate method the relative disappearance rates of the compound under investigation, i.e. the aromatic hydrocarbons, and a reference compound are monitored simultaneously in the presence of the radicals.



Control experiments showed that the aromatic hydrocarbons were also subject to losses in the absence of radicals, mainly due to wall deposition.



No wall deposition losses were observed for the reference hydrocarbons used in all the kinetic studies. On the basis of equations 2.7, 2.8 and 2.9 the following rate laws are valid for the aromatic and reference compounds:

$$-\frac{d[\textit{aromatic}]}{dt} = k_1[\textit{radical}][\textit{aromatic}] + k_3[\textit{aromatic}] \quad 2.10$$

$$-\frac{d[\textit{reference}]}{dt} = k_2[\textit{radical}][\textit{reference}] \quad 2.11$$

Integration and combination of equations 2.10 and 2.11 leads to:

$$\ln\left(\frac{[\textit{aromatic}]_{t_0}}{[\textit{aromatic}]_t}\right) - k_3(t - t_0) = \frac{k_1}{k_2} \ln\left(\frac{[\textit{reference}]_{t_0}}{[\textit{reference}]_t}\right) \quad 2.12$$

where k_1 and k_2 are the rate coefficients for the reactions of the radicals with the aromatic hydrocarbon and reference compound, respectively. The terms $[\textit{aromatic}]_{t_0}$, $[\textit{aromatic}]_t$, $[\textit{reference}]_{t_0}$ and $[\textit{reference}]_t$ are the initial concentration of the aromatic compound at time t_0 , its concentration at time t , the initial concentration of the reference hydrocarbon at time t_0 , and its concentration at time t , respectively. Hence plots of $(\ln([\textit{reactant}]_{t_0}/[\textit{reactant}]_t) - k_3(t-t_0))$ against $\ln([\textit{reference}]_{t_0}/[\textit{reference}]_t)$ should yield a straight line of slope k_1/k_2 and zero intercept. The rate coefficient k_1 can be placed on an absolute basis using the known rate coefficient k_2 for the reaction of the reference hydrocarbon with the radical.

2.2.2.2 NO₃ kinetic experiments on 1,2 dihydroxybenzenes

Rate coefficients for the reactions of NO₃ radicals with a number of 1,2-dihydroxybenzene compounds have been measured in two photoreactor systems using the relative rate method outlined in this chapter: (i) at the Bergische

Universität Wuppertal (Barnes *et al.*, 1994) and (ii) at the European Photoreactor (EUPHORE), Valencia, Spain (Becker, 1996). 2,3-Dimethyl-2-butene was chosen as reference hydrocarbon because it is one of the few compounds that has a well-established rate coefficient of a magnitude similar to that which was expected for the reaction of NO_3 with the 1,2-dihydroxybenzenes. In addition, 2,3-dimethyl-2-butene has interference-free adsorptions in the infrared, which do not overlap with those of the aromatic compounds under study. Unfortunately none of the other possible reference compounds checked in this study met the selection criteria.

Two different types of experiment were performed in both chambers. Firstly, experiments were performed in which N_2O_5 was added as prepared and secondly, experiments were performed in which high concentrations of NO_2 were added to N_2O_5 from the beginning of the experiments in order to shift the equilibrium between N_2O_5 , NO_2 and NO_3 radicals towards N_2O_5 and to ensure that the reaction times were extended beyond the reactant mixing time in the reactor. In addition, the experiments with high NO_2 served as a check for any possible interference from radical species generated from the NO_3 radical reactions (such as OH radicals) and also possible influences of NO_2 and/or N_2O_5 on the measured rate coefficient.

Studies at the Bergische Universität Wuppertal

The experiments were performed at 1000 mbar total pressure of synthetic air and at a temperature 298 ± 2 K. The experimental procedure was as follows. The 1,2-dihydroxybenzene compound under investigation and the reference hydrocarbon, 2,3-dimethyl-2-butene, were injected into the chamber under reduced pressure. Because the aromatic compounds are solid a special heated inlet was used. The chamber was then pressurized to 1000 mbar with synthetic air. For the first 5 min the concentration-time behaviours of the two compounds were monitored by FT-IR spectroscopy, i.e. 5 spectra derived from 64 interferograms co-added over a period of 1 min were recorded. N_2O_5 was then flushed into the chamber through a glass line at a flow rate of $50\text{-}100 \text{ ml min}^{-1}$ for 15 min by evaporating solid N_2O_5 . This procedure delivered N_2O_5 to the chamber at a rate of about $20\text{-}25 \text{ ppbV min}^{-1}$. N_2O_5 was prepared as described in Appendix I and stored

at -78°C in dry ice. In total, the measurement period time for one experiment was about 20 min.

The initial reactant concentration ranges were (in cm^{-3} units) $(1.2 - 4.8) \times 10^{13}$ for the 1,2-dihydroxybenzene compounds and reference hydrocarbon and $(0 - 2.4) \times 10^{13}$ for NO_2 . At least 5 experiments were performed for each dihydroxybenzene compound.

Control experiments showed that wall loss of the 1,2-dihydroxybenzenes in clean air in the chamber was typically between 35 - 40% per hour. No wall deposition loss was observed for the reference hydrocarbon.

Studies at the EUPHORE chamber

The experiments were performed at atmospheric pressure and 296 ± 2 K in purified air. Four kinetic experiments were performed on 1,2-dihydroxybenzene and three on each of the 1,2-dihydroxybenzene methylated isomers. The experimental procedure was as follows. The chamber was flushed with purified air overnight for approximately 10-12 h before the start of each experiment. The dihydroxybenzene compounds were added to the chamber using a spray inlet system. Prior to injection a weighted amount of 1,2-dihydroxybenzenes was first dissolved in a minimum of distilled water (~ 5 ml). 2,3-Dimethyl-2-butene and NO_2 were injected by means of a syringe into a glass tube (impinger) connected to the chamber via a Teflon line. The initial reactant concentration ranges were (in cm^{-3} units) $(5 - 7.2) \times 10^{12}$ for the reactant compounds and reference hydrocarbon and $(0 - 7) \times 10^{12}$ for NO_2 . N_2O_5 was produced by titration of a flow of NO_2 with O_3 prior to entry into the chamber and was added continuously to the chamber through a Teflon line. This procedure resulted in a delivery rate for N_2O_5 to the chamber of about $1.2 \text{ ppbV min}^{-1}$.

Each experiment on the dihydroxybenzene/reference/ N_2O_5 reaction system was performed over a period of approximately 2 h in the dark using *in situ* FT-IR spectroscopy (Nicolet Magna spectrometer) to monitor the compounds. Infrared spectra were derived from 130 co-added scans, which yielded a time resolution of 2.5 min. The experiment was usually terminated when ca. 70-80% of the reactant had been consumed. The reaction chamber was pressurized continuously during

the experiments to compensate for losses due to leaks and air drawn by the external analytical instrumentation. This dilution was monitored by FT-IR using SF₆ as an inert tracer gas. The dilution loss was typically 3-4% h⁻¹. The sum of the surface deposition and dilution rates for the dihydroxybenzenes were determined by observing the decay of their IR absorption features prior to addition of N₂O₅ and NO₂. Loss rates of about 20% h⁻¹ were measured. In the case of the reference hydrocarbon no wall deposition loss was observed but the dilution loss was taken into account in the data analysis.

Because of the different behaviour of aromatics and alkenes in air (e.g. diffusion) possible inhomogeneous cloud formation close to the inlet in the chamber is a possible experimental artefact. In order to check the homogeneity of the mixing of the reactants in the chamber a test experiment was performed. Using *o*-cresol as the reference hydrocarbon, the rate coefficient for the reaction of NO₃ with 2,3-dimethyl-2-butene was measured. The rate coefficients for the reactions of both *o*-cresol and 2,3-dimethyl-2-butene with NO₃ are considered as well as established.

All the hydrocarbons studied (1,2-dihydroxybenzene, 1,2-dihydroxy-3-methylbenzene and 1,2-dihydroxy-4-methylbenzene) as well as the reference hydrocarbon (2,3-dimethyl-2-butene) were used as supplied by Aldrich Chemical Company and had stated purities of > 98 %.

2.2.2.3 OH kinetic experiments on nitrocresols

The kinetic investigations on the reactions of OH radicals with the nitrocresols were carried out in a 1080 l cylindrical quartz-glass photoreactor in synthetic air (760 ± 10) Torr by (296 ± 3) K. A Nicolet Nexus FT-IR spectrometer was used for reactant and reference monitoring. IR spectra were recorded at a spectral resolution of 1 cm⁻¹. Between 8 and 12 spectra were recorded in each kinetic experiment; each spectrum was comprised of 128 co-added interferograms. Prior to the kinetic experiments, 5 experiments were performed for every nitrocresol compound in order to obtain the photolysis and wall loss rates for these compounds. These two constants were used in corrections of the OH kinetic rate data. OH radicals were produced during the photolysis of nitrocresols. Using

isoprene as scavenger for OH radicals ($k_{\text{OH}} = 8.52 \times 10^{-12} \text{ cm}^3 \text{ s}^{-1}$, Atkinson and Arey, 2003) it was possible to calculate the concentration of OH radicals produced by the photolysis and thus calculate a “correct” value for the photolysis frequency.

6-Methyl-2-nitrophenol was obtained from Olariu (2001) who prepared it by addition of sodium nitrite to *o*-toluidine dissolved in a concentrated solution of sulphuric acid, following a method described by Winzor (1935).

Ethene was used as the reference compound. In the cases of 4-methyl-2-nitrophenol and 5-methyl-2-nitrophenol a second reference compound, n-butane, was also used.

Gaseous compounds (CH_3ONO , NO, ethene, n-butane and isoprene) were injected into the reactor using calibrated gas-tight syringes with the reactor under reduced pressure. Solid compounds (nitrocresols) were introduced into the chamber in airflow through a special heated inlet system. The initial reactant concentrations (in cm^{-3} units) were as follows: C_5H_8 2×10^{14} , C_4H_{10} (6-8) $\times 10^{13}$, nitrocresols (4.8 - 9.2) $\times 10^{13}$, CH_3ONO 5×10^{13} , C_2H_4 (6 - 8) $\times 10^{13}$ and NO 3×10^{14} .

2.2.3 Photolysis of nitrophenols. HONO formation

The formation of HONO from the photolysis of nitrophenols was studied in the glass flow photoreactor system shown in Figure 2.3. The following nitrophenols, as provided by the manufacturer, were investigated: 2-nitro-1-hydroxybenzene (2-nitrophenol: 2NP, Aldrich, 98 % purity), 3-methyl-2-nitro-1-hydroxybenzene (3-methyl-2-nitrophenol: 3M2N, Fluka 98 % GC purity), 4-methyl-2-nitro-1-hydroxybenzene (4-methyl-2-nitrophenol: 4M2N, Aldrich, 99 % purity) and 3-methyl-6-nitro-1-hydroxybenzene (5-methyl-2-nitrophenol: 5M2N, Aldrich, 97 % purity).

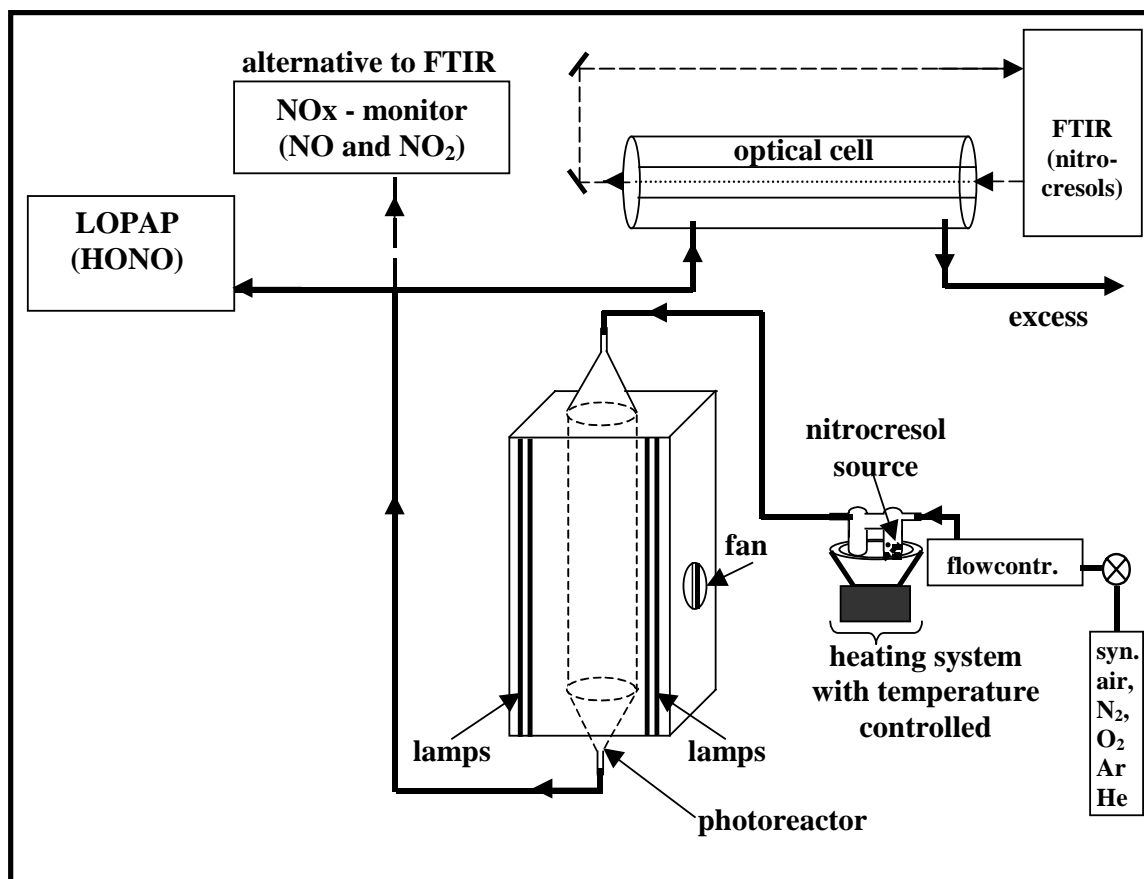


Figure 2.3 Experimental set-up used for investigations on the photolysis of nitrophenols

A gas phase mixture containing a nitrophenol was generated by flushing 2.5 l min⁻¹ pure synthetic air (flow controller: Bronkhorst, 2.5 l min⁻¹) over a solid or liquid sample of the nitrophenol, which was immersed in a temperature regulated water bath. The vapour pressure of the nitrophenol in the gas phase was adjusted by varying the temperature of the water bath. For some experiments with 3M2N the influence of the buffer gas on the HONO formation rate was investigated using calibrated flows of N₂ (99.999 and 99.9999), O₂ (99.999), Ar (99.999) or He (99.9999) in place of synthetic air.

The gas containing the nitrophenol was flushed through the photoreactor, for which either a 9 mm i.d. glass tube (length 46 cm, S/V = 4.4 cm⁻¹, borosilicate glass) or a cylindrical glass flow tube (length 80 cm, 50 mm i.d., conic entrance and exit junctions, S/V: 0.75 cm⁻¹, borosilicate glass) was used. The photoreactors were placed in an aluminium housing, in which six UV/VIS lamps (Phillips TL/05, 20

Watt, 300-500 nm, λ_{\max} = 370 nm, length 57 cm) were installed symmetrically around the photoreactor. The lamps are wired in parallel and can be switched individually to allow control of the light intensity. A fan installed in the aluminium housing prevented strong heating of the photoreactor. The temperature increase over ambient temperature (298 ± 5 K) during irradiation was around 3-4 K.

Typically, the effluent from the photoreactor was analyzed for HONO, nitrophenols and in a few experiments also for NO₂. Nitrous acid was measured with a newly developed, highly sensitive instrument (LOPAP), which is described in detail elsewhere (Heland *et al.*, 2001; Kleffmann *et al.*, 2002).

Briefly, HONO is sampled in a stripping coil by a fast chemical reaction and converted into an azo dye, which is photometrically detected by long path absorption in light conducting Teflon tubes. The two-channel set-up of the instrument corrects for interferences (Kleffmann *et al.*, 2002) including those caused by mixtures of NO₂ and semi-volatile diesel exhaust components (Gutzwiller *et al.*, 2002). In recent intercomparison campaigns with the DOAS technique, in the field and in a smog chamber, excellent agreement was obtained for daytime conditions (Kleffmann *et al.*, 2006). For the experimental conditions applied in the present study, the instrument had a detection limit of 5 pptV for a time resolution of 2.5 min.

The concentration of the nitrophenol was determined using a FTIR spectrometer coupled to a 10 l White type multiple reflection cell operated at a total optical path length of 32.8 m. The cell was connected to the exit of the photoreactor (Figure 2.3). IR spectra were recorded at a spectral resolution of 1 cm⁻¹ using a Nicolet NEXUS FT-IR spectrometer. Spectra were recorded by co-adding 128 scans per spectrum over a time period of 2 min while sampling continuously during the experiments. Cross sections as reported by Olariu (2001) were used at the following spectral wavenumbers to calculate the nitrophenol concentrations: 1627 and 1343 cm⁻¹ for 2-nitrophenol; 1609 and 1351 cm⁻¹ for 3-methyl-2-nitrophenol; 1639, 1335 and 1191 cm⁻¹ for 4-methyl-2-nitrophenol; 1634, 1603, 1335 and 1203 cm⁻¹ for 5-methyl-2-nitrophenol.

A Perkin-Elmer Lambda 40 double-beam UV/VIS spectrometer equipped with a halogen/deuterium lamp was used to obtain the absorption spectrum of

3M2N in dichloromethane as solvent. The UV/VIS Spectrometer was operated at a resolution of 0.5 nm in the wavelength range 190-1100 nm. WinLab software was used to analyse the recorded spectra.

For some experiments, the NO₂ dependence of the photolytic HONO formation rate and the upper limit of the NO₂ formation rate during the photolysis of pure nitrophenols were determined with a Luminol NO₂ monitor (Unisearch, LMA-3D). NO₂ was obtained from Messer Griesheim as a 10 ppmV premix-gas in N₂. The error in the NO₂ concentration was calculated from the accuracy of the NO₂ calibration mixture, specified by Messer Griesheim, and the statistical errors of the calibration curve.

Photolysis of NO₂ (NO₂+hν→NO+O) was studied as a photochemical reference reaction within the reactor. A NO_x (NO+NO₂) chemiluminescence analyser (Eco-Physics: AL 770 ppt) with a photolytic converter (Eco Physics: PLC 760) was used to measure the decrease of the NO₂ concentration upon irradiation at various photolysis times and different initial NO₂ concentrations. The photochemical conversion rate of NO₂ is quantified by the photolysis frequency J_(NO₂):

$$J(NO_2) = -\frac{1}{[NO_2]} \times \frac{\Delta[NO_2]}{\Delta t} \quad 2.13$$

J_(NO₂) was calculated numerically incorporating the chemistry of the Leighton equilibrium (Finlayson-Pitts and Pitts, 2000) and recommended rate constants (Atkinson *et al.*, 2005). For all six lamps, a value for J_(NO₂) of 0.018 s⁻¹ was determined inside the photoreactor. This result is in good agreement with J_(NO₂)=0.016 s⁻¹ calculated (Kleffmann, 2005) from the measured actinic flux spectra taking into account the reactor geometry and molecular data of NO₂, i.e. absorption cross sections and quantum yields (Hofzumahaus *et al.*, 1999). The Eco-Physics instrument could not be used for experiments with the nitrophenols, since the NO_x concentration measured by the instrument was significantly lower than the actual NO_x concentration in the presence of ppmV levels of nitrophenols, because of photochemical reactions leading to NO_x losses in the photolytic converter.

2.2.4 Photolysis of nitrophenols. Aerosol formation

The formation of aerosols in the 1080 I reactor was studied with an SMPS system presented in Figure 2.4. The SMPS consists of an electrostatic classifier TSI 3071 A and a particle counter TSI 3022 A. The classifier is connected to the reactor by a steel line. The particles generated in the gas phase inside the reactor were drawn in a laminar flow through a steel line to a DMA (Differential Mobility Analyzer) where the aerosols were classified according to their electrical mobility. The electrical field is adjustable between 10 and 12000 V.

The mono-dispersed aerosol distribution then enters the Condensation Particle Counter (CPC) where the particle concentration for the classified size is determined. The counter is connected to a computer in order to achieve data acquisition. The CPC consist of 3 major subsystems: the sensor, the microprocessor-based signal-processing electronics and the flow system. The sensor itself is made up of a saturator, condenser, and optical detector, as shown in Figure 2.4. After passage through the heated saturator and the cooled condenser the submicrometer particle becomes supersaturated. The droplets then pass through a lighted viewing volume where they scatter light. The optical part of the CPC, which counts the light scattered from individual droplets, consists of a laser diode, collimating lens and cylindrical lens, and photodetectors. The scattered-light pulses are collected by a photodetector and converted into electrical pulses. The electrical pulses are then counted and their rate is a measure of the particle concentration. Aerosol size distributions between 10 and 1000 nm could be measured as a function of gas flow and impactor used.

In addition to the SMPS system described above an ultrafine condensation particle counter (UCPC) TSI 3025 A was also used. The time set for this counter was 5 min per scan. This counter was used to observe the starting phase of the particle formation.

All the aerosol formation experiments were performed in the 1080 I quartz glass photoreactor as described previously. The experimental procedure during this work was as follows. Before each experiment a blind experiment was performed in order to check the background level of aerosols in clean air and also to ensure that no aerosol was coming from the reactor walls during the photolysis.

In all the blind experiments no particle formation was observed during 30 min photolysis time. With the chamber under reduced pressure the nitrophenols were added as described earlier in this chapter. Before the start of irradiation the nitrophenol was allowed to stand in the dark for 20 min in order to determine the wall loss rate. IR spectra were recorded at a spectral resolution of 1 cm^{-1} using a Nicolet NEXUS FT-IR spectrometer. FT-IR spectra were recorded continuously during the experiment by co-adding 128 scans per spectrum over a time period of 2 min. The SMPS sampling was timed to coincide with the recording of the FT-IR spectra.

Solid compounds (nitrocresols) were introduced into the chamber in airflow through a special heated inlet system. The initial reactant concentrations (in cm^{-3} units) were $(2 - 10) \times 10^{13}$.

Isoprene was injected in order to suppress the possible reaction of the nitrophenols with OH radicals formed during the experiment. The concentration of isoprene was varied between $10\text{-}100 \times 10^{13}\text{ cm}^{-3}$.

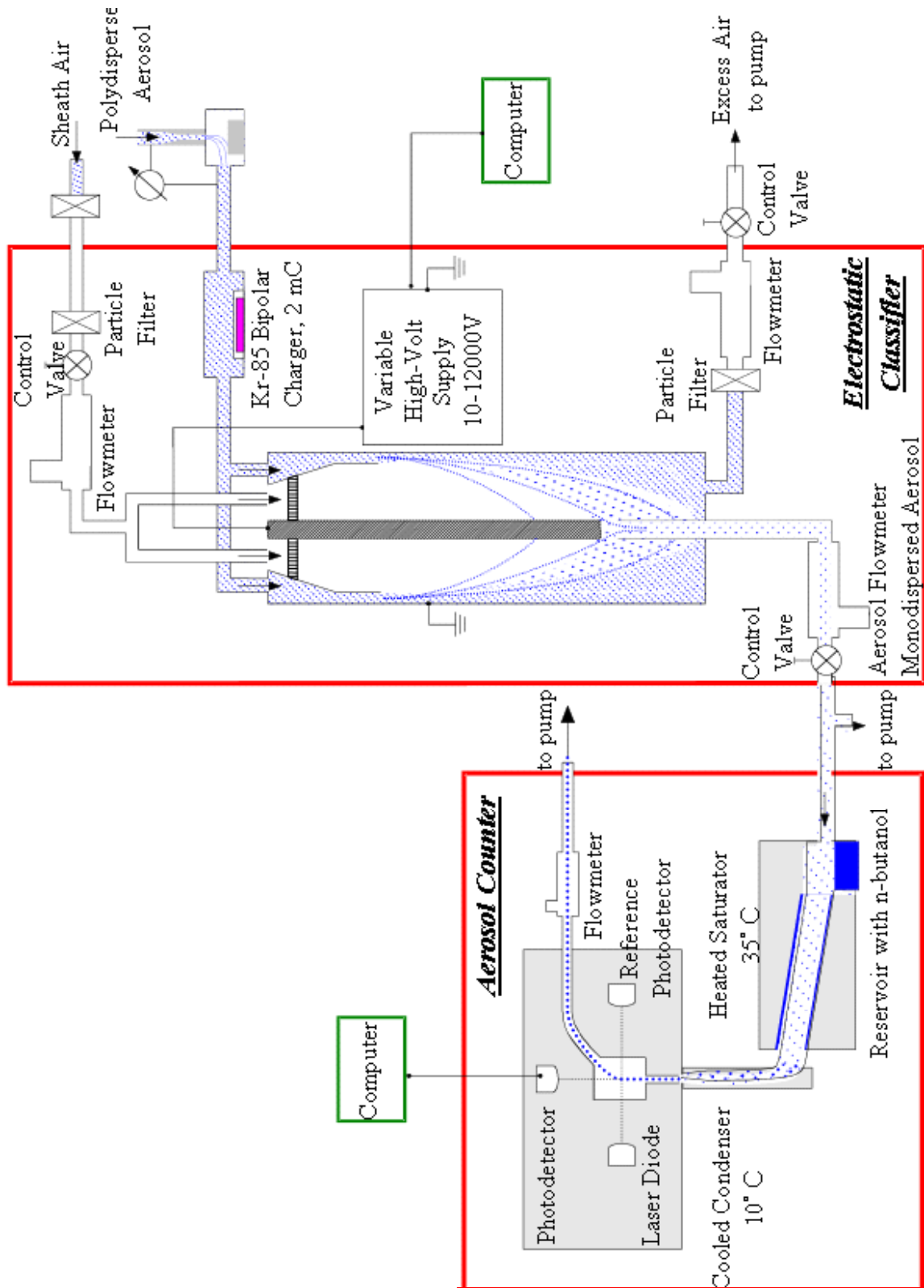


Figure 2.4 Detailed schematic diagram of the SMPS system (DMA and CPC) (adapted from Spittler (2001)).

Chapter 3

3. Kinetic investigations of the gas-phase reaction of NO₃ and OH radicals with some nitro/hydroxy substituted monoaromatic hydrocarbons

The compounds investigated in this work are the main products of the atmospheric degradation of phenol and the cresol isomers in the gaseous phase. It is known that 1,2-dihydroxybenzene (catechol) and its methylated derivatives are formed in high yields in the OH initiated gas phase reaction of phenol and cresols, respectively (Olariu *et al.*, 2002; Berndt and Böge, 2003). Formation of nitrophenol isomers has been observed from both the OH and NO₃ radical reactions of the compounds (Atkinson *et al.*, 1992; Bolzacchini *et al.*, 2001; Olariu *et al.*, 2002; Berndt and Böge, 2003).

3.1 Kinetics of the reaction of NO₃ radicals with 1,2-benzenediol and methylated substitutes

Except for two kinetic studies made in our laboratories, nothing is presently known about the atmospheric chemistry of catechols. Olariu *et al.* (2002) and Tomas *et al.* (2003) have determined rate coefficients for the reaction of catechol with OH radicals and with O₃, respectively. The work presented here, which in part is already published (Bejan *et al.*, 2002; Olariu *et al.*, 2004), provides new information on the rate coefficients for the gas phase reactions of NO₃ radicals with a number of catechols.

3.1.1 Results

The kinetic data obtained from investigations on the reactions of NO₃ with selected catechols, performed in both the 1080 l quartz glass reactor in Wuppertal and in the EUPHORE chambers in Valencia, are plotted in accordance with eq. (2.12) in Figures 3.1–3.6.

Reasonably linear plots were obtained in both chambers. As can be seen in all the figures, there is no discernable difference in the results between the experiments performed at low or high NO₂ for both chambers; i.e., the kinetic behaviour was independent of the [N₂O₅]/[NO₂] ratio. This supports that the reactions of the 1,2-dihydroxybenzenes take place with NO₃ radicals and not with N₂O₅ or NO₂.

In the present work only 2,3-dimethyl-2-butene was used as a reference compound. The reaction of all other reference compounds tested with NO₃ were either too slow or an interference free analysis of their infrared absorption bands was not possible. A value of $k(2,3\text{-dimethyl-2-butene} + \text{NO}_3) = (5.72 \pm 0.21) \times 10^{-11} \text{ cm}^3 \text{ s}^{-1}$ at 298 K (Atkinson, 1994) has been used as rate coefficient for the reaction of NO₃ radicals with 2,3-dimethyl-2-butene to put the measured relative rates on an absolute basis.

A possible problem, which can arise in the EUPHORE chamber, is the inhomogeneity of the reactants as a consequence of the large chamber volume. Possible complications from “persistent cloud” formation close to the inlet port have been tested for in a separate experiment using the reference compound. This test experiment consisted of measuring the rate coefficient for the reaction of NO₃ with 2,3-dimethyl-2-butene relative to another reference compound whose kinetic rate coefficient is well established. o-Cresol was employed as a second reference organic compound with a recommended rate coefficient of $k(\text{o-cresol} + \text{NO}_3) = 1.4 \times 10^{-11} \text{ cm}^3 \text{ s}^{-1}$ at 298 K (Calvert *et al.*, 2002). Good linearity was obtained in the test experiment and a rate coefficient of $k(2,3\text{-dimethyl-2-butene} + \text{NO}_3) = 5.6 \times 10^{-11} \text{ cm}^3 \text{ s}^{-1}$ was measured which is in perfect agreement with the rate coefficient of $(5.72 \pm 0.21) \times 10^{-11} \text{ cm}^3 \text{ s}^{-1}$ for the reaction recommended by Atkinson (1994).

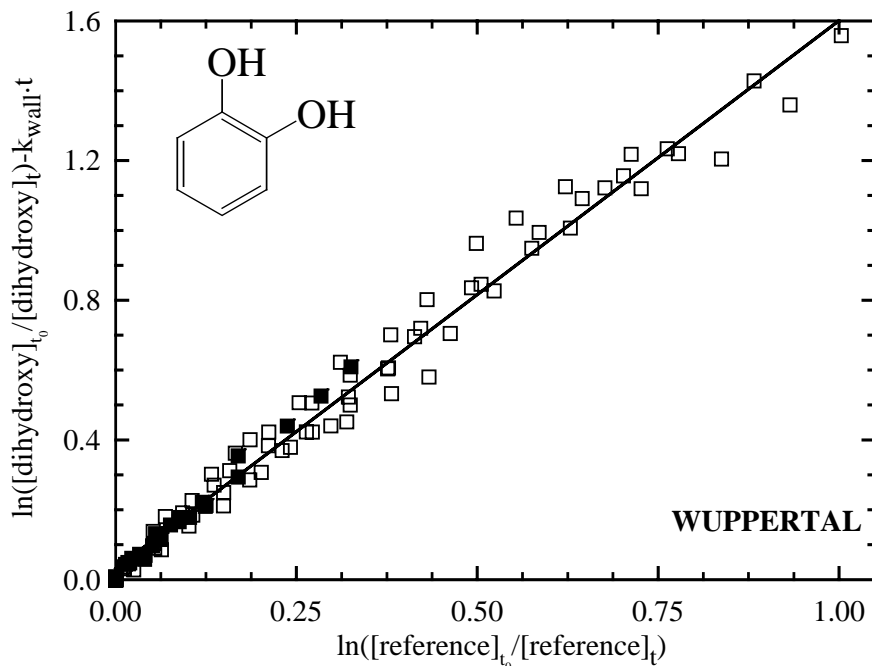


Figure 3.1 Plot of the kinetic data according to equation (2.12) for the reaction of 1,2-dihydroxybenzene with NO_3 radicals measured relative to 2,3-dimethyl-2-butene in the 1080 l quartz glass reactor chamber: (\square) low NO_2 ; (\blacksquare) high NO_2 .

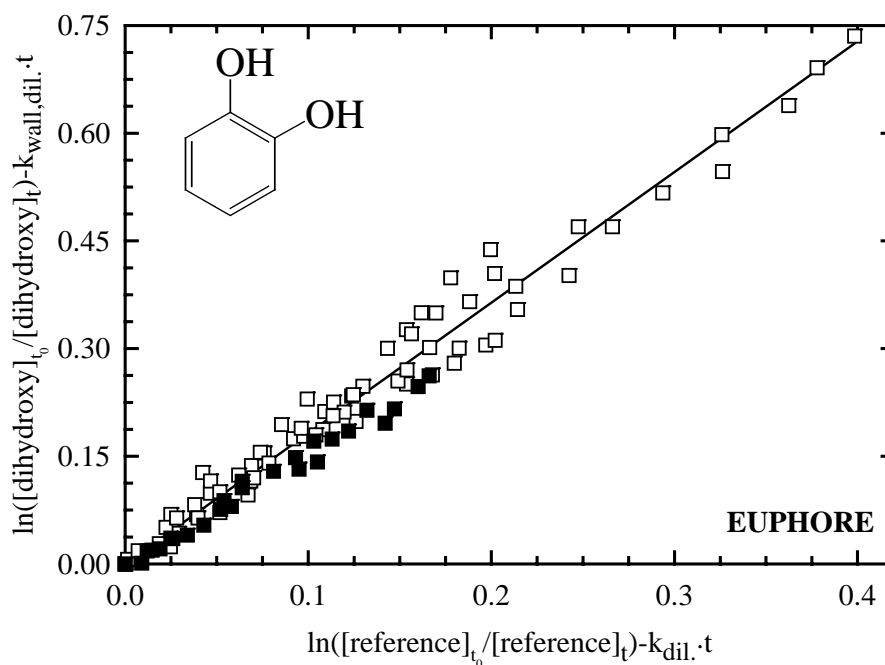


Figure 3.2 Plot of the kinetic data according to equation (2.12) for the reaction of 1,2-dihydroxybenzene with NO_3 radicals measured relative to 2,3-dimethyl-2-butene in the EUPHORE chamber: (\square) low NO_2 ; (\blacksquare) high NO_2 .

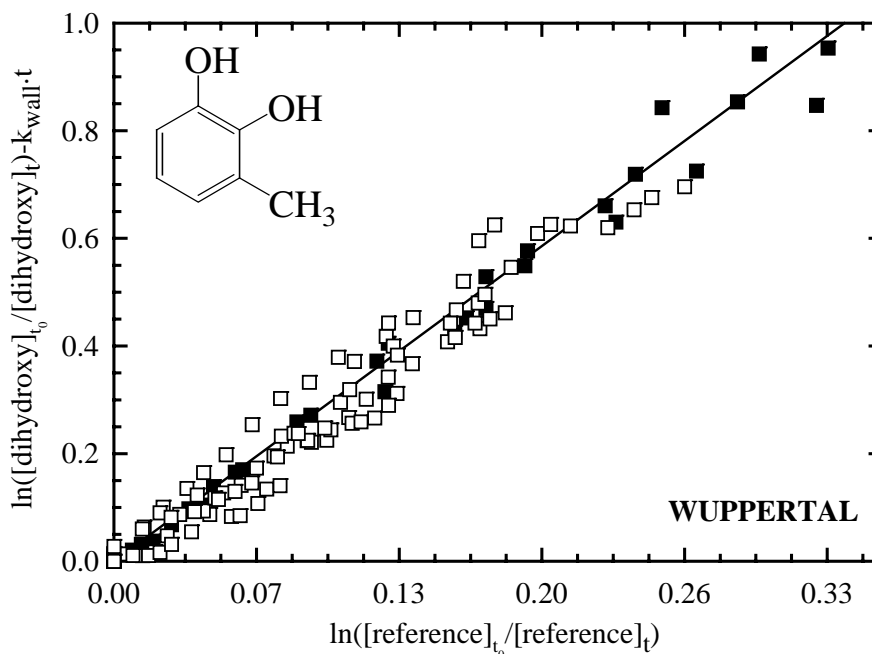


Figure 3.3 Plot of the kinetic data according to equation (2.12) for the reaction of 1,2-dihydroxy-3-methylbenzene with NO_3 radicals measured relative to 2,3-dimethyl-2-butene in the 1080 l quartz glass reactor chamber: (\square) low NO_2 ; (\blacksquare) high NO_2 .

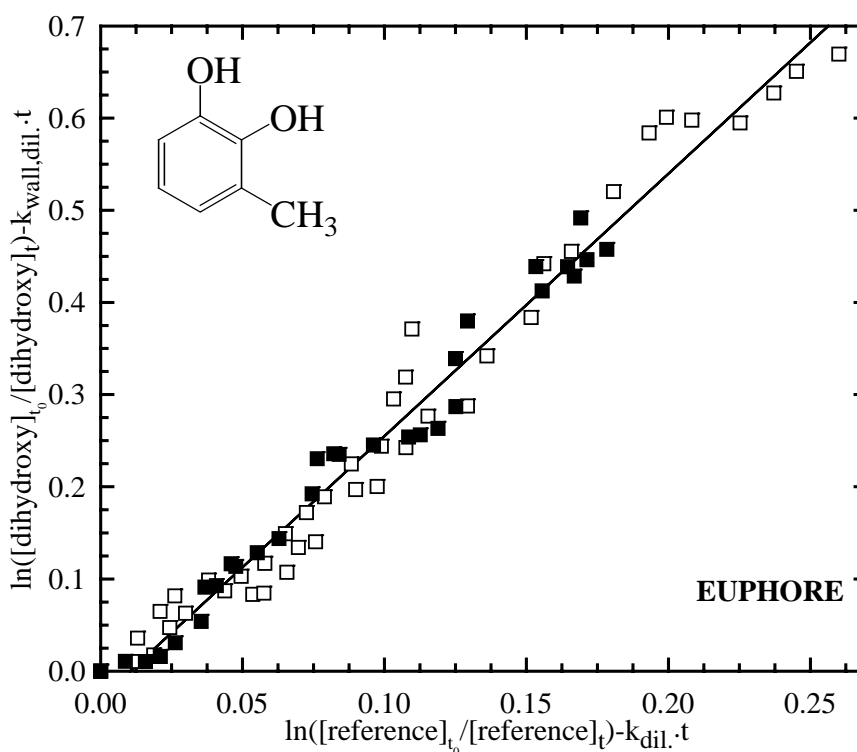


Figure 3.4 Plot of the kinetic data according to equation (2.12) for the reaction of 1,2-dihydroxy-3-methylbenzene with NO_3 radicals measured relative to 2,3-dimethyl-2-butene in the EUPHORE chamber: (\square) low NO_2 ; (\blacksquare) high NO_2 .

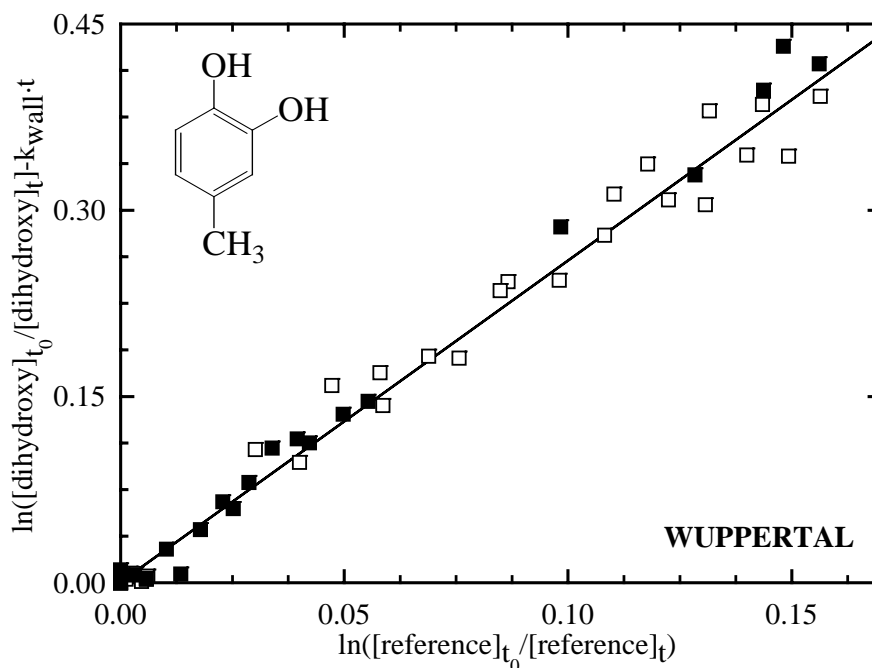


Figure 3.5 Plot of the kinetic data according to equation (2.12) for the reaction of 1,2-dihydroxy-4-methylbenzene with NO_3 radicals measured relative to 2,3-dimethyl-2-butene in the 1080 l quartz glass reactor chamber: (\square) low NO_2 ; (\blacksquare) high NO_2 .

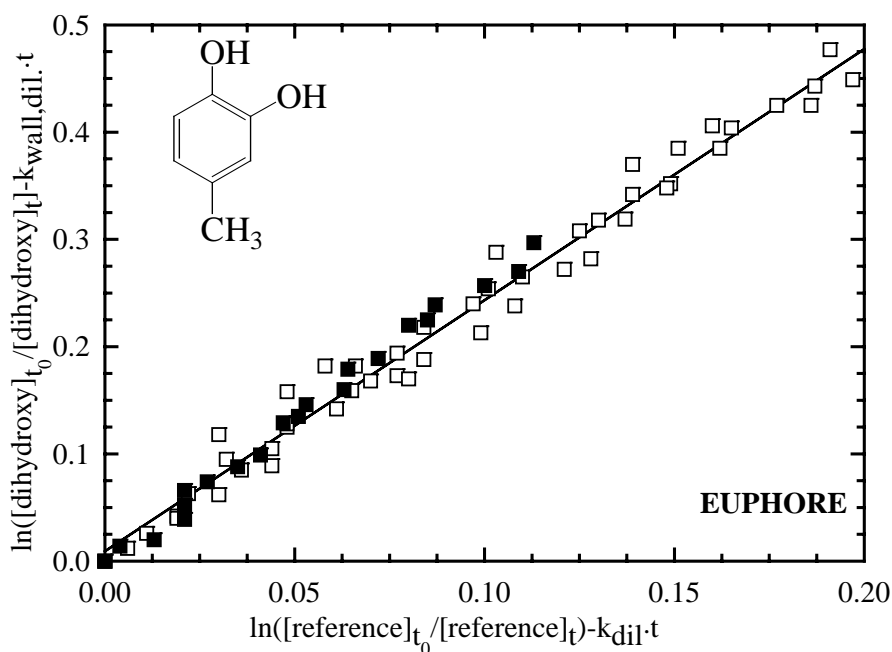


Figure 3.6 Plot of the kinetic data according to equation (2.12) for the reaction of 1,2-dihydroxy-4-methylbenzene with NO_3 radicals measured relative to 2,3-dimethyl-2-butene in the EUPHORE chamber: (\square) low NO_2 ; (\blacksquare) high NO_2 .

The k_1/k_2 ratios determined from the slopes of the straight-line plots in Figures 3.1-3.6 in accord with eq. (2.12) are listed in Table 3.1. The errors quoted in Table 3.1 are a combination of the 2σ statistical errors from the linear regression analysis, the error given for the recommended value of the reference compound in the literature, and the errors arising from the subtraction procedure and from the wall-deposition correction of the reactant. The corrections for wall depositions of the catechols in the Wuppertal chamber experiments were approximately 40% compared to reaction with NO_3 ; in the EUPHORE chamber the corrections for wall and dilution losses were also typically 40% compared to NO_3 reaction.

Good agreement was found between the rate coefficients measured in each of the chambers. The quality of the agreement is demonstrated in Figure 3.7 where the kinetic data obtained for 1,2-dihydroxybenzene in the Wuppertal and EUPHORE chambers are plotted collectively according to eq. (2.12). Since the values of the rate coefficients determined in the two chambers are indistinguishable within the experimental uncertainties, final values $k_1(\text{average})$ are given in Table 3.1, which are the average of the individual measurements, together with error limits, which encompass the extremes of the individual measurements.

In order to increase confidence in the rate coefficients determined for the 1,2-dihydroxybenzenes the reference compound in the EUPHORE chamber was monitored by two different techniques, i.e. in-situ FT-IR and on-line GC-FID. No differences were observed in the rate coefficients determined using these techniques. An example of the measurements using both monitoring techniques is shown in Figure 3.8 for 3-methyl-1,2-dihydroxybenzene.

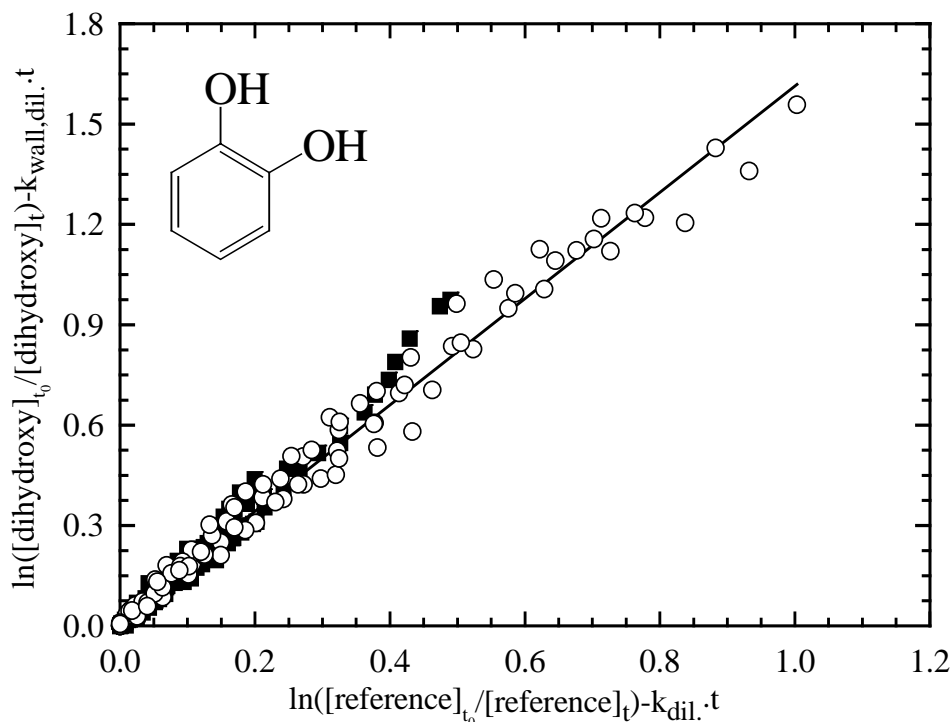


Figure 3.7 Plot of the kinetic data according to equation (2.12) for the reaction of 1,2-dihydroxybenzene with NO_3 radicals measured in the 1080 l quartz glass WUPPERTAL reactor chamber (\circ) and in the EUPHORE chamber (\blacksquare). The reference hydrocarbon is 2,3-dimethyl-2-butene.

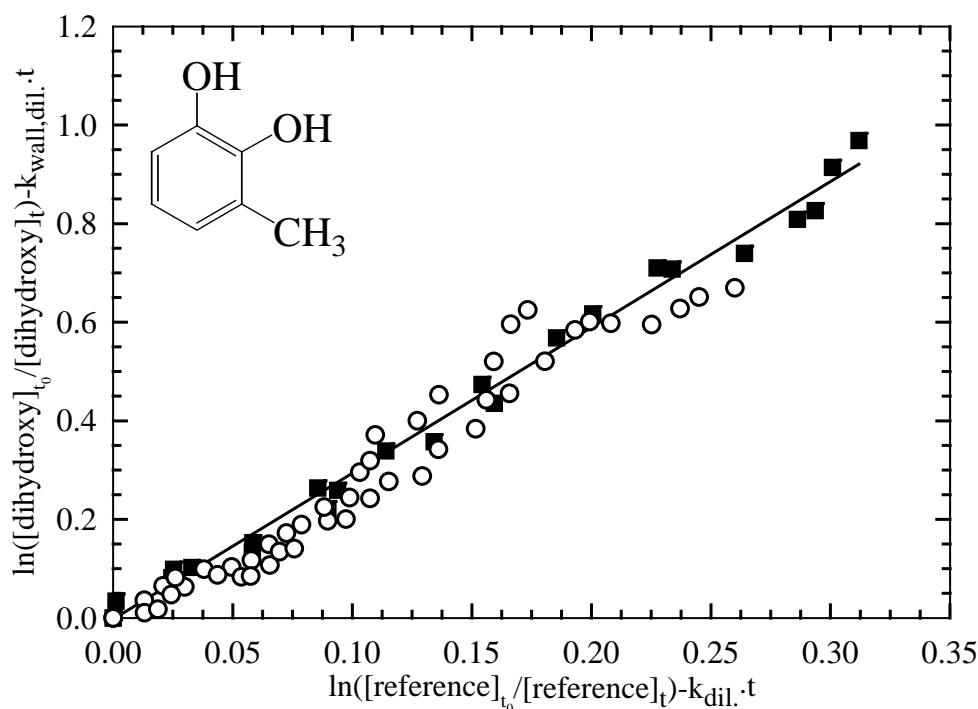
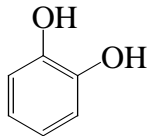
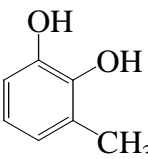
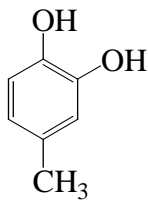


Figure 3.8 Plot of the kinetic data according to equation (2.12) for the reaction of 3-methyl-1,2-dihydroxybenzene with NO_3 radicals measured in the EUPHORE chamber using two different techniques for monitoring the reference: FT-IR (\circ) and GC-FID (\blacksquare). The reference hydrocarbon is 2,3-dimethyl-2-butene.

Table 3.1 Rate coefficients for the reaction of NO₃ radicals with 1,2-dihydroxybenzene, 1,2-dihydroxy-3-methylbenzene and 1,2-dihydroxy-4-methylbenzene.

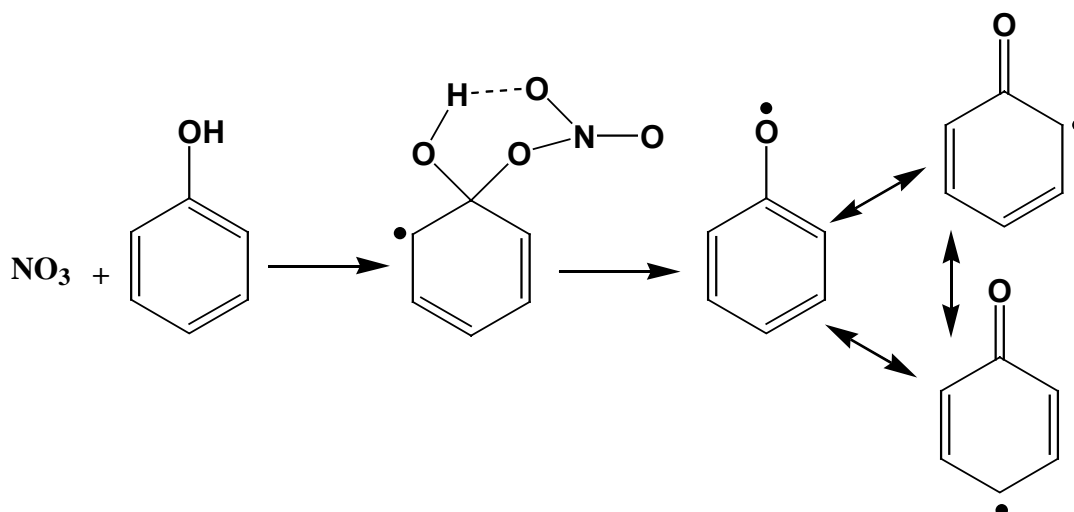
Compound	1080 l reactor		EUPHORE chamber		k ₁ (average) (10 ⁻¹¹ cm ³ s ⁻¹)	τ _i = 1/k _i [NO ₃]
	k ₁ /k ₂	k ₁ (10 ⁻¹¹ cm ³ s ⁻¹)	k ₁ /k ₂	k ₁ (10 ⁻¹¹ cm ³ s ⁻¹)		
 1,2-dihydroxybenzene	1.58±0.07	9.03 ± 3.7	1.88±0.11	10.6 ± 4.3	9.8 ± 5.0	42 s
 1,2-dihydroxy-3-methylbenzene	3.01±0.10	17.3 ± 5.6	2.93±0.06	17.1 ± 4.8	17.2 ± 5.6	24 s
 1,2-dihydroxy-4-methylbenzene	2.80±0.10	16.0 ± 5.2	2.36±0.06	13.4 ± 5.0	14.7 ± 6.5	28 s

3.1.2 Discussion

This study represents the first determination of the rate coefficients for the reaction of NO₃ radicals with 1,2-dihydroxybenzene, 1,2-dihydroxy-4-methylbenzene, and 1,2-dihydroxy-3-methylbenzene. No literature data for comparison are available.

As seen from Table I, the reactivity of the 1,2-dihydroxybenzenes takes the following order: kNO₃ (1,2-dihydroxybenzene) < kNO₃(1,2-dihydroxy-4-methylbenzene) < kNO₃(1,2-dihydroxy-3-methylbenzene). Since the reaction of NO₃ with phenolic compounds is believed to proceed via an overall H-atom abstraction mechanism, which is preceded by an electrophilic addition of NO₃ to the aromatic ring (Calvert *et al.*, 2002), this order is what would be expected from a

consideration of the structures of the compounds. The initial addition step is addition of the NO_3 radical to the ring in the ipso position of one of the hydroxy groups to form a six membered transition state with subsequent elimination of nitric acid, producing a phenoxy radical as shown below (Atkinson, 1991). The electronic structure of the phenoxy radical can be represented as an admixture of three principal resonance structures.



This mechanism explains the faster reactivity of hydroxylated monoaromatic compounds toward NO_3 radicals compared to the corresponding methylated monoaromatic compounds. The faster rate coefficients for the reactions of the methylated 1,2-dihydroxybenzenes compared to 1,2-dihydroxybenzene can be attributed to the positive inductive effect of the methyl group, which increases the electron density at the one of the OH positions.

At present there is no reliable method to quantitatively estimate rate coefficients for the reactions of the NO_3 radical with aromatic hydrocarbons. However, in Figure 3.9 a comparison has been made between the recommended rate coefficients for the reaction of NO_3 radicals with hydroxylated and alkylated monocyclic aromatic compounds at 298 K (Calvert *et al.*, 2002). The rate coefficient for the reaction of NO_3 with 1,2-dihydroxybenzene at 298 K is about a factor of 24 higher than that for phenol [$k_{\text{NO}_3} = (3.8 \pm 0.6) \times 10^{-12} \text{ cm}^3 \text{ s}^{-1}$]. For 1,2-dihydroxy-3-methylbenzene, the measured NO_3 rate constant is factors of 12.3 and 15.6 higher than those for the corresponding reactions of o-cresol [$k_{\text{NO}_3} = (1.43 \pm 0.16) \times 10^{-11} \text{ cm}^3 \text{ s}^{-1}$] and m-cresol [$k_{\text{NO}_3} = (1.1 \pm 0.2) \times 10^{-11} \text{ cm}^3 \text{ s}^{-1}$], respectively. For 1,2-dihydroxy-4-methylbenzene, the rate coefficient is a factor of

14.5 higher than that for m-cresol and p-cresol [$k_{\text{NO}_3} = (1.1 \pm 0.2) \times 10^{-11} \text{ cm}^3 \text{ s}^{-1}$], respectively.

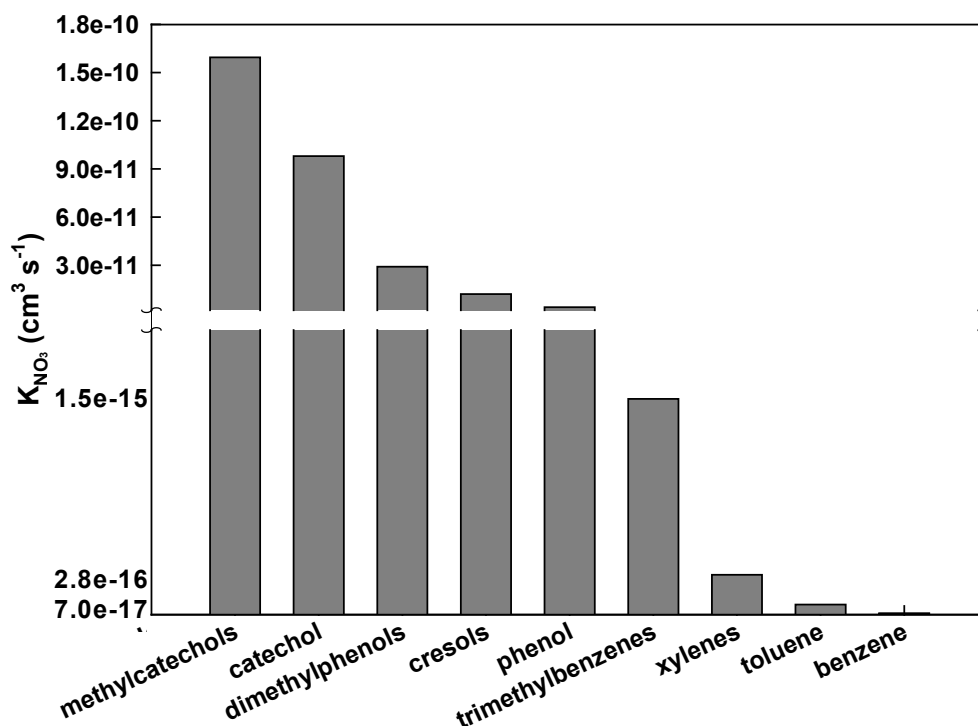


Figure 3.9 Trend of experimental kinetic rate coefficients for the reaction of methylated hydroxyaromatic compounds with NO_3 radicals. For the isomers an average of the rate coefficients has been used. For benzene an upper limit of $k_{\text{NO}_3} = 3 \times 10^{-17} \text{ cm}^3 \text{ s}^{-1}$ has been used.

On average, the addition of the second hydroxyl group to phenol and the cresols to form 1,2-dihydroxybenzenes increases the reactivity of the compounds toward the NO_3 radical by a factor of about 16. The observed differences in reactivity can be ascribed to the activating effect of the hydroxyl groups toward electrophilic reactions and the magnitude of the o- and p-site directing strengths of the substituents. Using the NO_3 rate coefficient database for aromatics as presented pictorially in Figure 3.9, it should now be possible to make reasonable estimates of rate coefficients for the reactions of NO_3 radicals with hydroxymethylated benzenes which have not yet been experimentally determined. For example, the rate coefficients for the reactions of NO_3 with trimethylphenols, which have not yet been measured, will probably be in the range of [$k_{\text{NO}_3} = (3 - 9) \times 10^{-11} \text{ cm}^3 \text{ s}^{-1}$].

3.1.3 Atmospheric implications

1,2-Dihydroxybenzene and its methylated derivatives react rapidly with NO_3 radicals, and this almost certainly constitutes the major nighttime atmospheric sink for these compounds. Using the kinetic data obtained in the present study, in combination with an average nighttime tropospheric nitrate radical concentration of $[\text{NO}_3] = 2.4 \times 10^8 \text{ cm}^{-3}$ (Geyer *et al.*, 2001) an estimation can be made of the atmospheric residence time τ_i of a compound i due to its reaction with NO_3 radicals using the relationship: $\tau_i = (k_i[\text{NO}_3])^{-1}$. The residence times thus obtained are presented in Table 3.1. The 1,2-dihydroxybenzenes will have very short atmospheric lifetimes in the night and, therefore, can influence chemical oxidant formation only on a local scale.

The rate coefficients for the reaction of 1,2-dihydroxybenzene, 1,2-dihydroxy-4-methylbenzene and 1,2-dihydroxy-3-methylbenzene with OH radicals are 1.04×10^{-10} , 2.05×10^{-10} and $1.56 \times 10^{-10} \text{ cm}^3 \text{ s}^{-1}$, respectively (Olariu *et al.*, 2000). Using this kinetic data for OH and the NO_3 kinetic data from the present study, the relative contribution of each species to the degradation of the dihydroxybenzenes during the daytime can be estimated. Based on a daytime average tropospheric OH radical concentration of $1.6 \times 10^6 \text{ cm}^{-3}$ (Crutzen and Zimmermann, 1991; Prinn *et al.*, 1995; Joeckel *et al.*, 2003) and NO_3 radical concentration of $3.1 \times 10^6 \text{ cm}^{-3}$ (Geyer *et al.*, 2001) it can be shown that 1,2-dihydroxybenzene will react during the daytime about 60 % with OH and about 40 % with NO_3 radicals. Therefore, reaction with NO_3 is also an important daytime oxidation processes for these compounds. Finally, an additional important sink for dihydroxybenzene compounds in the atmosphere will be removal by wet and dry deposition. Dihydroxybenzenes are polar molecules with very high Henry's law constants at 25 °C (Mackay *et al.*, 1995) and, therefore, can also be efficiently scavenged by rain and fog droplets.

As mentioned in the results section the mechanism of the reaction of NO_3 with 1,2-dihydroxybenzene and its methylated derivatives is probably initial addition of NO_3 to the ring followed by H-atom abstraction from an OH group.

In preliminary tests the formation of 4-nitrocatechol, which has a very low vapor pressure, has been observed as a primary product. As a comparison, the 4-

nitrophenol has a vapour pressure of 0.27 Torr at 25°C (see <http://www.epa.gov/oppt/chemfact/nitro-sd.pdf>). Therefore, the products from the NO₃-initiated oxidation of 1,2-dihydroxybenzenes (or their further oxidation products) are potentially important precursors for the formation of secondary organic aerosol (SOA). Detailed studies of the oxidation products from the NO₃-initiated oxidation of 1,2-dihydroxybenzenes, particularly with respect to quantification of their SOA formation potential, seem warranted.

3.2 Photolysis rates and kinetics of the reaction of OH radicals with selected nitrocresols

Nitrocresols are secondary products of many atmospheric chemical reactions involving aromatic hydrocarbons and are formed mainly in the urban atmosphere. Very little is presently known about the gas phase atmospheric chemistry of nitrocresols. This work supplies new information on the rate coefficients for the gas phase reactions of the OH radical with nitrocresols. Photolysis rates for the nitrocresols have been determined in the Wuppertal quartz glass reaction chamber from which estimates of the photolysis rates of the compounds under atmospheric conditions have been made.

3.2.1 Results

The experimental kinetic data plotted in Figures 3.10-3.13 according to eq (2.12) were obtained from a minimum of 8 experiments with ethene as the reference hydrocarbon and a minimum of 4 experiments with n-butane as the reference hydrocarbon. The plots show reasonable linearity considering that the reactions are fairly slow and also the difficulties, which arise in the infrared spectral subtraction procedures and the handling of these sticky aromatic hydrocarbons. Table 3.2 lists the rate coefficients extracted from the plots in Figures 3.10-3.13 for the reaction of OH radicals with the four nitrocresols investigated. Rate coefficients of 8.52×10^{-12} and 2.36×10^{-12} (cm³ s⁻¹) were used for the references ethene and n-butane, respectively (Atkinson and Arey, 2003).

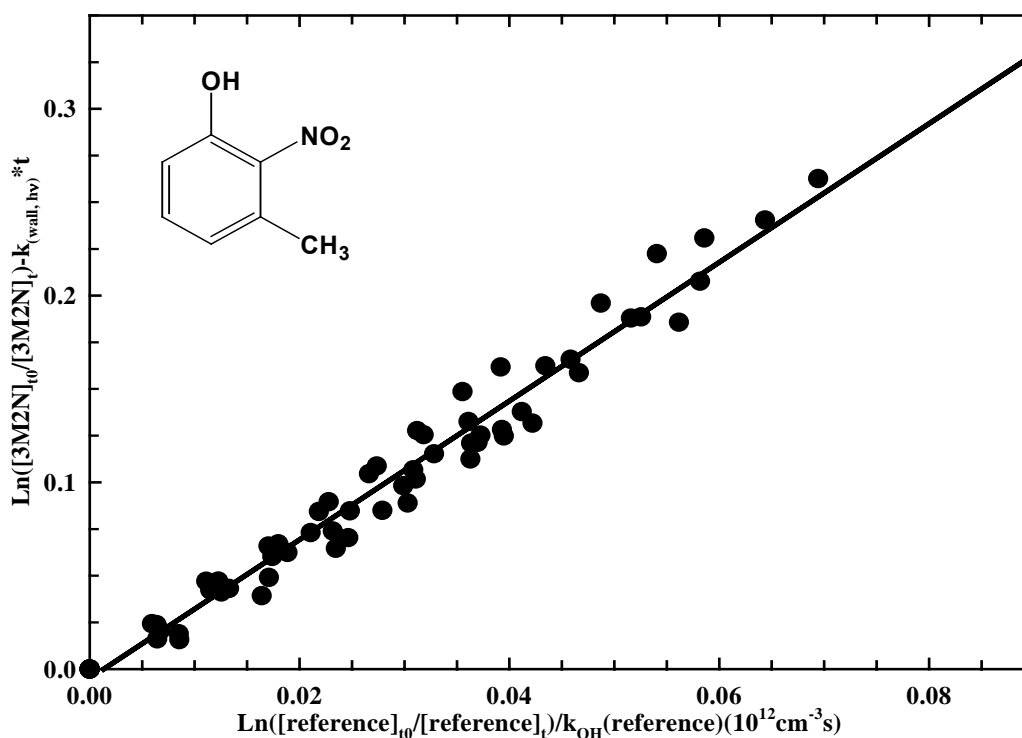


Figure 3.10 Kinetic data plot for the reaction of 3-methyl-2-nitrophenols (3M2N) with OH radicals using (•) ethene as the reference hydrocarbon.

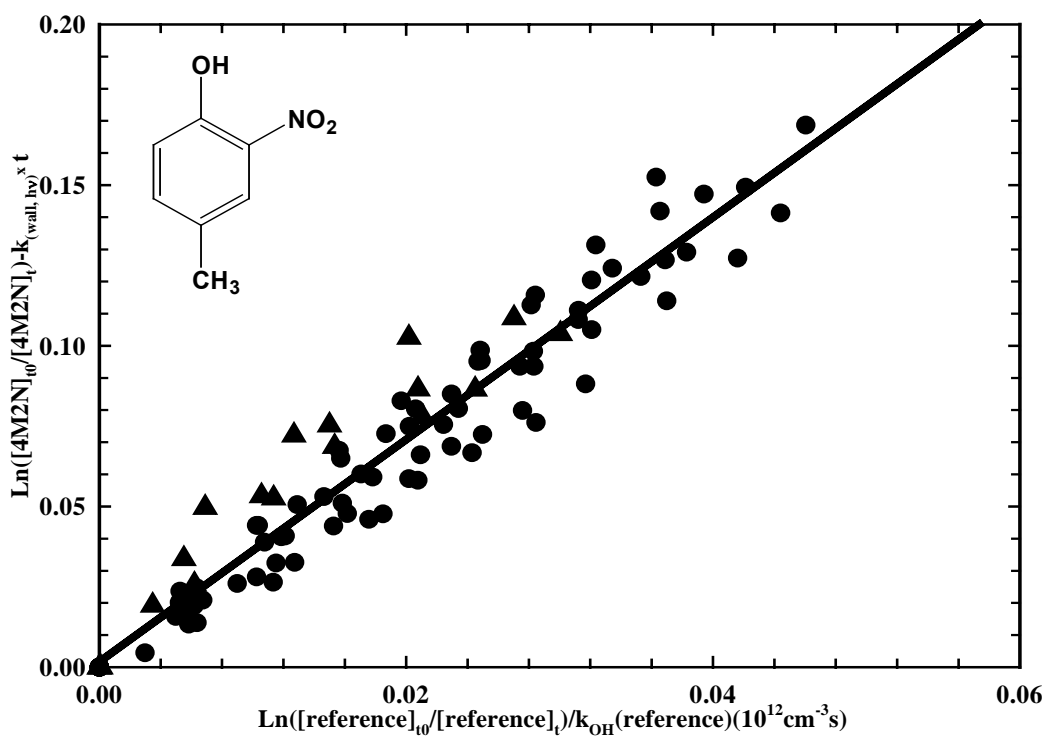


Figure 3.11 Kinetic data plot for the reaction of 4-methyl-2-nitrophenols (4M2N) with OH radicals using (•) ethene and (▲) n-butane as reference hydrocarbons.

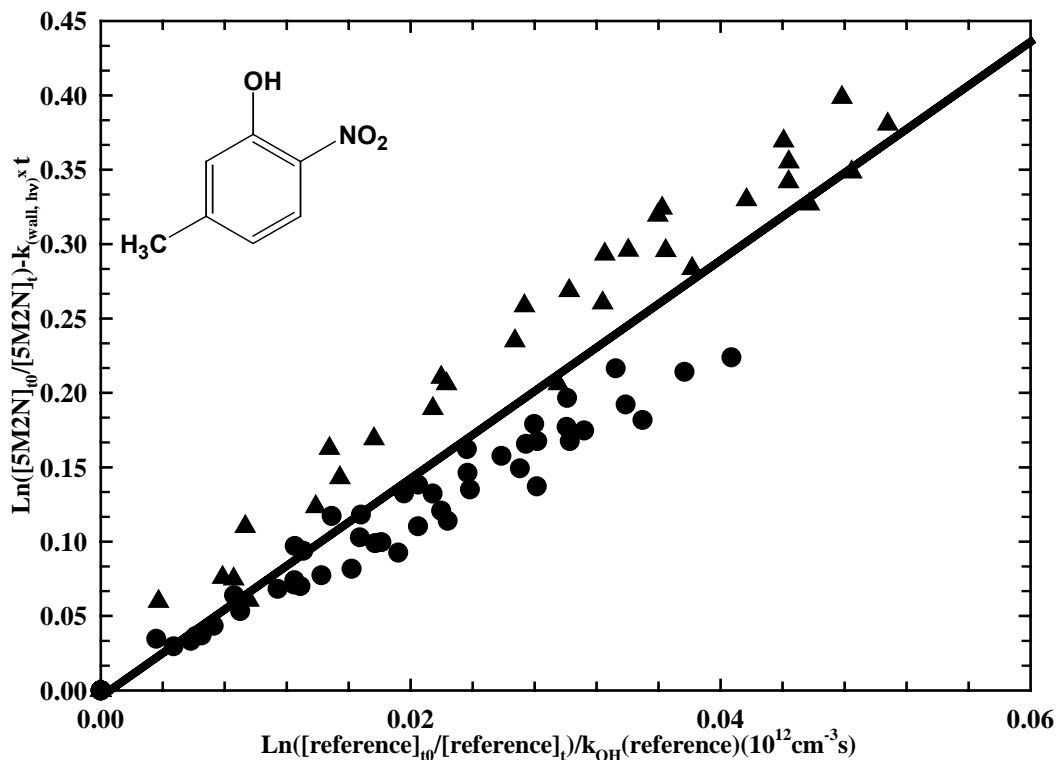


Figure 3.12 Kinetic data plot for the reaction of 5-methyl-2-nitrophenols (5M2N) with OH radicals using (•) ethene and (▲) n-butane as reference hydrocarbons.

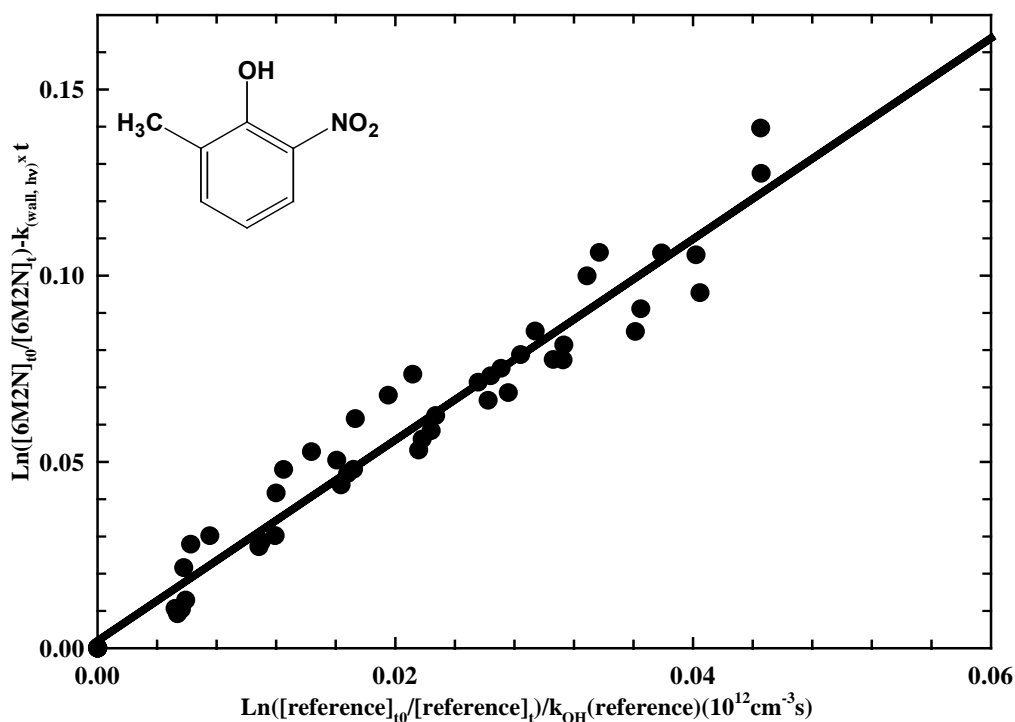
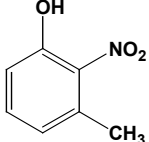
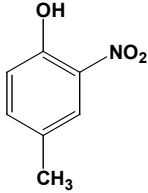
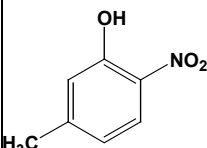
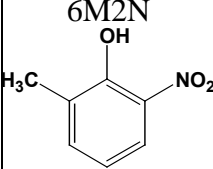


Figure 3.13 Kinetic data plot for the reaction of 6-methyl-2-nitrophenols (6M2N) with OH radicals using (•) ethene as the reference hydrocarbon.

Table 3.2 Rate coefficients for the reactions of OH with four *i*-methyl-2-nitrophenols (*i* = 3, 4, 5, 6).

compound	reference	k_1/k_2	k_1 ($10^{-12}\text{cm}^3\text{s}^{-1}$)	$k(\text{average})$ ($10^{-12}\text{cm}^3\text{s}^{-1}$)	$k(\text{literature})^a$ ($10^{-12}\text{cm}^3\text{s}^{-1}$)
3M2N 	ethene	0.43 ± 0.02	3.69 ± 0.16	3.69 ± 0.16	11.2
4M2N 	ethene	0.41 ± 0.02	3.51 ± 0.17	3.46 ± 0.18	5.38
	n-butane	1.55 ± 0.23	3.66 ± 0.54		
5M2N 	ethene	0.67 ± 0.04	5.71 ± 0.31	7.34 ± 0.52	11.2
	n-butane	1.42 ± 0.67	7.73 ± 0.58		
6M2N 	ethene	0.32 ± 0.02	2.70 ± 0.17	2.70 ± 0.17	-

(a) The literature values are computer estimates based on the structure-activity relationship (Meylan and Howard, 1993).

Photolysis of methylated nitrophenols is a potential source of OH radicals (Bejan *et al.*, 2006) and thus also a potential source of error in the determination of the correction for photolysis in the OH kinetic analysis. To obtain the exact values of the photolysis rates for the compounds it was necessary to perform separate experiments in which the OH radicals were scavenged. Using isoprene as scavenger it was possible to calculate the OH radical concentration and thus calculate the overestimation in the measured photolysis rate due to reaction with OH. The calculated concentrations of OH radicals produced in the photolysis of the various nitrocresols are presented in Table 3.3.

The loss processes (wall deposition and photolysis) make a large contribution of around 50-55% to the measured total loss of most of the compounds investigated. In the case of 5-methyl-2-nitrophenol the contribution was

between 29 - 33%. This lower contribution from photolysis and wall loss to the overall loss for this compound can be explained by the higher reactivity of 5-methyl-2-nitrophenol toward OH radicals compared to the other nitrocresols. The losses due solely to photolysis were approximately 23-27% in all cases.

Table 3.3 Photolysis rates and the steady-state OH radical concentration estimated during the photolysis of all four *i*-methyl-2-nitrophenols (*i* = 3, 4, 5, 6) investigated.

compound	3-methyl-2-nitrophenol	4-methyl-2-nitrophenol	5-methyl-2-nitrophenol	6-methyl-2-nitrophenol
photolysis rate ^(a) (s ⁻¹)	1.67±0.11 x10 ⁻⁴	8.86±1.07x10 ⁻⁵	1.07±0.14x10 ⁻⁴	7.81±1.11x10 ⁻⁵
OH concentration (cm ⁻³)	~3x10 ⁵	~2x10 ⁵	~3x10 ⁵	~2x10 ⁵

(a) Values for the photolysis rate obtained in the 1080 L quartz glass reactor.

3.2.2 Remarks and conclusions

This work represents the first reported experimental kinetic study of the reaction of OH radicals with methylated nitrophenols, therefore, a comparison with other experimentally obtained data is not possible. Because of the difficulties in handling the compounds the measured rate coefficients should be used with caution and require validation using different experimental techniques.

Up to now there has only been a theoretical estimation of the rate coefficients for the atmospheric gas-phase reactions of these compounds with OH radicals (Meylan and Howard, 1993). According to the estimate both 3M2N and 5M2N should have the same rate coefficient of $1.12 \times 10^{-11} \text{ cm}^3 \text{ s}^{-1}$ and 4M2N a value of $5.4 \times 10^{-12} \text{ cm}^3 \text{ s}^{-1}$. The rate coefficient of 6M2N was not estimated. The results of the present work are in disagreement with the estimated values; all of the measured values are lower than the estimates with the differences being factors of 2 and 3 in the cases of 5M2N and 3M2N, respectively.

The measured rate coefficients are higher than those reported for OH + 2-nitrophenol (Atkinson *et al.*, 1992a) and lower than those reported for OH with the cresol isomers (Calvert *et al.*, 2002). This is in line with reactivity expectations. The rate coefficient for all four nitrocresols is around $10^{-12} \text{ cm}^3 \text{ s}^{-1}$, however, the present results appear to indicate an influence of the position of the methyl group on the aromatic ring on the rate coefficient. Based on established chemical activating/deactivating effects for ring substituents (discussed below), the rate for OH + 5M2N would be predicted to have a higher rate than the others, and OH + 6M2N should have the lowest rate coefficient; 3M2N and 4M2N would be expected to have fairly similar rate coefficients.

The reaction of phenolic compounds with OH radicals occurs predominantly by electrophilic addition of OH to the aromatic ring (Atkinson, 2000). NO_2 is a *meta* director because electrophilic attack at the *ortho* and *para* positions generates an especially poor resonance structure and the CH_3 group is an *ortho-para* director. OH has a strong electron donating resonance effect that activates the ring. For all of the four compounds investigated NO_2 and OH are fixed on adjacent positions on the aromatic ring. Thus the position of the CH_3 substituent has a profound affect on the reactivity of the aromatic compounds with OH radicals, as can be seen in Figure 3.14.

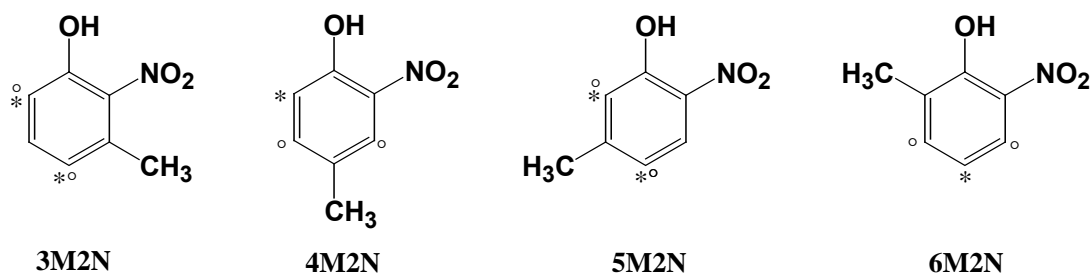


Figure 3.14 The nitrocresol isomers considered in this study and the sites that are activated by the hydroxyl (*) and methyl (°) groups toward electrophilic addition.

The OH and CH_3 entities both donate electron density to the aromatic ring and activate the *ortho* and *para* positions toward electrophilic addition. The

directing + *I* effect of the methyl group is considerably less than the + *E* effect of OH, but nevertheless the CH₃ group still plays an important role. OH activation and NO₂ deactivation effects are in the 4th and 6th positions for all compounds, so additional activation from CH₃ becomes important.

The faster rate coefficient for the reaction of 5M2N compared with those of the other *i*-M2Ns (*i*=3,4,6) can be ascribed to enhanced activation of the 4th and 6th ring positions by both the methyl and OH groups (*ortho*- by CH₃, and both *ortho*- and *para*- by OH).

A similar effect is present in 3M2N, but the + *I* effect of CH₃ is somewhat suppressed by the – *E* effect of the NO₂ group. Within the experimental error limits, the rate coefficients for 4M2N and 6M2N are almost the same. This is expected because the number of possible addition sites for the OH radical is the same for both compounds.

Except for the study of Bardini (2006) the gas phase photolysis of nitrocresols has not received any attention until now. It is not possible to compare directly the photolysis frequencies obtained for the nitrophenols under natural sunlight conditions by Bardini (2006) with those determined in this work using fluorescent lamps. However, except for 6-methyl-2-nitrocresol, which was not studied by Bardini, the trend in the magnitude of J-values measured for the methylated 2-nitrophenols in the indoor photoreactor in Wuppertal is very similar to the trends observed by Bardini in natural sunlight for the same compounds, i.e. the same order of photoreactivity is also observed with 3M2N>5M2M>4M2N~6M2N.

A rough estimate of the magnitude of the photolysis rates for methylated nitrophenols under atmospheric conditions can be made using the values obtained in the experiments with the superactinic lamps. This is accomplished by scaling the values obtained in the reactor and presented in Table 3.3 with a factor comprised of the ratio of the NO₂ photolysis measured in the atmosphere and that measured in the reactor. For example, a factor of $J_{\text{NO}_2}(\text{atmosphere})/J_{\text{NO}_2}(\text{in the reactor}) = (8.5 \pm 0.5) \times 10^{-3} \text{ s}^{-1} / (2.0 \pm 0.2) \times 10^{-3} \text{ s}^{-1} = 4.25$ is obtained when using an atmospheric noontime photolysis frequency of NO₂ typical for clear sky conditions at a latitude of 40° N for July 1 (Klotz *et al.*, 1997).

The photolysis frequencies obtained on scaling the values obtained in the photoreactor to atmospheric conditions are plotted in Figure 3.15 where they are compared with the values measured in the EUPHORE reactor by Bardini (2006).

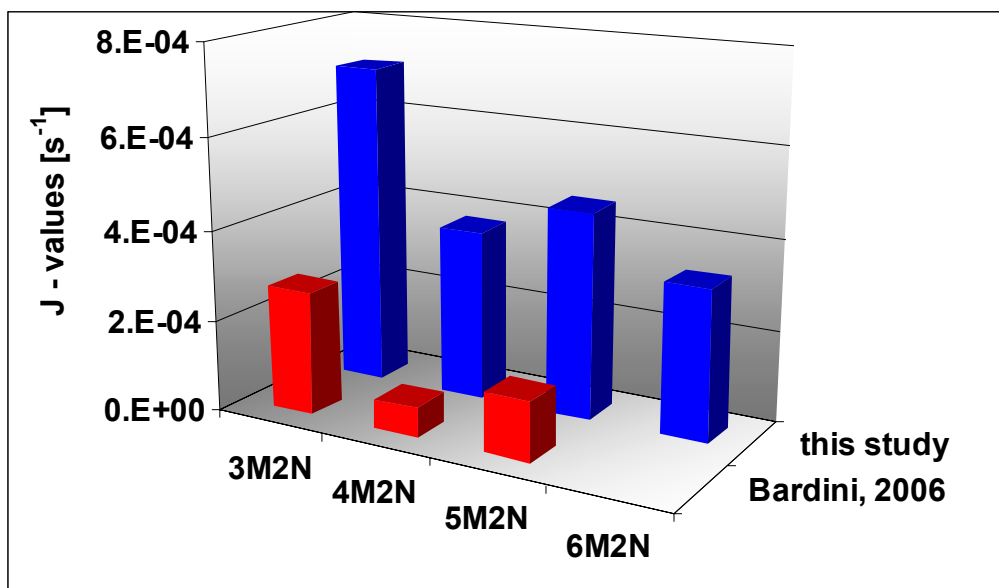


Figure 3.15 Comparison of the J-values measured for the 2-nitrocresols in the photoreactor scaled to atmospheric conditions (see text) with those measured by Bardini (2006) in the outdoor EUPHORE chamber.

The J values measured in the reactor when scaled to atmospheric conditions are significantly larger than the values measured in EUPHORE under natural light conditions by Bardini (2006). This is not too surprising for a number of reasons i) the light distribution in the photoreactor does not truly mimic that of the atmosphere, ii) scaling by using J_{NO_2} values is a rough approximation since the nitrophenol and NO_2 UV spectra are different and iii) the value of $J_{\text{NO}_2}(\text{atmosphere})$ chosen for scaling may be different to that at the time of the measurements of Bardini (2006). Bardini used a value of $J_{\text{NO}_2}(\text{atmosphere}) = 1 \times 10^{-2} \text{ s}^{-1}$.

In recent studies the formation of secondary aerosol formation has been measured during the photolysis of nitrophenols in the reaction chamber (Bejan *et al.*, 2004). The possible influences of aerosols on the kinetic rate have been studied by Sorensen *et al.* (2002). They found no discernable effect of aerosol on the rate of loss of the organic compounds via reaction with OH radicals.

3.2.3 Atmospheric implications

The rate coefficients for the OH radical initiated oxidation of 2-nitrocresols can be used to calculate the tropospheric lifetime of the 2-nitrocresols with respect to reaction with OH radicals. Similarly the scaled photolysis frequencies for the 2-nitrophenols can be used to roughly estimate their tropospheric lifetime with respect to photolysis. The estimated lifetimes of the 2-nitrophenols with respect to photolysis and reaction with OH calculated using the data obtained in this study are presented in Table 3.4. It is clear from Table 3.4 that photolysis will be the dominant gas phase loss process for the 2-nitrocresols even if the scaled photolysis frequencies are significantly overestimated.

Table 3.4 Atmospheric lifetimes of the 2-nitrocresols with respect to photolysis and reaction with OH radicals.

compound	3-methyl-2-nitrophenol	4-methyl-2-nitrophenol	5-methyl-2-nitrophenol	6-methyl-2-nitrophenol
$\tau_{hv}^{(a)}$ (min)	~ 23	~ 44	~ 37	~ 50
$\tau_{OH}^{(b)}$ (h)	~ 47	~ 50	~ 24	~ 64

(a) Calculated using an atmospheric photolysis rate estimated by multiplication of the measured photolysis rate in the photoreactor by a scaling factor (see text).

(b) Daily average OH = $1.6 \times 10^6 \text{ cm}^{-3}$ (Prinn *et al.*, 1995).

Nitrocresols are reactive species, so their overall effective atmospheric lifetime will be determined by a number of atmospheric processes like the kinetic rates of gas phase production and loss, rates of equilibrium partitioning and rates of the reactions in the aqueous phase. The net transfer of a gas into a liquid is the result of a series of processes: gas phase diffusion to the surface, mass accommodation, Henry's law solubility, liquid phase diffusion and liquid phase reaction.

2-Nitrocresols are polar molecules. Unfortunately no Henry's law coefficients are known. For 2-nitrophenol, cresols and phenol at 298 K, the Henry's law coefficients are fairly large with values of 84 M atm^{-1} , 1114 M atm^{-1} , 3174 M atm^{-1} respectively. The Henry's law coefficient value for 2-nitrophenol is known to

increase by a factor 2.1 when the temperature decreases by 10 degrees (Harrison *et al.*, 2002).

A mass accommodation coefficient (α) of 8.3×10^{-4} at 298 K has been measured for 2-nitrophenol by Leysens *et al.* (2005). Using this value results in a calculated accommodation time for 2-nitrophenol of around 10 min. If this calculation is generally applicable to other methylated nitrophenols then mass accommodation is a fast process for this class of compound and could compete with gas phase photolytic losses.

Chapter 4

4. Mechanistic investigations on the photolysis of nitrophenols: A new gas phase source of HONO formation

Mechanistic investigations relevant to the atmospheric degradation of nitrophenols, with regard to the observation of its photolysis products, were carried out using a special photoreactor flow tube system at the Bergische University Wuppertal. Despite the numerous studies on the gas phase atmospheric chemistry of many aromatic hydrocarbons, very little attention has been given to the atmospheric fate of nitrophenols.

Experiments performed in the 6 m quartz glass reactor on the photolysis of nitrophenol have shown the formation of OH radicals. The suggested source of the OH radicals is formation of HONO followed by HONO photolysis leading to OH radicals and NO.

This is the first mechanistic study on the photolysis of nitrophenols leading to HONO formation.

4.1 Results

The gas phase photolysis of nitrophenols was first studied at Wuppertal University in a 6.2 m quartz glass reactor presented in Figure 2.1 in Chapter 2. In

order to prevent interference by possible OH radical formation in the reactor during the photolysis, isoprene was added to scavenge the OH radicals. It is now well established that the photolysis of nitrous acid formed at the chamber walls by reactions of NO₂ can produce OH radicals in environmental chambers (Besemer and Nieboer, 1985; Rohrer *et al.*, 2005, Zador *et al.*, 2006). In the presence of isoprene it was assumed that only photolysis would be responsible for the decay of the nitrophenols. A fast decay of isoprene was observed during the irradiation of the nitrophenols that suggested a source of OH radicals other than heterogenic chemical production on the surface of the chamber.

There have been many studies on surface processes leading to HONO formation (Zhou *et al.*, 2001, 2002a, 2002b; George *et al.*, 2005; Stemmler *et al.*, 2005, 2006), however, the preliminary work in the photoreactor indicated that the HONO formation was mainly a gas phase process. Because of the difficulty in decoupling gas phase from heterogeneous formation processes for HONO in the large quartz glass reaction chamber a flow tube photoreactor has been used in order to reduce the contribution of wall effects to HONO formation (see Chapter 2).

When mixtures of nitrophenols at ppmV levels were irradiated in the flow tube photoreactor an instantaneous formation of HONO at ppbV levels was observed in the gas phase in all cases (see Figure 4.1). HONO formation was not observed in the dark. Using FTIR no significant change in the nitrophenol concentrations upon photolysis could be established. This, however, is due to the low precision of the FTIR measurements. The ratio of $\Delta[\text{Nitro}]/[\text{Nitro}]$ is $\ll 1\%$. The upper limit of the loss of nitrophenols during the irradiation was < 50 ppbV for all the experiments. When the flow tube photoreactor was not thoroughly cleaned between experiments, HONO formation was also observed during the irradiation of the photoreactor flushed with synthetic air only.

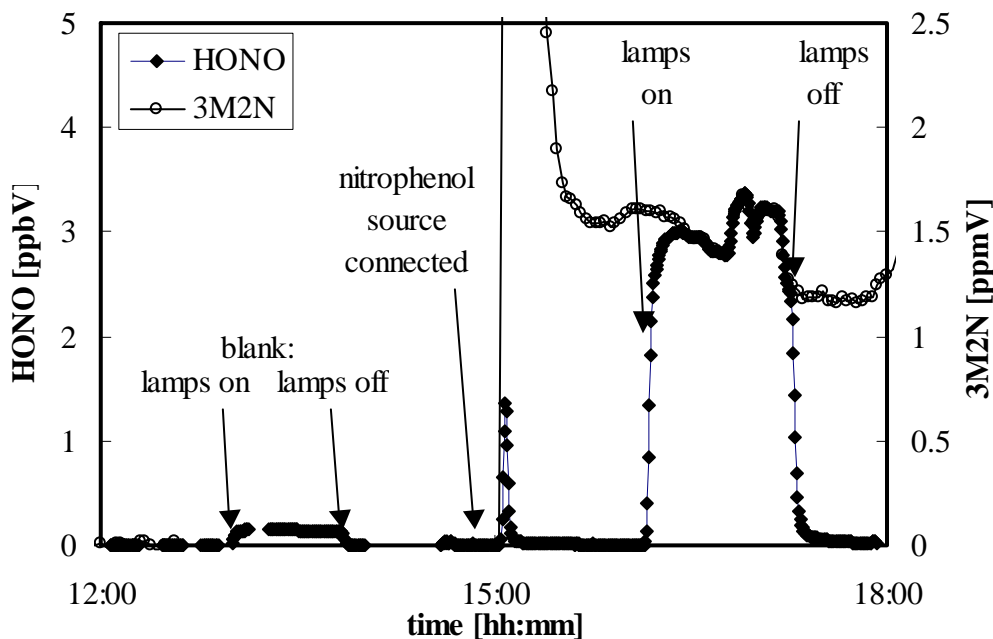


Figure 4.1 HONO formation during the irradiation of the empty flow tube reactor flushed with synthetic air (blank) and during the irradiation of 3M2N in synthetic air ($J_{(\text{NO}_2)} = 0.018 \text{ s}^{-1}$, $t_{\text{reac}} = 27 \text{ s}$).

However, this blank formation was normally significantly lower than the HONO formation observed in the presence of the nitrophenols (see Figure 4.1) and was taken into consideration in the evaluation of the data. The stability of the nitrophenol source varied significantly during the experiments, however, the HONO concentration during irradiation followed perfectly the fluctuations in the nitrophenol concentration (see Figure 4.1).

A linear correlation between the HONO and nitrophenol concentration was observed in separate experiments for all of the nitrophenols investigated. An example of this linear correlation is shown in Figure 4.2 for 3M2N. During the experiments the HONO formed from the photolysis of the nitrophenols can also photolyse. However, HONO loss by photolysis within the reactor is estimated to be $< 5\%$.

ten Brink and Spolestra (1998) have suggested that a dark decay of HONO also occurs. The dark decay is a second order decomposition process in which NO and NO_2 are formed (Chan *et al.*, 1976). However, because of the short reaction time of $< 27 \text{ s}$ in the flow reactor, this process can be totally neglected.

During the photolysis of nitrophenols there is appreciable aerosol formation (Bejan *et al.*, 2004). The effect of aerosols on the HONO decay can, however, be neglected (ten Brink and Spolestra, 1998). Moreover, the very short reaction time is not sufficient to permit an aerosol catalytic effect.

When two flow tube photoreactors with significantly different surface to volume ratios (S/V) and volumes were used, the HONO concentration in the effluent differed significantly between the reactors. The ratio of the HONO yield per ppmV of 3M2N used was a factor of 40 smaller for a 9 mm i.d. photoreactor compared to a 50 mm i.d. photoreactor (see slopes in Figure 4.2). The 40 times lower HONO yield perfectly matched the ratio of the photolysis time of the gas phase in both photoreactors, for which a value of 41 was calculated. In contrast, the ratio of the product $S/V \times t_{\text{reac}}$ changed by only a factor of 7.

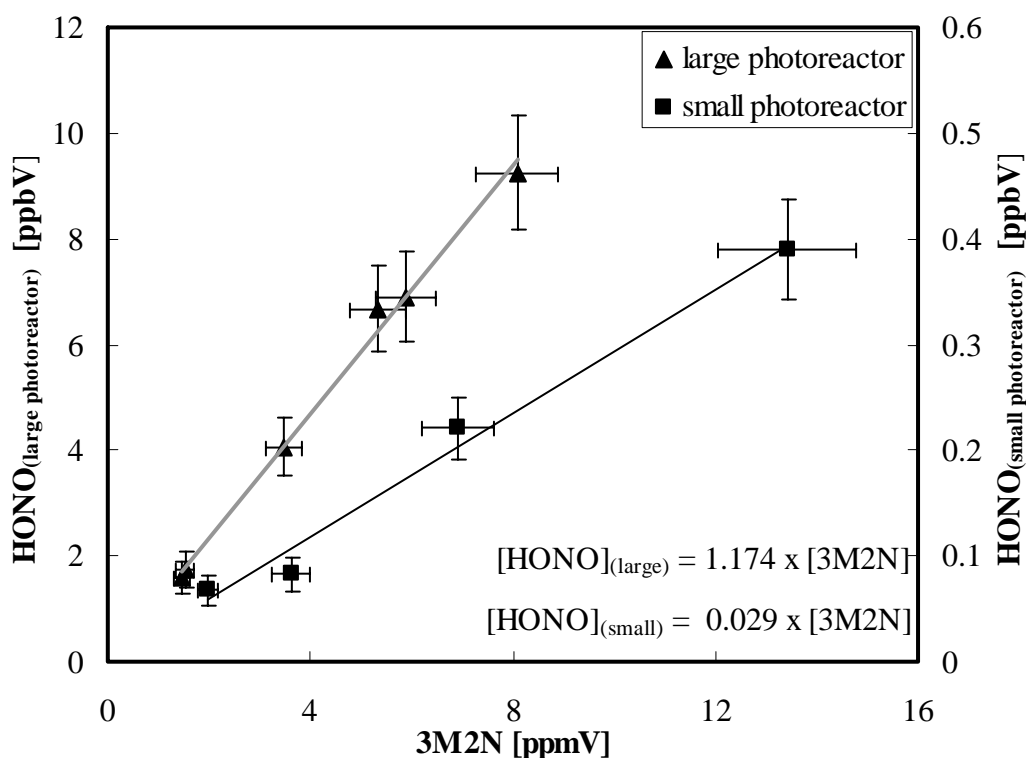


Figure 4.2 HONO formation as a function of the concentration of 3M2N in two different photoreactors ($S/V_{\text{(large)}} = 0.75 \text{ cm}^{-1}$, $t_{\text{reac(large)}} = 26.7 \text{ s}$, $S/V_{\text{(small)}} = 4.44 \text{ cm}^{-1}$, $t_{\text{reac(small)}} = 0.64 \text{ s}$).

The influence of the light intensity on the HONO formation rate during the photolysis of 3M2N was also studied for the large flow tube photoreactor by variation of the number of lamps switched on. A linear correlation between the HONO formation and the number of lamps switched on was observed (see Figure 4.3).

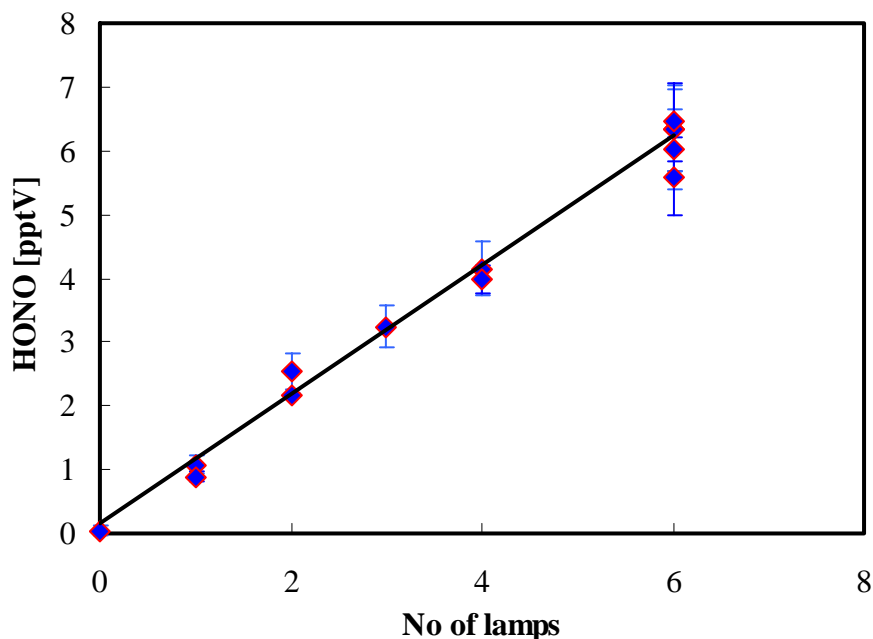


Figure 4.3 HONO formation during the photolysis of 3M2N in the large flow tube photoreactor as a function of the number of operating lamps ($t_{\text{reac}}(\text{large}) = 26.7$ s).

Since NO_2 might have been formed during the irradiation of the nitrophenols and since NO_2 can be photochemically converted into HONO on organic surfaces, (George *et al.*, 2005; Stemmler *et al.*, 2005, 2006) the influence of NO_2 on the HONO formation rate was studied for 3M2N. A significant increase in the HONO formation was observed when NO_2 was added (see Figure 4.4). The additional HONO formation was non-linearly correlated with the initial NO_2 concentration. This is similar to what has been observed in recent studies on organic surfaces (George *et al.*, 2005; Stemmler *et al.*, 2005, 2006).

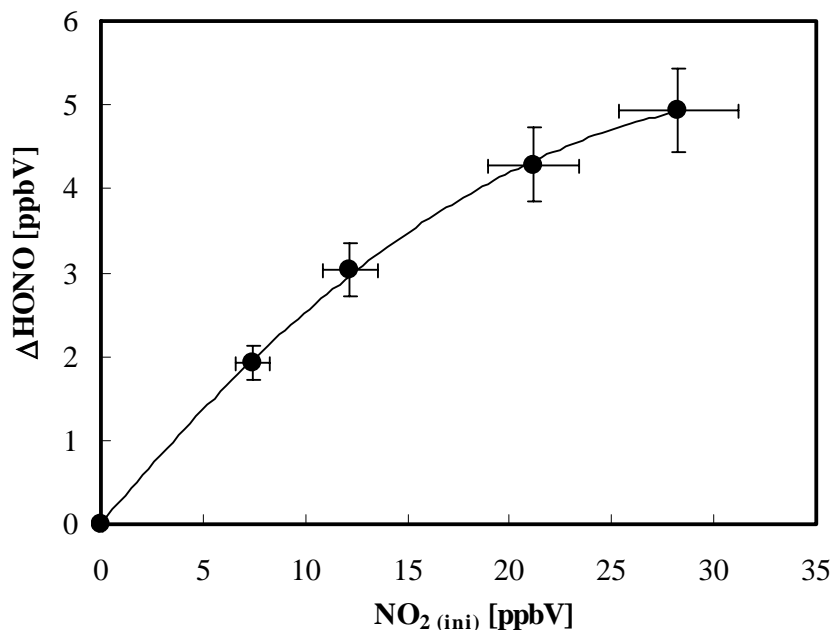


Figure 4.4 Additional HONO formation by NO₂ photochemistry during the irradiation of 3M2N (2.5 ppmV) in the large flow tube photoreactor using 6 lamps as a function of the initial NO₂ concentration ($t_{\text{reac}} = 26.7$ s, $J_{(\text{NO}_2)} = 0.018$ s⁻¹). The photolytic HONO formation in the absence of NO₂ was ~3 ppbV.

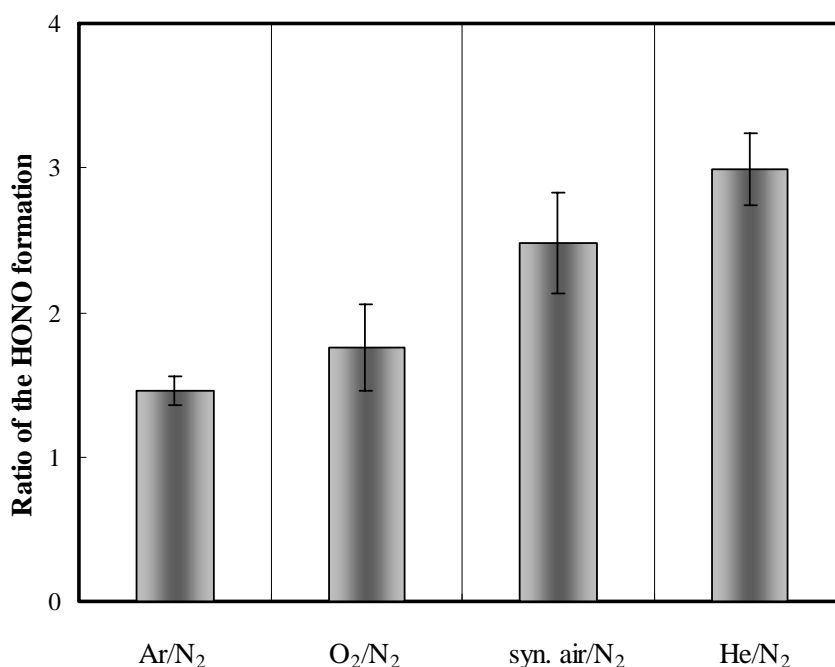


Figure 4.5 Ratio of the HONO formation during the irradiation of 3M2N in a certain buffer gas to the formation in pure nitrogen normalized to the same concentration of 3M2N. Purity of buffer gas were N₂ (99.999 and 99.9999), O₂ (99.999), Ar (99.999) or He (99.9999).

Only an upper limit of ≤ 0.14 ppbV NO_2 could be estimated for the NO_2 formation during the irradiation of pure 3M2N mixtures (2.5 ppmV). The photolysis of any NO_2 that might have been formed in the photoreactor was taken into consideration for the calculation of this upper limit. These observations strongly support that only a small fraction of the observed HONO yield during the irradiation of pure nitrophenol mixtures occurs by mechanisms involving NO_2 .

The influence of the buffer gas on the HONO formation rate was also investigated for the photolysis of 3M2N. As can be clearly seen in Figure 4.5, the nature of the buffer gas had an impact on the HONO formation. Compared to pure nitrogen (99.999% or 99.9999%), the HONO yield increased by factors of 1.5, 1.8, 2.5 and 3.0 in Ar, O_2 , synthetic air and He, respectively.

Figure 4.6 shows the photolysis of the other nitrophenols studied in this work, 2NP, 4M2N and 5M2N, as a function of the concentration of the nitrophenols in synthetic air. For all of the compounds a linear dependency between HONO formation and the nitrophenol concentration was observed. 2NP, 4M2N and 5M2N were photolysed with all 6 lamps at a reaction time of 26.7 s in the large flow tube reactor. $J_{(\text{NO}_2)}$ in the reactor was 0.0184 s^{-1} . Figure 4.7 shows the variation of the concentration of HONO formation for the different ortho-nitrophenols.

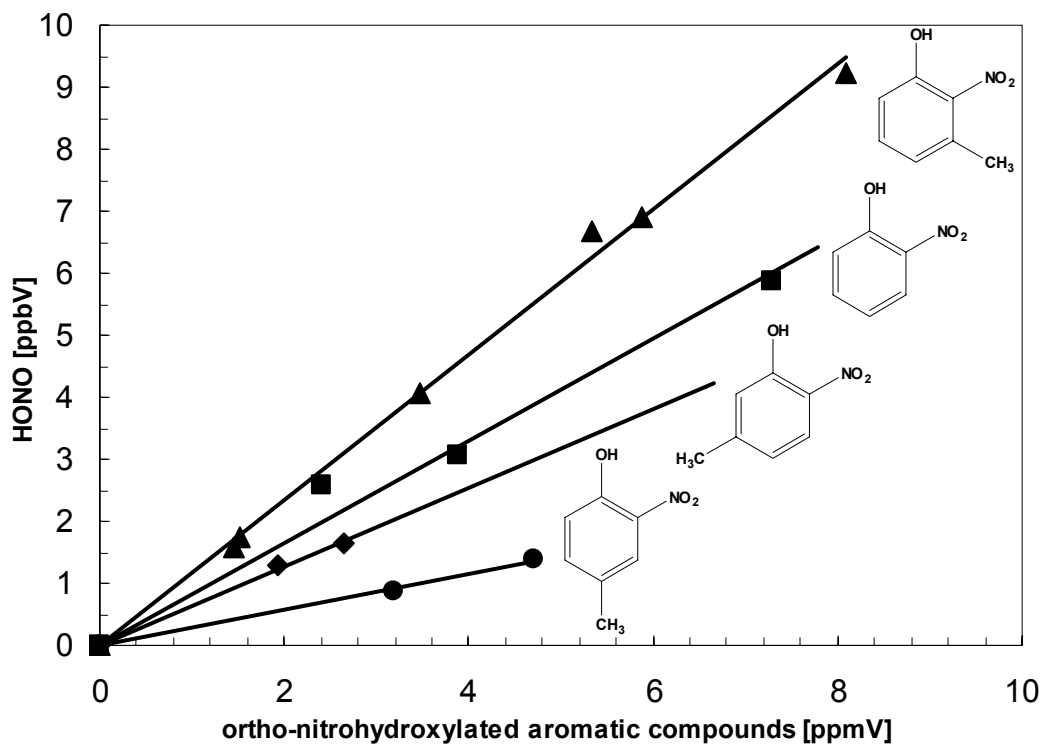


Figure 4.6 HONO formation as a function of the concentration of the ortho-nitrohydroxylated monoaromatic compounds.

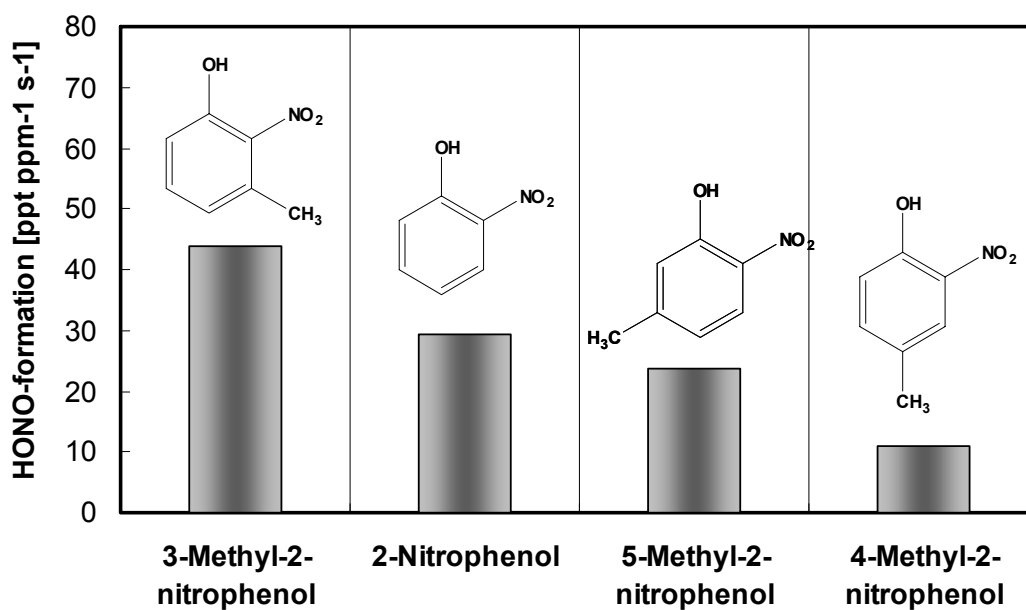


Figure 4.7 HONO formation rate (ppt ppm⁻¹ s⁻¹) from the different ortho-nitrohydroxylated monoaromatic compounds.

The formation of HONO from the different nitrophenols can be quantitatively related to the photolysis frequency of the nitrophenol by,

$$J(\text{nitrophenol} \rightarrow \text{HONO}) = \frac{1}{[\text{nitrophenol}]} \times \frac{\Delta[\text{HONO}]}{\Delta t} \quad 4.1$$

The results are listed in Table 4.1. From the measured photolysis frequency of 3M2N a quantum yield $\phi(3\text{M2N} \rightarrow \text{HONO})$ has been estimated using equation 4.2 under the assumption that this quantity is independent of wavelength (Finlayson-Pitts, 2000).

$$J = \int \sigma(\lambda) \times \phi(\lambda) \times F(\lambda) d\lambda \quad 4.2$$

A value of $\phi(3\text{M2N} \rightarrow \text{HONO}) \approx 1.5 \times 10^{-4}$ was calculated using the equation 4.2 and based on the actinic flux spectrum from the reactor and an absorption spectrum of 3M2N obtained in liquid dichloromethane (see Figure 4.8). Since the absorption cross section of 3M2N is unknown for the gas phase, it was assumed that the cross sections for the gas and liquid phases are similar. The UV absorption spectrum of 3-methyl-2-nitrophenol shows three distinct absorption bands. The first two bands at $\sim 200\text{-}250$ nm and $270\text{-}330$ correspond to $\pi - \pi^*$ electronic transitions within the aromatic ring. The broad absorption band at $350\text{-}440$ nm is due to an $n - \pi^*$ electronic transition within the NO_2 chromophore (Silverstein *et al.*, 2005). Bardini (2006) has also studied the bathochromic effect of solvent. No significant shift in the absorption bands in the UV spectra of the nitrophenols was observed when using acetonitrile, methanol or 1-propanol as the solvent.

For further verification of the mechanism, the photolysis of different 3- and 4-nitrophenols was attempted. However, because of the much lower vapour pressures of these compounds they could not be detected by FTIR, i.e. the vapour pressure at the temperature of the experimental set-up (room temperature) was much lower than the detection limit of the FTIR.

Table 4.1 Photolysis frequency, $J(\text{nitrophenol} \rightarrow \text{HONO})$, of HONO formation for different nitrophenols in the flow tube photoreactor under conditions with $J_{(\text{NO}_2)} = 0.018 \text{ s}^{-1}$ in synthetic air (errors: 2σ)

Compound	$J(\text{nitrophenol} \rightarrow \text{HONO})/10^{-5} \text{ s}^{-1}$
3M2N	4.4 ± 0.3
2NP	2.9 ± 0.6
5M2N	2.4 ± 0.3
4M2N	1.1 ± 0.1

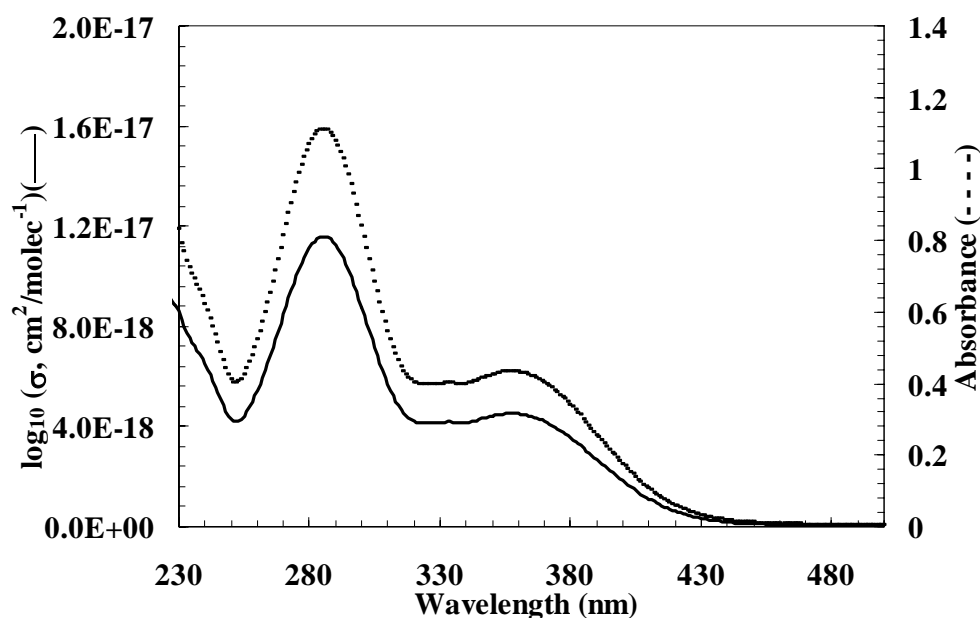


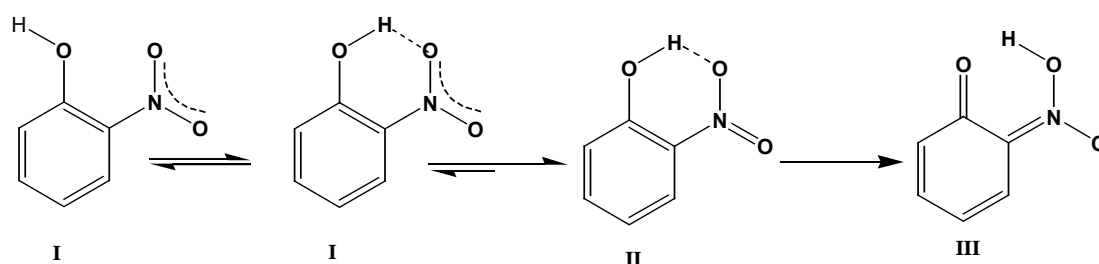
Figure 4.8 Plot of the cross section (base 10) for 3M2N measured in dichloromethane solvent.

4.2 Discussion

4.2.1 Internal rotation proton transfer between OH and NO₂ groups positioned ortho to one another

The properties of 2-nitrophenol (OH and NO₂ groups positioned ortho to each other, structure I) and its methylated analogues are significantly different compared to those of the 3- and 4-nitrophenols, i.e. the melting points of the 3- and 4-nitrophenols are higher, the vapour pressures of 3- and 4-nitrophenols are 1000

times lower, and there are marked differences in the infrared absorption spectra (see Figure 4.9). The equilibrium between the *cis* and *trans* isomers in structure I is strongly shifted to the *cis* isomer (Schreiber, 1989). The differences in physical properties are caused by strong intramolecular hydrogen bonding in the 2-nitrophenols as shown in structure II; the effect of “chelation” on physical properties is well known (Baitinger *et al.*, 1964; Leavel and Curl, 1973; Schreiber, 1989; Borisenko *et al.*, 1994; Borisenko and Hargittai, 1996; Chen *et al.*, 1998; Kovacs *et al.*, 1998, 2000).



In infrared spectroscopy evidence of “chelation” is based on the absence of the characteristic OH absorption infrared peak around 3650 cm^{-1} in phenols with an *ortho* nitro group (see Figure 4.9). For 2-nitrophenols the frequency of the OH stretching band is decreased by 400 cm^{-1} compared to other phenols while that of the OH torsion is increased by 380 cm^{-1} (Kovacs *et al.*, 1998). Due to the constraining effect of the intramolecular hydrogen bonding, the NO_2 torsional frequency is also increased with respect to that of nitrobenzene.

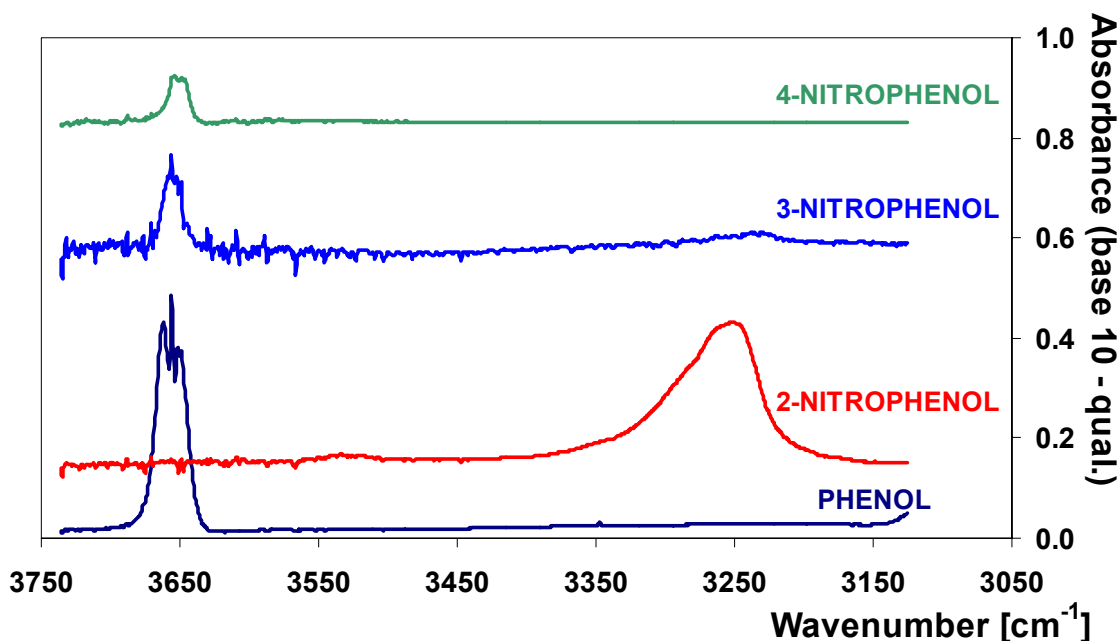


Figure 4.9 Infrared spectroscopic evidence of intramolecular hydrogen bonding in 2-nitrophenol.

The hydrogen bond can be considered the first step in a proton transfer process, leading to a nitronic acid structure III (Chen *et al.*, 1998; Chen and Chieh, 2003). For the nitronic acid structure III arising from nitrobenzene, dissociation leading to the formation of HONO has been predicted for the gas phase on the basis of theoretical calculations (Polasek *et al.*, 2001). Thus, photo-dissociation of 2-nitrophenol and its methylated derivatives via structure III and formation of HONO in the gas phase might also be possible, as has been observed in the liquid phase (Ishag and Moseley, 1977; Alif *et al.*, 1991; Bing *et al.*, 2005). To date, no observations of nitrous acid formation from the gas phase photolysis of nitrophenols have been reported in the literature.

4.2.2 Gas-phase process or surface chemistry?

As shown in the Results section, the instantaneous HONO formation observed during the photolysis of several nitrophenols was linearly correlated with the light intensity in the photoreactor (Figure 4.3), the concentration of the nitrophenols (Figures 4.2 and 4.6), and the photolysis time. However, the HONO formation was found to be independent of the S/V ratio of the reactor, see Figure 4.2. These observations all support that a gas phase process is forming HONO. In

the case of a heterogeneous reaction source a dependence on S/V would be expected. In addition, the perfect correlation of the HONO formation with the concentration of the nitrophenols, even for rapid concentration changes (Figure 4.1), would not be expected for a surface process, where adsorption of the nitrophenols on the surface would lead to a measurable delay between the nitrophenol concentration changes and the HONO concentration.

4.2.3 Can impurities be responsible for HONO formation?

Due to the low estimated quantum yield of $\sim 10^{-4}$ and purities of the different nitrophenols of only 97–99%, HONO formation might also result from the photolysis of nitrogen-containing impurities with a two orders of magnitude higher photolysis frequency than those of the nitrophenols. However, a linear concentration dependency was observed for all of the nitrophenols investigated (see Figure 4.6). Since the concentration of the nitrophenols was varied by changing the temperature of the nitrophenol source, impurities can only explain the observed HONO formation if the temperature dependencies of the vapour pressures of the hypothetical impurities are similar to those of the different nitrophenols investigated. In addition, during the experiments the physical state of the samples changed between liquid and solid, depending on the temperature of the nitrophenol source, without affecting the HONO yield. In experiments in which 3M2N with a higher purity (99% instead of 98%) was used, no effect on the photolysis frequency $J(\text{nitrophenol} \rightarrow \text{HONO})$ was observed.

A further indication that impurities are unimportant is given by the time dependence of the HONO formation during the blank experiments (see Figure 4.1). The HONO formation in these experiments was attributed to the photolysis of adsorbed nitrophenols on the walls, since in blank experiments, in which the photoreactor was cleaned prior to the experiment, significantly lower HONO formation was observed. If impurities of $\sim 2\%$ caused the HONO formation in the experiment with 3M2N shown in Figure 4.1, the photolysis frequency of the impurities should have been $\sim 2 \times 10^{-3} \text{ s}^{-1}$ (50 times higher than the value for 3M2N, see Table 4.1) leading to a lifetime of only ~ 8 min for the impurities on the reactor walls. During the blank experiment shown in Figure 4.1 the reactor was irradiated for 45 min, which would thus result in an almost complete destruction of the

impurities. However, the HONO formation only decreased from 0.15 to 0.13 ppbV (see Figure 4.1), which is attributed to the decrease of the amount of adsorbed 3M2N by desorption from the walls. In conclusion, HONO formation in the experiments by the photolysis of impurities is improbable.

4.2.4 Is the HONO originating from a mechanism involving NO₂?

Recently, photolytic HONO formation was observed during the heterogeneous reaction of NO₂ with phenolic hydrocarbons (George *et al.*, 2005; Stemmler *et al.*, 2005, 2006). This was also observed in the present study when NO₂ was added to the nitrophenols under irradiation (see Figure 4.4). However, in the present investigation, during the photolysis of pure nitrophenol–bath gas mixtures no NO₂ formation was observed. Thus, from the upper limit of the NO₂ yield of ≤ 0.14 ppbV for a concentration of 3M2N of 2.5 ppmV in the large photoreactor, and from the observed NO₂ dependence in the case of 3M2N (see Figure 4.4) the contribution of HONO formation by reactions involving NO₂ is estimated to be $< 3\%$. Accordingly, the contribution to the formation of HONO by photolytic NO₂ reactions during the photolysis of pure nitrophenols should be negligible. This conclusion is also supported by the gas phase nature of the process observed (see above). In contrast, for the photolytic HONO formation by NO₂ reactions in the presence of phenolic compounds, a surface process has been proposed (George *et al.*, 2005; Stemmler *et al.*, 2005, 2006).

4.2.5 Mechanistic investigations

The linear dependence of the HONO formation on the concentration of the nitrophenols (see Figures 4.2 and 4.6) also excludes an intermolecular reaction between two nitrophenol molecules, for which a quadratic concentration dependency would be expected. Instead, an elimination of HONO from the nitronic acid structure **III**, formed by photoexcitation of structure **II** of 2-nitrophenol, is proposed. In the study of Chen *et al.* (1998), structure **III** was proposed as a thermal decomposition product of 2-nitrophenol and it appears to be feasible that it is also formed by photoexcitation. In addition, abstraction of HONO was calculated to be energetically possible from a similar nitronic acid structure **III** of nitrobenzene (Polasek *et al.*, 2001) and might also explain the HONO formation in the gas phase

observed in the present study for the photolysis of nitrophenols. HONO formation has also been observed during the photolysis of 2-nitrophenol in the liquid phase (Ishag and Moseley, 1977; Alif *et al.*, 1991; Bing *et al.*, 2005) and was explained, at least in part, by the elimination of HONO leading to an organic biradical (Alif *et al.*, 1991).

In a recent article, Nagaya *et al.*, (2006) have studied in detail the intramolecular hydrogen bond between the OH and NO₂ groups in the 2-nitrophenol molecule. They identified the conformation of the aci-nitro isomer of 2-nitrophenol and examined the photoreaction mechanism with the aid of DFT and time-dependent DFT calculations. Nagaya *et al.* (2006) confirmed the existence of the unstable intermediate proposed in this work.

To obtain further insight into the mechanism leading to HONO formation upon photolysis, the influence of the buffer gas was studied. From the different experiments in the absence of oxygen the following trend in the HONO yield was observed: HONO(He)>HONO(Ar)>HONO(N₂) (see Figure 4.5). From this observation it is concluded that HONO formation is caused, at least in part, by a sequence of reactions involving a photoinduced intramolecular H atom transfer to form a primary excited state III**, followed by energy transfer to form an excited state, structure III*, with subsequent elimination of HONO, i.e. reactions (a), (c) and (d) in the mechanism shown in Figure 4.10. To explain the observed buffer gas dependency of the HONO yield it is proposed that the excited state III** can be additionally quenched by the buffer gas, the effectiveness of which will depend on the nature of the quenching gas being used, see reaction (b).

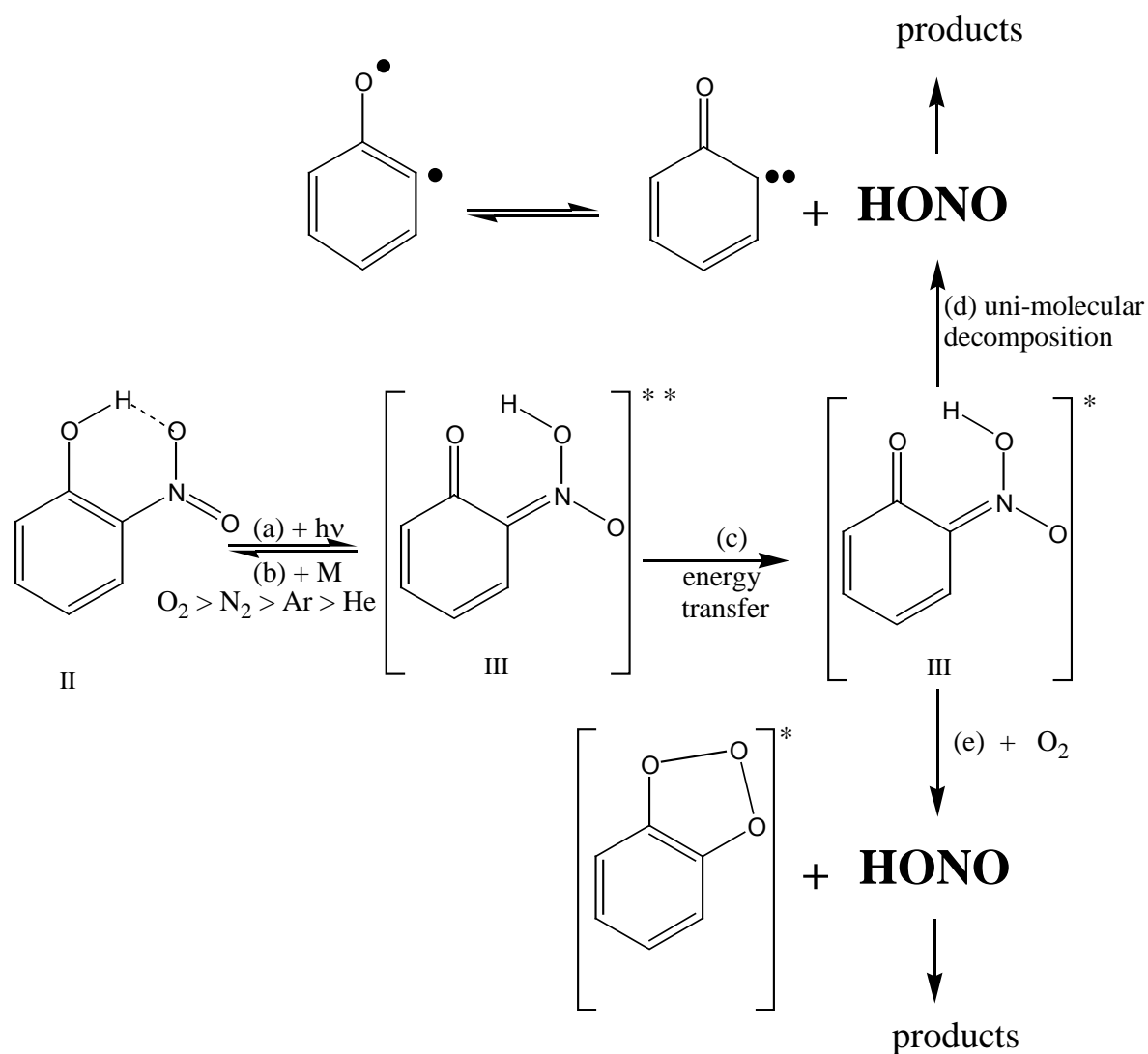


Figure 4.10 Reaction mechanism proposed to explain HONO formation during the photolysis of 2-nitrophenol in the gas phase.

For the liquid phase, the formation of a biradical leading to the formation of a ketene was proposed to explain HONO formation during the irradiation of 2-nitrophenols (Alif *et al.*, 1991) and might also be a co-product of HONO during the gas phase photolysis, see Figure 4.11.

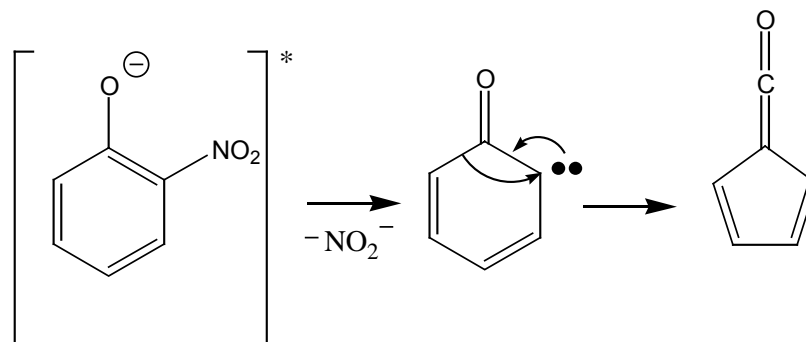


Figure 4.11 Formation of cyclopentadiene ketene from the phototransformation of 2-nitrophenol in aqueous solution (Alif *et al.*, 1991)

The proposed reactions (a)–(d) cannot, however, explain the observations in the presence of oxygen, for which a similar or even lower HONO formation compared to nitrogen would be expected, since oxygen is known to be an efficient quencher. However, O_2 can potentially serve as both a quencher in the reactions and a reactant in bimolecular steps, depending on the electronic structure of the reactants and products (Pilling and Seakins, 1995). In the present experiments, the HONO yields in synthetic air and pure oxygen were significantly higher than that obtained in pure nitrogen (see Figure 4.5). Thus, in order to explain this anomaly, a further reaction is proposed, in which HONO is formed in a reaction of oxygen with the excited state III^* , i.e. reaction (e) in the mechanism shown in Figure 4.10. With this additional process the decrease in HONO formation observed on switching from synthetic air to pure oxygen (see Figure 4.5) can be explained. For relatively low oxygen concentrations (synthetic air) the concentrations of III^{**} and III^* are still high and reaction (e) will lead to a high HONO yield. When the oxygen concentration is further increased (100% O_2) the concentrations of III^{**} and III^* will significantly decrease, due to efficient quenching of III^{**} , reaction (b), so reaction (e) will become less important. Although the mechanism explains the observations reasonably well, it should be remembered that it is only based on the observed HONO yield. None of the other reaction products, e.g., the proposed ketene, (Alif *et al.*, 1991) were detected with the FTIR spectrometer. The mechanism is still highly speculative and needs to be validated by additional product and spectroscopic studies, and theoretical calculations.

As reported by Bejan *et al.*, (2004) and described in detail in Chapter 5 the instantaneous formation of submicron particles has been observed during the

photolysis of nitrophenols. Based on the mechanism proposed in this study, the formation of particles from the photolysis of nitrophenols is not unexpected. For example, the proposed biradical, reaction (**d**) in mechanism from Figure 4.10, will most probably undergo further reactions such as isomerisation, leading to the formation of acids (Alif *et al.*, 1991) or reactions with nitrophenols, probably generating higher molecular species with vapour pressures low enough to generate particles. Detailed product studies will be necessary in order to explain the observed formation of particles during the photolysis of nitrophenols.

Although in most experiments 3M2N was used, the photolytically induced HONO formation from other nitrophenols was also investigated. Although not as efficient as 3M2N, HONO formation was observed for all of the ortho-nitrophenol compounds investigated (see Figure 4.6). Thus, it is to be expected that higher molecular ortho-nitrophenols, such as nitro-PAH derivatives and also polynitrophenols and polyhydroxy-nitroaromatics will also form HONO during photolysis.

Using *ab initio* and DFT studies (density functional theory) a photoinduced hydrogen transfer leading to the nitronic acid structure **III** was also recently proposed for 2-nitrotoluene (Il'ichev and Wirz, 2000). Thus, it is possible that nitroaromatic compounds with even weaker hydrogen donors than the phenolic OH group in the ortho-position to the nitro group might form HONO during irradiation. This opens a field for further studies on photoinduced HONO formation from a wide variety of nitroaromatic hydrocarbons.

4.3 Atmospheric implications

In order to make a rough estimate of the homogeneous HONO formation rate upon photolysis of ortho-nitrophenols in the atmosphere, a concentration of 1 ppbV for these compounds has been assumed, which is taken as being representative of urban conditions. Recently, gas phase mixing ratios of ~60 pptV of ortho-nitrophenol were measured at an urban site (Harrison *et al.*, 2005). Since photolytic HONO formation is expected for all phenolic aromatic hydrocarbons with a nitro group in an ortho-position to the OH group, including higher molecular nitro-PAHs, polynitro- and polyhydroxy-aromatics, an upper limit for the mixing ratio of 1 ppbV is considered reasonable for the total collective concentration of all these

compounds present in the urban troposphere. In addition, as speculated above, other classes of nitroaromatics might also form HONO upon photolysis.

Since a linear dependence of the HONO yield on the nitrophenol concentration was observed, the results obtained here have been extrapolated linearly to atmospheric concentrations. However, it should be borne in mind that the experiments were performed in the ppmV range and thus the extrapolation to atmospheric conditions needs to be verified by experiments using much lower concentrations of the nitrophenols.

A linear dependence of the HONO yield on the light intensity (i.e., the number of lamps switched on) and on measured $J_{(\text{NO}_2)}$ was observed for a spectral range of 300–500 nm ($\lambda_{\text{max}} = 370$ nm) within the reactor. Because the wavelength dependency of the process was not studied, a direct extrapolation of the results to atmospheric conditions is uncertain. However, since (i) the nitrophenols studied absorb in the spectral range of the lamps used, (ii) the NO_2 photolysis is most efficient at wavelengths <400 nm, and (iii) the lower spectral limit of the lamps is comparable to atmospheric conditions, the measured ratio $J(3\text{M}2\text{N} \rightarrow \text{HONO})/J_{(\text{NO}_2)}$ was used to estimate the photolytic HONO formation under atmospheric conditions. Calculations using actinic flux spectra from the atmosphere indeed show that the ratio $J(3\text{M}2\text{N} \rightarrow \text{HONO})/J_{(\text{NO}_2)}$ is similar to the photo-reactor conditions and virtually independent of time if a wavelength independent quantum yield $\phi(3\text{M}2\text{N} \rightarrow \text{HONO})$ is assumed (Bohn, 2005).

Based on experimental data obtained for 3M2N and applying the assumptions described above, a photolytic HONO formation rate of 100 pptV h^{-1} is estimated for a maximum $J_{(\text{NO}_2)}$ value of 10^{-2} s^{-1} in the presence of 1 ppbV of nitrophenols.

Results obtained in recent field campaigns (Zhou *et al.*, 2002; Kleffmann *et al.*, 2003, 2005; Vogel *et al.*, 2003) have suggested the presence of an additional photolytic HONO source. In two studies, (Kleffmann *et al.*, 2005; Acker *et al.*, 2006) the existence of a daytime source of HONO was unequivocally demonstrated based only on experimental observation. For semi-urban and rural conditions, daytime sources of HONO of 500 pptV h^{-1} and 400 pptV h^{-1} were calculated. Thus, the mechanism proposed in the present study might explain a significant fraction of

the observed HONO formation in the urban atmosphere, besides other postulated photolytic HONO sources (Zhou *et al.*, 2001, 2002a, 2002b; George *et al.*, 2005; Stemmler *et al.*, 2005, 2006). However, this estimate needs to be verified using data from experiments performed under atmospheric conditions, and also investigations on the wavelength dependencies of the photolysis processes.

Chapter 5

5. Secondary organic aerosol formation from the photolysis of nitrophenols

Experiments on the SOA formation from the photooxidation of BTX in the EUPHORE chamber have indicated that the nitrophenols may play a key role in the aerosol formation observed in the oxidation systems (Martín-Reviejo and Wirtz, 2005). In order to investigate this possibility the formation of secondary organic aerosol (SOA) from the photolysis of a series of nitrophenols has been investigated for the first time in this work. Results are presented here from observations of secondary organic aerosol formation during the irradiation of nitrophenols with actinic lamps in a large volume quartz glass chamber. Of 10 possible nitrophenol isomers, 4 have been investigated: 2-nitrophenol, 3-methyl-2-nitrophenol, 4-methyl-2-nitrophenol and 4-nitrophenol. The experiments have mainly focused on the SOA formation from the photolysis of 2-nitrophenol.

Since the photolysis is known to produce OH radicals, the influence of adding an OH scavenger on the SOA formation has been investigated as well as changes in the irradiation intensity. Qualitative information regarding the aerosol yield has been obtained using a gas/aerosol absorption model. Possible atmospheric implications of the observations are discussed.

5.1 Results

The experiments on the photolysis of the nitrophenols were carried out in the quartz glass photoreactor described in Chapter 2. In addition to the experiments performed in order to investigate the formation of aerosols during the photolysis of nitrophenols, experiments were also performed to determine the effect of NO_x and the presence of an OH radical scavenger on the aerosol formation.

The nitrophenols were photolysed using the VIS lamps (emission in the range of 320 – 480 nm with the maximum intensity at 360 nm) as described in Chapter 2.

Prior to the initiation of the photolysis by switching on the lamps, the reaction mixture, nitrophenol/air, was left to stand in the dark for 15 min; no particles were observed during this pre-irradiation period (see Figure 5.1). Test experiments were also performed with only synthetic air in the chamber. The air was irradiated for the same period of time as that used in the experiments with nitrophenol in the chamber. In these experiments formation of no more than 200 particles cm⁻³ was observed.

A rapid formation of aerosols has been observed immediately after switching on the lamps for all of the nitrophenols investigated. The formation of very small particles with a mean diameter of 20-40 nm was observed for each compound in the first scan of the SMPS instrument, which has a time resolution of 5 min (an example for 2-nitrophenol is shown in Figure 5.1). Coagulation of the particles with increasing photolysis time resulted in a continuous increase of the mean particle diameter.

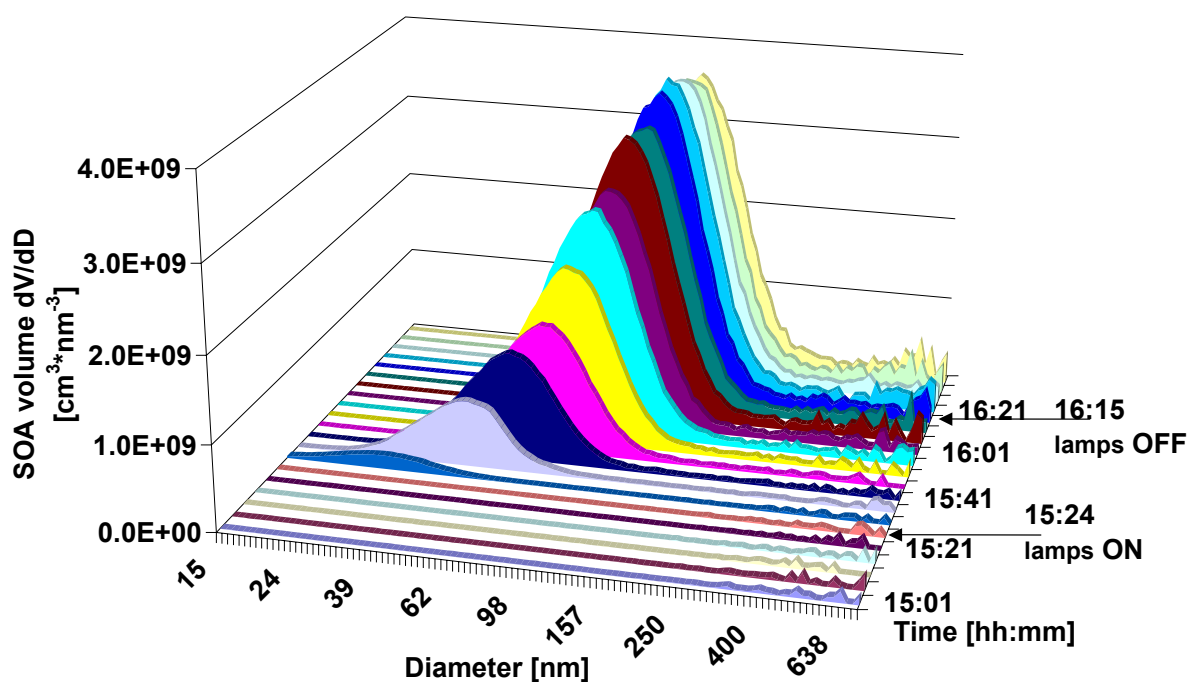


Figure 5.1 Secondary organic aerosol distribution observed during the photolysis of 2-nitrophenol without a scavenger for OH radicals.

Concentration-time profiles showing the decrease in the reactant concentration and the increase in the aerosol mass is shown in Figure 5.2 for 2-nitrophenol. As can be seen from Figure 5.2 conversion of only a very small amount of the nitrophenols is sufficient for aerosol formation.

Figure 5.2, also shows the very fast rise in the particle number concentration as detected with the sensitive UCPC instrument. An aerosol formation burst in the reactor was detected in less than 1 min after initiation of the photolysis for all of the nitrophenols. Typically, only 10 - 15 ppbV of the nitrophenol had reacted before the aerosol appearance. The initial reactant concentrations were 0.4-1.2 ppmV.

The concentrations of the reactants have been corrected for wall deposition. In Figure 5.1, a decrease in the aerosol formation is evident after termination of the photolysis. The dark decay has been used to calculate the deposition rate of the aerosol in the chamber. Physical processes such as electrostatic attraction to the chamber walls are also partially responsible for the particle losses. Corrections of 10-15 % were applied to the aerosol mass.

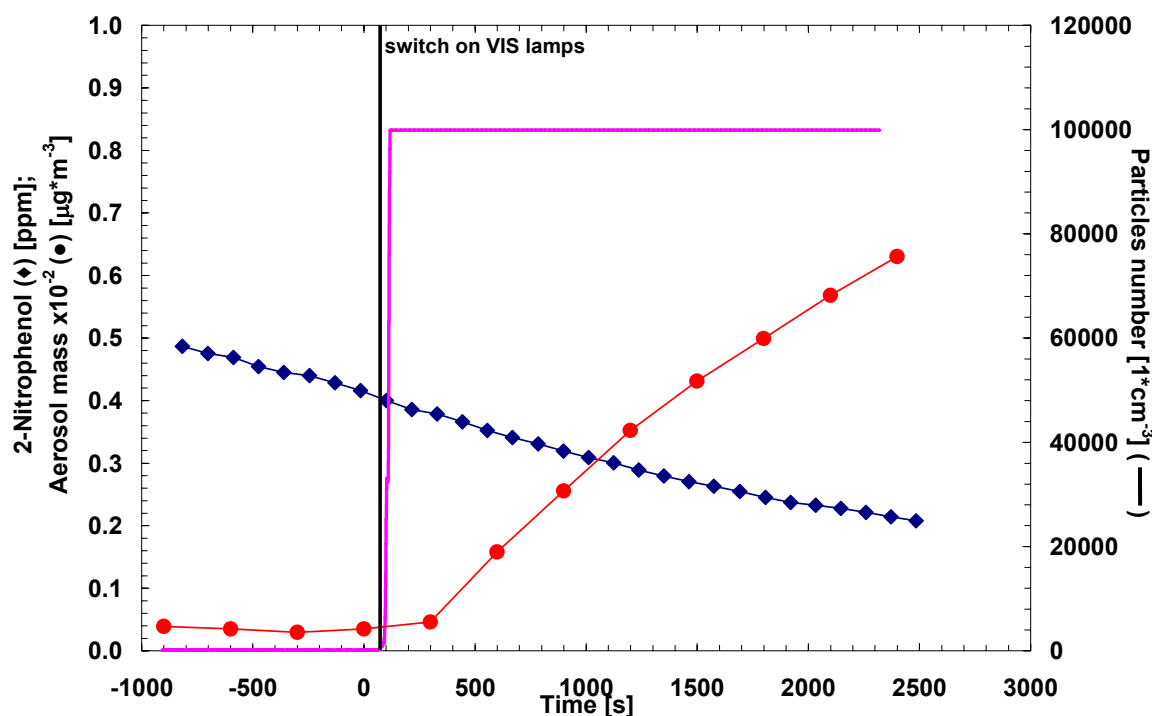


Figure 5.2 Concentration-time profiles of 2-nitrophenol (♦), aerosol mass (●) and formation of particles (—) from one experiment.

The aerosol mass formed during the photolysis time was obtained using the aerosol volume distribution and assuming unity density. The mass of aerosol formed during the photolysis was plotted against the amount of the nitrophenol reacted. The slopes give the formation yields of the aerosol formed. Examples are shown in Figure 5.3 for 2-nitrophenol and 2-nitro-p-cresol.

Significant aerosol formation was observed for the four nitrophenols investigated. For 2-nitrophenol the aerosol formation yield in the absence of OH scavenger and NO_x varied between 18% - 24%; slightly higher values were observed when the initial concentration was higher. The aerosol yields were also higher when all the lamps were used to initiate the photolysis; in experiments in which the number of lamps was reduced the aerosol yields were generally much lower. An overview of aerosol yields obtained for 2-nitrophenol and the associated experimental conditions is given in Table 5.1.

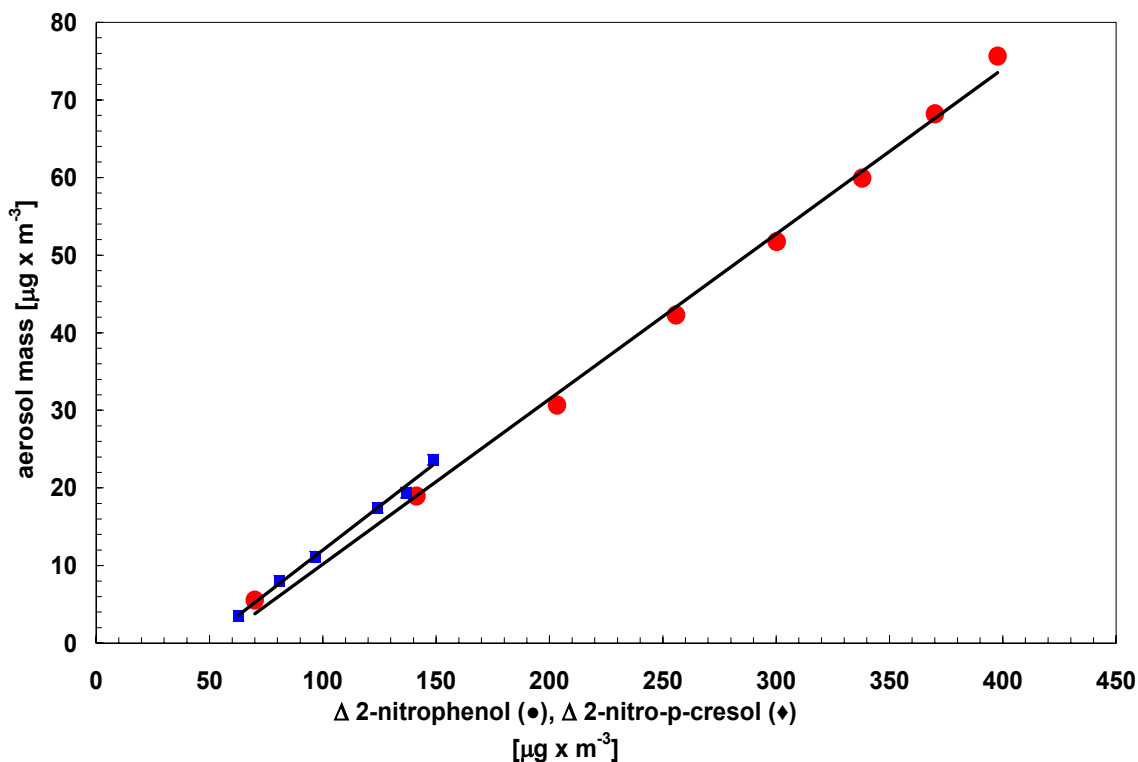


Figure 5.3 Examples of the aerosol mass yield as a function of reacted 2-nitrophenol (●) and 2-nitro-p-cresol (◆).

Table 5.1 Overview of the results obtained from aerosol studies performed on the photolysis of 2-nitrophenol.

experiment name	2NP (ppmV)	aerosol yield (%)	wall loss $\times 10^{-5}$	photolysis $\times 10^{-5}$	conditions
100305	0.80	22.2 ± 1.15	7.3 ± 0.22	10.3 ± 0.49	
111002	0.49	21.3 ± 0.98	18.4 ± 1.53	9.3 ± 0.44	
061102	1.23	19.6 ± 2.64	9.8 ± 0.91	8.4 ± 0.60	
110305	1.12	6.9 ± 1.00	7.3 ± 0.45	5.8 ± 0.29	scav.*
120305	0.66	2.9 ± 0.44	7.4 ± 2.60	7.0 ± 0.30	scav.*
180305	1.14	7.5 ± 2.10	8.8 ± 0.72	4.6 ± 0.10	scav.*
060705_1	0.70	**	8.2 ± 0.43	7.3 ± 0.78	NO _x
060705_2	0.92	**	9.0 ± 0.68	6.5 ± 0.24	NO _x
070705	0.61	**	11.0 ± 1.44	9.7 ± 0.58	NO _x

*Experiments performed with the addition of isoprene as OH radical scavenger,

** No aerosol yield calculation.

The reaction of nitrophenols with OH radicals is very slow (Bejan *et al.*, 2005b), whereas that of OH with isoprene is very fast ($1 \times 10^{-10} \text{ cm}^3 \text{ s}^{-1}$ at 298 K; Atkinson, 2003). The amount of isoprene present in the experiments (0.5 - 4 ppmV) was sufficient to scavenge more than 97% of the OH radicals produced during the experiments.

The aerosol yields measured in the absence of the scavenger were higher than those measured in the presence of isoprene (see Table 5.1) indicating an inhibitory effect of the OH scavenger on the aerosol formation.

Figure 5.4 presents an example of a photolysis experiment with 2-nitrophenol in which isoprene was used as the scavenger for OH radicals. The graph shows clearly that after the initial nucleation the particles grow in size during the photolysis period by uptake of condensable material from the gas phase. After termination of the photolysis the particle size distribution changed due to a combination of further coagulation and deposition to the walls. This dark period was used to determine the aerosol deposition rate.

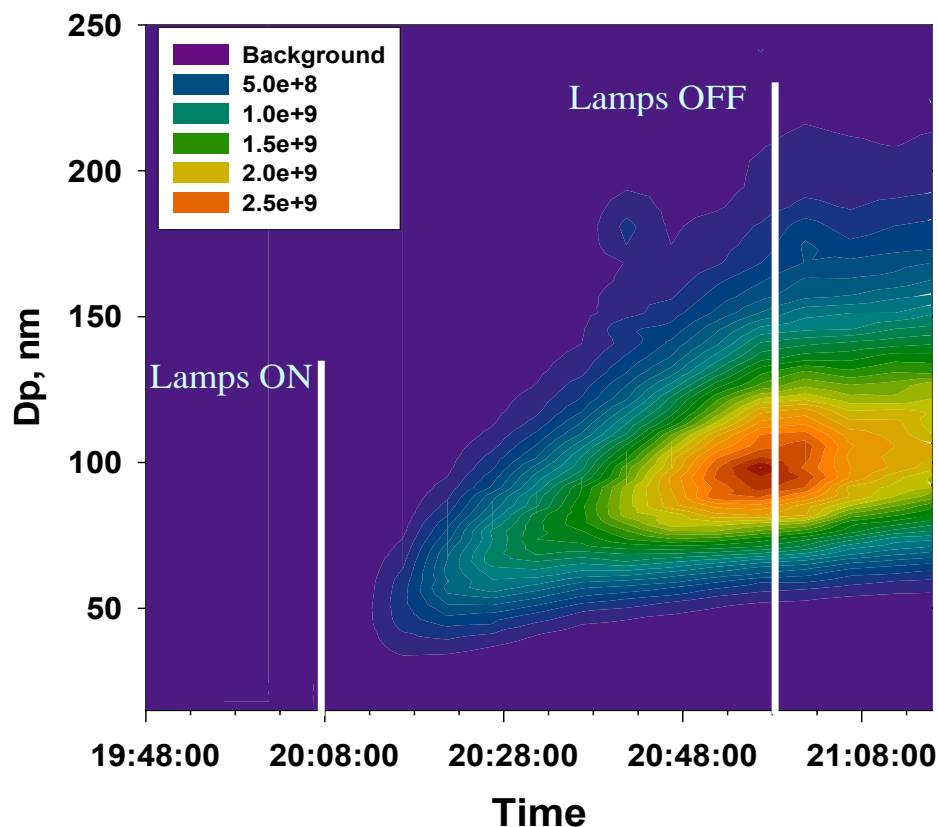


Figure 5.4 Time dependence of the aerosol size distribution measured during a typical photolysis experiment on 2-nitrophenol in which isoprene was used as a scavenger for the OH radicals formed in the system.

By addition of NO_x in the range 0.5–4 ppmV, the SOA formation in the photolysis of nitrophenols was almost totally suppressed. Nevertheless, the formation of a small number of particles could be detected with the UCPC. It was not possible to calculate an aerosol yield for the reaction systems in which NO_x was present. The UCPC data showed a decrease in the number of particles in the presence of NO_x .

5.2 Discussion

5.2.1 OH radical influence on aerosol formation

As presented in Chapter 4, the photolysis of nitrophenols is a source of HONO (Bejan *et al.*, 2006). In order to suppress the reaction of OH radicals with nitrophenols in the systems studied, isoprene was used as an OH radical scavenger. Although SOA formation has been reported for the photooxidation of

isoprene (Claeys *et al.*, 2004; Böge *et al.*, 2006; Kroll *et al.*, 2006; Surratt *et al.*, 2006) no aerosol formation was observed from isoprene at the concentration levels and on the experimental timescales used in the present studies.

The effect of radical scavengers on the aerosol formation in studies on the ozonolysis of alkenes has been reported previously in the literature. The studies of Docherty and Ziemann (2003), Ziemann (2003) and Keywood *et al.* (2004) have clearly demonstrated that the radicals produced from the reactions of the OH (produced in the ozonolysis of alkene) with the scavenger have an effect on the SOA yield. The extent and direction of the effect have also been shown to be dependent on the specific alkene (Keywood *et al.*, 2004). Keywood *et al.* (2004) present evidence in their paper that acylperoxy radicals formed in the system play a central role.

5.2.2 NO_x influence on aerosol formation

In the photolysis of nitrophenols under high NO_x conditions it would appear that the formation of aerosol producing oxidation products is strongly inhibited. It is now well established from theoretical and experimental studies that the concentration of NO_x present in an aromatic hydrocarbon photooxidation system can modify the degradation chemistry of the aromatic hydrocarbons (Volkamer *et al.*, 2002; Berndt and Böge, 2006) and consequently also the aerosol formation (Hurley *et al.*, 2001; Martin-Reviejo and Wirtz, 2005; Song *et al.*, 2005).

From the present experimental work it was not possible to show whether the average levels of NO_x in the ambient atmosphere (typically between 10 to 50 ppb in urban areas) will be effective in suppressing the aerosol formation. In order to do this it will be necessary to use a technique capable of measuring low concentrations of NO_x. However, results from the photolysis experiments of Bardini (2006) on nitrophenols in the EUPHORE photoreactor, in which low levels of NO_x were present, suggest that under moderately polluted conditions the formation of aerosol from the photolysis of nitrophenols will probably still be quite substantial.

Unfortunately in the present work it has also not been possible to ascertain the identity of the product(s) inhibiting the aerosol in the photolysis of nitrophenols

at high NO_x . It can only be speculated that reaction of the postulated aromatic biradical intermediate (see Figure 5.6 below) with NO_x is forming some photochemically inactive aromatic nitro compound(s) with a reasonably high vapour pressure. It is evident that more experimental work is required in order to better assess the effects of the NO_x concentration on SOA formation from the photolysis of nitrophenols.

5.2.3 Expression for SOA yield

Qualitative information regarding the aerosol yield can be obtained using a gas/aerosol absorption model (see Appendix IV). The fractional aerosol yield (Y), as defined by Odum *et al.* (1996), is the fraction of a reactive organic gas (ROG) converted to aerosol, and is given by the expression:

$$Y = \Delta M_0 / \Delta \text{ROG} \quad 5.1$$

where ΔM_0 is the aerosol mass concentration produced for a given amount of nitrophenol photolyzed, ΔROG .

As proposed by Odum *et al.* (1996) the semi-volatile compounds produced in the photolysis of nitrophenols can partition between the gas and aerosol phases, which can be represented by the expression

$$Y = M_0 \sum_i \frac{\alpha_i k_i}{1 + k_i M_0} \quad 5.2$$

which includes the total aerosol yield in terms of the individual product stoichiometric coefficients α_i , the partition coefficients K_i and the total aerosol mass M_0 .

Figure 5.5 shows plots of the aerosol mass yield plotted as a function of the aerosol mass concentration, for two experiments involving the photolysis of 2-nitrophenol and 2-nitro-p-cresol. The gas-phase partitioning could be fitted assuming the presence of only one compound in both phases. As expected from the model the mass yield approaches a limiting value if the total mass rises infinitely.

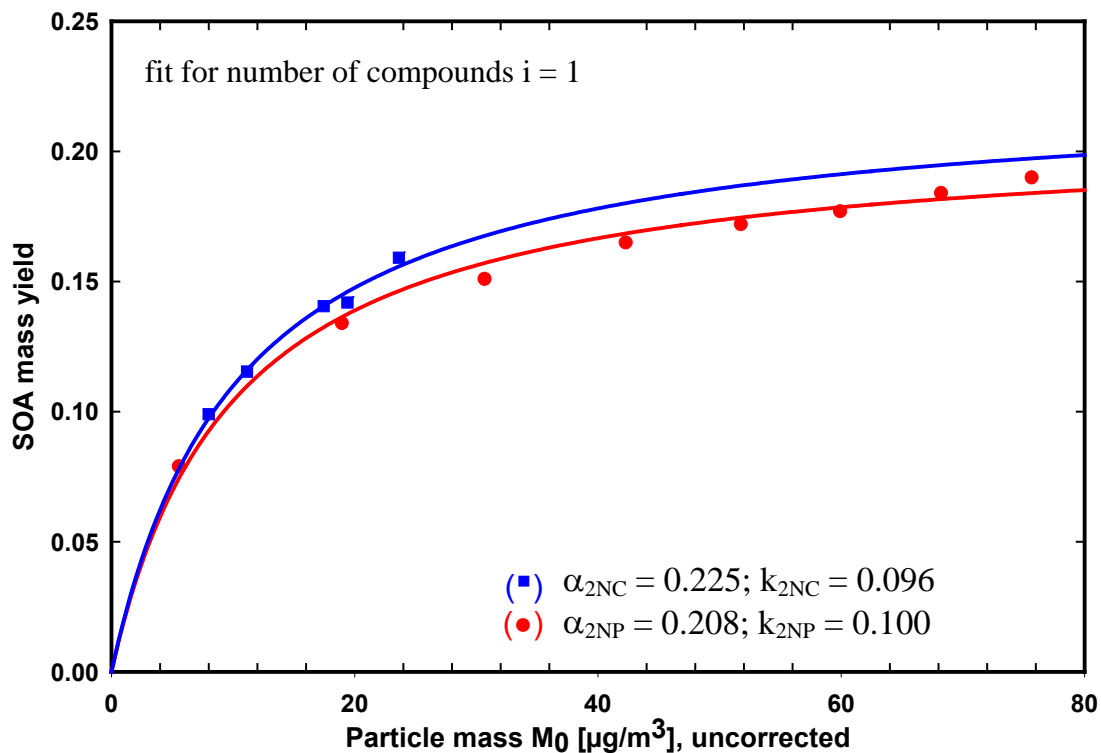


Figure 5.5 Application of a partitioning model for estimation of the aerosol yield from the photolysis of 2-nitrophenol and 2-nitro-p-cresol

The α coefficient obtained using Odum's model, is almost equal to the aerosol yield (Figure 5.5). This suggests that the product(s) formed in the photolysis process is (are) very non-volatile, and that partitioning to the particle phase is favoured.

5.2.4 Potential explanation of SOA formation in the photolysis of nitrophenols

Unfortunately due to the low conversion of the nitrophenol compounds detection of photolysis products using FT-IR spectrometer was not possible under any of the experimental conditions. A possible mechanism to explain the aerosol formation is suggested in Figure 5.6.

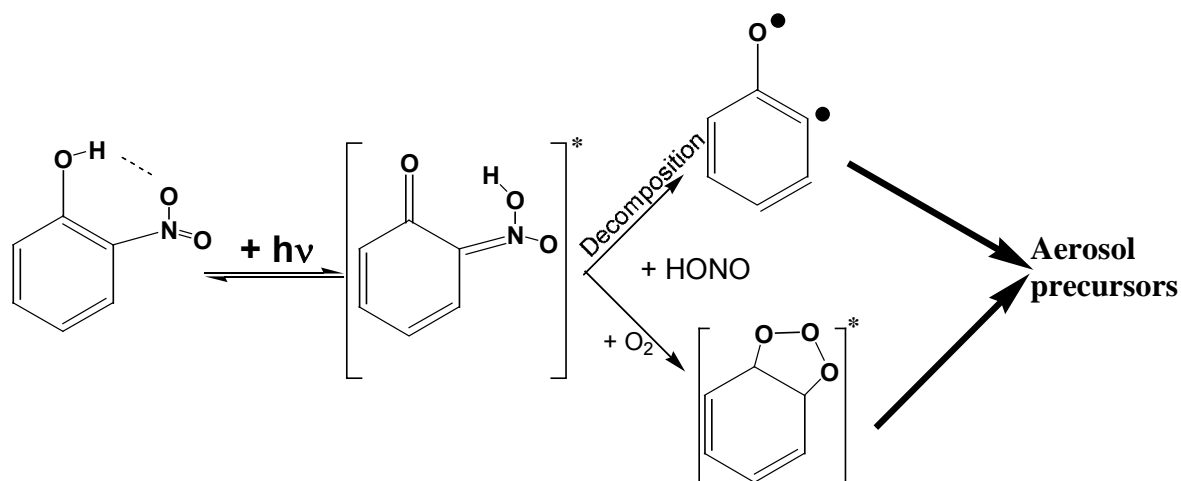


Figure 5.6 A possible mechanism to explain the aerosol formation observed in the photolysis of nitrophenols.

In this study, as discussed in Chapter 4, the instantaneous formation of HONO has been observed during the gas phase photolysis of nitrophenols. Based on the mechanism proposed in Chapter 4, the formation of particles from the photolysis of nitrophenols can be expected. The proposed biradical resulting from the generation of HONO, will most probably undergo further reactions such as reaction with O₂ and isomerisation, leading to the formation of acids as presented in Figure 5.7 (Alif *et al.*, 1991), or reactions with the parent nitrophenol, probably generating higher molecular species with vapour pressures low enough to generate particles.

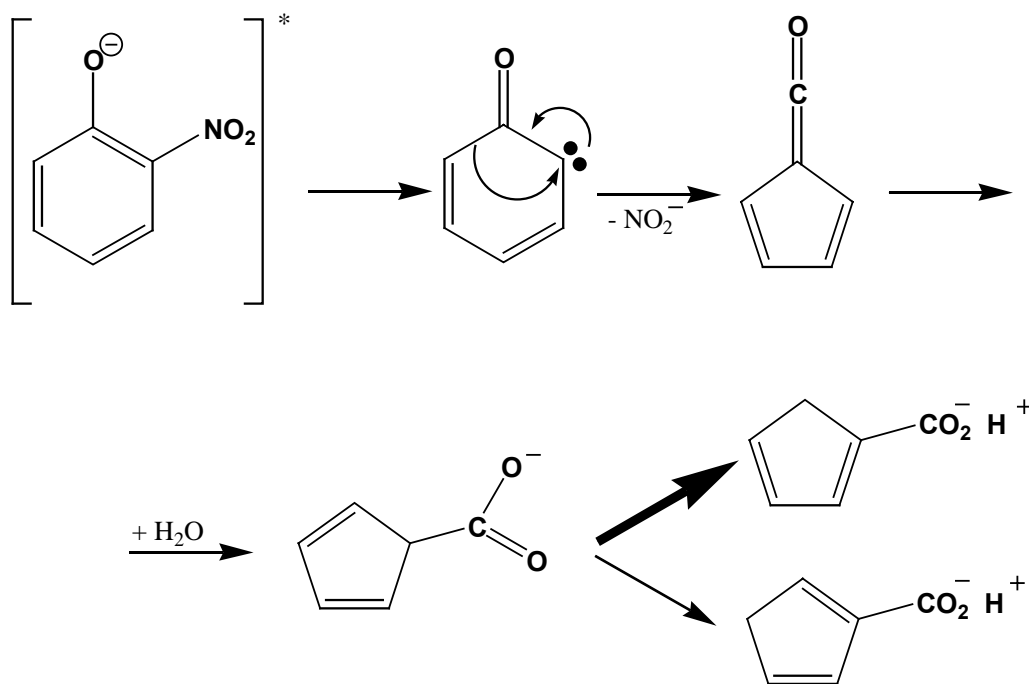


Figure 5.7 Mechanism proposed by Alif *et al.* (1991) to explain the carboxylic acid formation observed in the photolysis of nitrophenols in aqueous solution.

In an attempt to gain more information on the mechanism of aerosol formation during the photolysis of nitroaromatic compounds, the photolysis of 2-nitrotoluene was investigated under similar conditions to test for mechanistic similarities. Aerosol formation was also observed from the photolysis of 2-nitrotoluene without NO_x addition. In addition, Bejan *et al.* (2007) have demonstrated that the photolysis of 2-nitrotoluene also produces HONO. These observations suggest that for 2-nitrotoluene a photolysis and SOA formation mechanism similar to that of 2-nitrophenol is probably operative, i.e. the possible formation of a biradical via a nitronic acid intermediate.

A significant finding of this work was that photolysis of nitrophenols produces high yields of secondary organic aerosols. Detailed product studies will be necessary in order to explain the observed formation of particles during the photolysis of both the nitrophenols and 2-nitrotoluene. Because of the very low mass conversion other much more sensitive techniques will need to be used for product identification and quantification. This information would help to elucidate

the intermediates responsible for aerosol formation as well as to validate the proposed mechanism for the photolysis of these compounds.

Chapter 6

6. Summary

The overall objective of this work was to obtain a better understanding of the gas phase chemistry of aromatics. The purpose was to provide an evaluation of the atmospheric fate of the following aromatic compounds, which are important products in the oxidation of BTX: 1,2-dihydroxybenzene, 3-methyl-1,2-dihydroxybenzene, 4-methyl-1,2-dihydroxybenzene, 2-nitrophenol, 3-methyl-2-nitrophenol, 4-methyl-2-nitrophenol, 5-methyl-2-nitrophenol, 6-methyl-2-nitrophenol.

The data obtained within the present work can be used to improve the knowledge on the atmospheric degradation of aromatic hydrocarbons. The rate coefficients of the OH and NO₃ radical initiated oxidation of some nitro/hydroxy substituted monoaromatic hydrocarbons improve the kinetic data base required to model the degradation mechanisms of aromatic compounds and to develop structure reactivity relationships for OH and NO₃ radical with VOCs. The mechanistic investigations on the photolysis of nitrophenols and formation of HONO as a new gas phase source and secondary organic aerosol investigation from the photolysis of nitrophenols improve our present understanding of the

reactions that are operative in the atmospheric oxidation of the aromatic hydrocarbons.

The results of this work can be divided in three major parts: (1) kinetic data for the gas-phase reactions of NO_3 and OH radicals with some nitro/hydroxy substituted monoaromatic hydrocarbons, (2) mechanistic information on the photolysis of nitrophenols as a new atmospheric gas phase source of HONO, (3) information on secondary organic aerosol formation from the photolysis of nitrophenols.

1) Relative rate coefficients have been measured for the reactions of NO_3 radicals with 1,2-dihydroxybenzene, 3-methyl-1,2-dihydroxybenzene and 4-methyl-1,2-dihydroxybenzene. The kinetic data on the reactions of NO_3 with selected catechols were obtained from investigations performed in two chambers: the 1080 l quartz glass reactor in Wuppertal and in the EUPHORE chambers in Valencia. The following rate coefficients (in units of $\text{cm}^3 \text{s}^{-1}$) were obtained: $(9.8 \pm 5.0) \times 10^{-11}$ for 1,2-dihydroxybenzene, $(17.2 \pm 5.6) \times 10^{-11}$ for 1,2-dihydroxy-3-methylbenzene and $(14.7 \pm 6.5) \times 10^{-11}$ for 1,2-dihydroxy-4-methylbenzene. The reactivity of the 1,2-dihydroxybenzenes takes the following order: k_{NO_3} (1,2-dihydroxybenzene) < k_{NO_3} (1,2-dihydroxy-4-methylbenzene) < k_{NO_3} (1,2-dihydroxy-3-methylbenzene). The experiments were performed at low and high NO_2 in both chambers; the kinetic behavior was independent of the $[\text{N}_2\text{O}_5]/[\text{NO}_2]$ ratio supporting that the reactions of the 1,2-dihydroxybenzenes takes place only with NO_3 radicals and not with N_2O_5 or with NO_2 . The reactions of 1,2-dihydroxybenzenes with NO_3 has been found to be a potentially important daytime oxidation processes for these compounds. It has been estimated that 1,2-dihydroxybenzene will react during the daytime about 60% with OH and about 40% with NO_3 radicals.

This work has provided rate coefficients for the gas phase reactions of the OH radical with 3-methyl-2-nitrophenol, 4-methyl-2-nitrophenol, 5-methyl-2-nitrophenol, 6-methyl-2-nitrophenol. The following rate coefficients (in units of $\text{cm}^3 \text{s}^{-1}$) were determined: $(3.69 \pm 0.16) \times 10^{-12}$ for 3-methyl-2-nitrophenol, $(3.46 \pm 0.18) \times 10^{-12}$ for 4-methyl-2-nitrophenol, $(7.34 \pm 0.52) \times 10^{-12}$ for 5-methyl-2-nitrophenol and $(2.70 \pm 0.17) \times 10^{-12}$ for 6-methyl-2-nitrophenol. Photolysis rates for the nitrocresols have been determined in the Wuppertal quartz glass reaction chamber from which

estimates of the photolysis rates of the compounds under atmospheric conditions have been made. The following photolysis rates (in units of s^{-1}) were determined for the four *i*-methyl-2-nitrophenols ($i = 3, 4, 5, 6$) investigated: $(1.67 \pm 0.11) \times 10^{-4}$ for 3-methyl-2-nitrophenol, $(8.86 \pm 1.07) \times 10^{-5}$ for 4-methyl-2-nitrophenol, $(1.07 \pm 0.14) \times 10^{-4}$ for 5-methyl-2-nitrophenol and $(7.81 \pm 1.11) \times 10^{-5}$ for 6-methyl-2-nitrophenol. The steady-state OH radical concentrations measured during the photolysis of the nitrophenols were $2 - 3 \times 10^5 \text{ cm}^{-3}$. The magnitude of the photolysis rates for the methylated nitrophenols under atmospheric conditions can be roughly estimated from the experiments.

These studies represent the first determinations of the rate coefficients for the gas-phase reactions of NO_3 and OH radicals with some nitro/hydroxy substituted monoaromatic hydrocarbons. The data is an important addition to the kinetic database on VOCs, which is used to develop structure-reactivity relationships for predicting rate coefficients for the reactions of NO_3 and OH radicals with VOCs and also the tropospheric lifetime of VOCs.

2) The photolysis of nitrophenols was found to be a gas phase source of HONO. To date, no observations of nitrous acid formation from the gas phase photolysis of nitrophenols have been reported in the literature.

A linear correlation between the HONO and nitrophenol concentration was observed in separate experiments for all of the nitrophenols investigated.

When two flow tube photoreactors with significantly different surface to volume ratios (S/V) were used, the HONO concentration in the effluent differed significantly between the reactors. The HONO formation was found to be independent of the S/V ratio of the reactors.

The possible effect of NO_2 formation has been considered. During the photolysis of pure nitrophenol–bath gas mixtures no NO_2 formation was observed. From a consideration of an upper limit for NO_2 formation, the contribution to HONO formation from mechanisms involving NO_2 have been estimated to be negligible.

The influence of light intensity on the HONO formation rate during the photolysis of 3M2N was also studied in the large flow tube photoreactor by varying

the number of lamps. A linear correlation between the HONO formation and the number of lamps switched on was observed.

The influence of the buffer gas on the HONO formation rate was also investigated for the photolysis of 3M2N. The nature of the buffer gas had a significant impact on the HONO formation.

Based on the HONO formation yields, a I photolysis mechanism has been proposed.

Since a linear dependence of the HONO yield on the nitrophenol concentration was observed, the results obtained here have been extrapolated linearly to atmospheric concentrations. Based on the experimental data obtained for 3M2N and applying the assumptions described in Chapter 4, a photolytic HONO formation rate in the atmosphere of 100 pptV h^{-1} is estimated for a maximum $J_{(\text{NO}_2)}$ value of 10^{-2} s^{-1} in the presence of 1 ppbV of nitrophenols.

3) The formation of secondary organic aerosol (SOA) from the photolysis of a series of nitrophenols was investigated for the first time. The effect of NO_x and the presence of an OH radical scavenger on the aerosol formation were also investigated. Significant aerosol formation was observed for the 4 nitrophenols investigated.

For 2-nitrophenol the aerosol formation yield in the absence of an OH radical scavenger and NO_x varied between 18 - 24%, with slightly higher values being observed, when the initial nitrophenol concentration was higher. The aerosol yields measured in the absence of the scavenger were higher than those measured in the presence of isoprene indicating an inhibitory effect of the isoprene on the aerosol formation. In the photolysis of nitrophenols under high NO_x conditions it would appear that the formation of aerosol producing oxidation products is strongly inhibited.

Qualitative information regarding the aerosol yield has been obtained using a gas/aerosol absorption model. The gas-phase partitioning could be fitted assuming the presence of only one compound in both phases. A possible mechanism to explain the aerosol formation observed in the photolysis of nitrophenols is proposed.

Synthesis**I. 1. Synthesis of methyl nitrite (CH₃ONO)**

Methyl nitrite has been prepared following the method of Taylor *et al.* (1980) with some small changes. Methyl nitrite was generated by the reaction of sodium nitrite (NaNO₂) with methanol (CH₃OH) in acidic medium (H₂SO₄+H₂O).

Quantities:

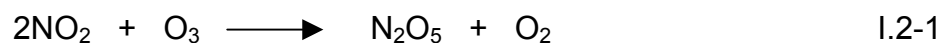
69 g (1 mol) of NaNO₂
solution of 26.8 ml H₂SO₄ (conc.) + 49 ml H₂O
solution of 48.7 ml CH₃OH + 38.5 ml H₂O

NaNO₂ and the CH₃OH solution in H₂O were mixed with a stirrer in a 2-liter three-neck flask. The flask is equipped with a dropping funnel in order to add the H₂SO₄/H₂O solution. Because this exothermic reaction is very fast the addition has to be slow and the flask must be cooled in an ice bath (273 K). The acid solution is added over a period of 2-3 hours. The gaseous methyl nitrite produced in the reaction was passed over an anhydrous calcium chloride (CaCl₂) bed to remove water and is then collected in a glass cylinder cold trap at the temperature of dry ice. The pale yellow liquid methyl nitrite was stored in the dark at 195 K to prevent thermal decomposition.

The FT-IR spectrum of freshly prepared methyl nitrite did not contain any traces of methanol. However, if methyl nitrite is left for a long period in the glass cylinder it has been observed that traces of methyl nitrate (CH₃ONO₂) can be formed.

I. 2. Synthesis of nitrogen pentoxide (N₂O₅)

N₂O₅ has been synthesized using a method proposed by Schott and Davidson (1958) without substantial changes.



Oxygen and NO₂ were taken gas cylinders and dried in a flow over P₄O₁₀. The driers contain glass balls in order to increase the contact surface of P₄O₁₀. The pre-dried oxygen is fed to an ozonizator where an oxygen-ozone mixture is formed. The oxygen-ozone is then mixed with the dried NO₂. The new mixture of all the gases is then directed through a glass impinger which contains a frite for better mixing. N₂O₅ synthesized in this reaction is collected and frozen in a cooling trap at -78°C in the form of colourless crystals. In order to prevent the possible formation and collection of N₂O₄ to the gas flows have to be carefully adjusted such that no yellow colour appears in the glass impinger. N₂O₅ was stored at -78°C.

N₂O₅ was added to the chamber using a nitrogen flow. The concentration of N₂O₅ added to the chamber can be controlled by adjusting the storage temperature.

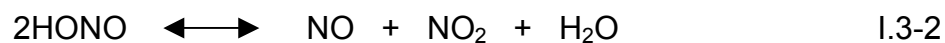
I. 3. Synthesis of nitrous acid (HONO)

Nitrous acid (HONO) has been prepared using the method described by Kleffmann (2004).

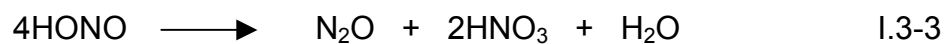
In a 100 ml three-neck flask, connected with a dropping funnel system and a thermometer, is placed 30 ml of a 25-30% sulphuric acid solution. 20 ml of a 1% NaNO₂ solution was added dropwise to the stirred H₂SO₄ solution over 30-50 minutes. The gaseous HONO formed was added to the chamber in a flow of nitrogen, which was passed through the flask. Together with HONO formed in reaction I.3-1, in the gas stream also contains NO, NO₂ and H₂O formed in reactions I.3-2 and I.3-3.

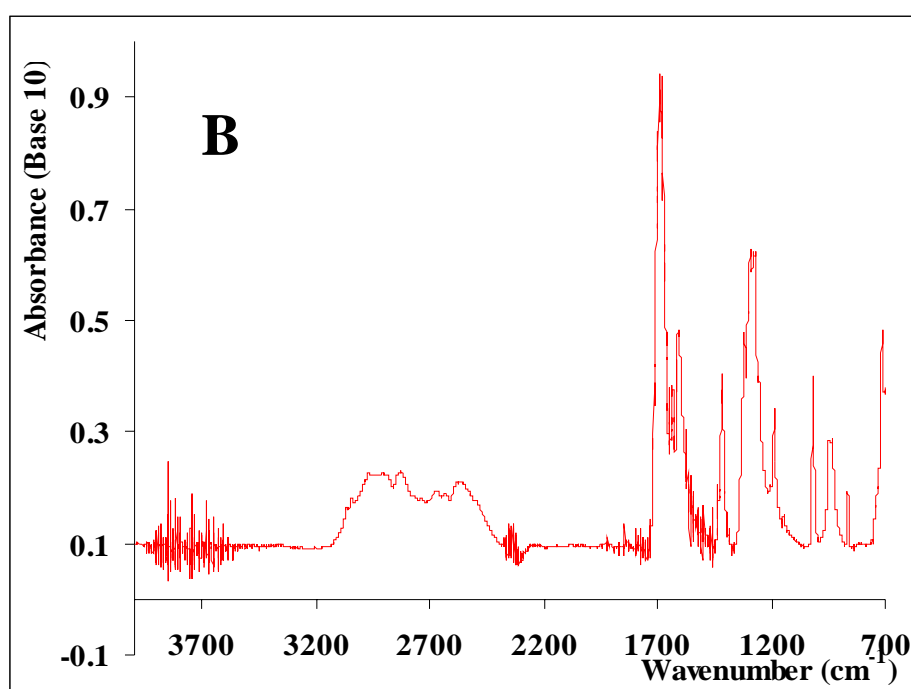
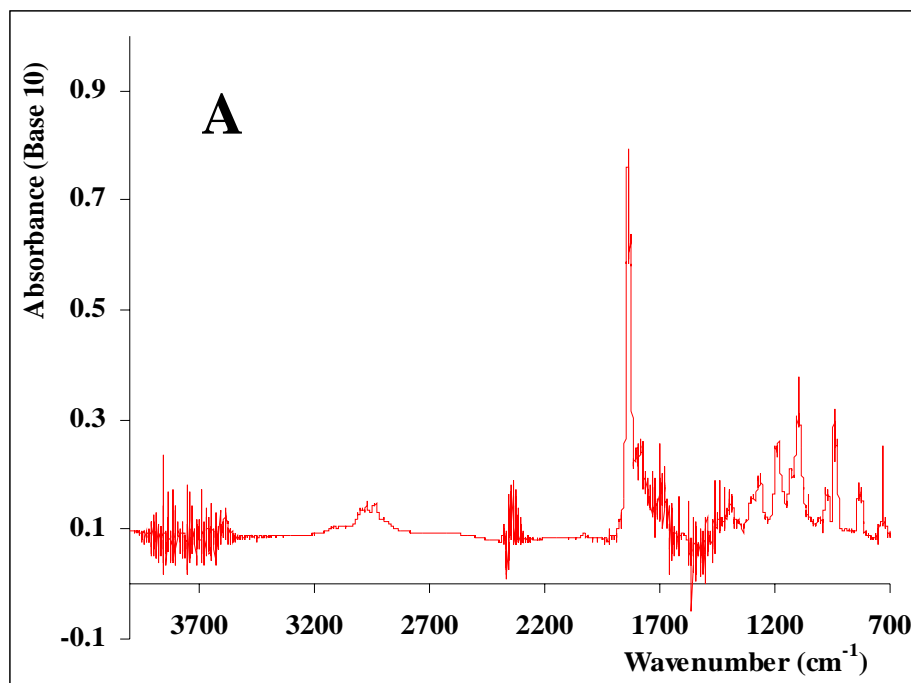


In the presence of water HONO is unstable and decomposes when heated or concentrated. At room temperature HONO also slowly decomposes (Finlayson-Pitts and Pitts, 2000).



Kleffmann *et al.* (1994, 1998) observed also the formation of N_2O during the decay of HONO, which they explained by a reaction on the wall surface. They suggested that the overall reaction can be represented by I.3-3:



Gas phase muconic acid infrared spectra

Qualitative reference spectra of *cis,cis*-muconic acid (A) and *trans,trans*-muconic acid (B). Difficulties were encountered in recording the spectra due to the extremely low vapor pressure and extremely high melting point of the compounds.

Appendix III**Origin and purity of the gases and chemicals used****III.1 Gases**

compound	origin	purity
synthetic air 20.5/79.5 = O ₂ /N ₂ %	Messer-Griesheim Air Liquid	hydrocarbons free 99.999%
O ₂	Messer-Griesheim	99.999%
N ₂	Messer-Griesheim	99.999%
N ₂	Messer-Griesheim	99.9999%
Ar	Messer-Griesheim	99.999%
He	Messer-Griesheim	99.999%
NO	Messer-Griesheim	99.5%
NO ₂	Messer-Griesheim	98%
SF ₆	Messer-Griesheim	99.99%
ethene	Messer-Griesheim	99.95
n-butane	Messer-Griesheim	99%

III.2 Chemicals

compound	state	origin	purity
1,2-dihydroxybenzene	solid	Aldrich	99%
1,2-dihydroxy-3-methylbenzene	solid	Aldrich	99%
1,2-dihydroxy-4-methylbenzene	solid	Aldrich	98%
2-nitrophenol	solid	Aldrich	98%
4-nitrophenol	solid	Sigma	99%
6-methyl-2-nitrophenol*	solid	synthesized	98%
3-methyl-2-nitrophenol	solid	Fluka/Aldrich	98/99%
5-methyl-2-nitrophenol	solid	Aldrich	97%
4-methyl-2-nitrophenol	solid	Aldrich	99%
2-nitrotoluene	liquid	Aldrich	99%
2,3-dimethyl-2-butene	liquid	Aldrich	99%
isoprene	liquid	Aldrich	99%
CH ₂ Cl ₂	liquid	Aldrich	99.9%

* the compound was synthesized by Olariu (2001)

Appendix IV**Gas/Particle partitioning and secondary organic aerosol yield**

Like ozone, SOA results from the atmospheric oxidation of reactive organic gases (ROGs), but whereas the oxidation of most ROGs results in ozone formation (Derwent *et al.*, 1996), SOA is generally formed only from the oxidation of ROGs comprised of six or more carbon atoms. This is because oxidation products must have high molecular weight and/or vapour pressures that are sufficiently low to enable them to partition into the aerosol phase (Odum *et al.*, 1996, 1997).

Efforts to represent SOA formation have primarily been based on using experimentally determined fractional aerosol yields (Seinfeld and Pandis, 1998).

The equilibrium gas/particle partitioning of a semivolatile organic species i between the gas phase and a particulate organic phase can be described by the vapour pressure relation (Pankow *et al.*, 1994):

$$p_i = x_i \gamma_i p_i^0 \quad \text{IV.1}$$

where p_i is the gas-phase partial pressure of species i , x_i is the mole fraction of species i in the organic aerosol phase, γ_i is the activity coefficient of species i in the aerosol-phase organic mixture, and p_i^0 is the vapour pressure of species i as a pure liquid. The activity coefficient γ_i describes the non-ideal interaction between dissolved species i and the other components of the solution. A value of γ_i above 1, means that the compound i is not easily miscible with the absorbing aerosol, and the non-ideal interactions favour that it remains in the gas phase.

Using p_i the concentration of the gas-phase G_i ($\mu\text{g m}^{-3}$) can be calculated with the ideal gas relation:

$$G_i = \frac{10^6 p_i MW_i}{RT} \quad \text{IV.2}$$

where: MW_i ($\mu\text{g m}^{-3}$) is the molecular weight of species i , R ($8.206 \times 10^{-5} \text{ m}^3 \text{ atm mol}^{-1} \text{ K}^{-1}$) is the ideal gas constant, T (K) is the temperature.

The total aerosol mass concentration M_0 is a sum of the aerosol-phase mass concentration of species i ($\mu\text{g m}^{-3}$):

$$M_0 = \sum_{i=1}^n A_i \quad \text{IV.3}$$

The mean molecular weight is the sum of all the fractions:

$$\overline{MW} = \sum_{i=1}^n x_i MW_i \quad \text{IV.4}$$

Using IV.3, IV.2 and IV.1 leads to equation IV.5:

$$K_i = \frac{A_i}{G_i M_0} = \frac{10^{-6} R T}{\overline{MW} \gamma_i p_i^0} \quad \text{IV.5}$$

where K_i is the equilibrium gas/particle partitioning coefficient of species i defined as the ratio of the aerosol to gas-phase mass concentration of species i , including the total mass of the organic particulate phase. K_i has the units ($\text{m}^3 \mu\text{g}^{-1}$), A_i is the concentration of compound i in the absorbing organic material phase, \overline{MW} is the mean molecular weight of the absorbing organic material, γ_i is the activity coefficient of species i in the aerosol-phase organic mixture $\gamma_i = \gamma_i(x_1, x_2, \dots, x_n; T)$ and $p_i^0 = p_i^0(T)$.

The fractional aerosol yield (Y) has been widely used to represent the SOA formation potential of ambient organics. Y is defined as the fraction of a reactive hydrocarbon compound (HC) that is converted to aerosol and is expressed by the first part of equation IV.6.

The aerosol yield calculated by Odum's equation is an overall secondary organic aerosol yield from the beginning of an experiment to a certain level of accumulated organic mass concentration in particles and is expressed by the second part of equation IV.6.

$$Y = \frac{\Delta M_0}{\Delta HC} = \frac{M_0}{\Delta HC} = M_0 \sum_i \left(\frac{\alpha_i K_i}{1 + K_i M_0} \right) \quad \text{IV.6}$$

In equation IV.6 α_i is the stoichiometric coefficient. Stoichiometric coefficients depend on the gas-phase chemical mechanism and represent the total

amount of semivolatile product formed, in both gas and aerosol phases, per amount of parent organic compound reacted.

In the limit of large organic aerosol mass concentration or low volatility of the products the total yield of SOA is independent of M_0 being the sum of the mass based stoichiometric coefficients of the products.

Appendix V**Gas-phase infrared absorption cross section****Table V.1** FT-IR absorption cross sections of dihydroxybenzene compounds (Olariu, 2001)

compound	absolute cross section		integrated cross section	
	wavenumber (cm ⁻¹)	$\times 10^{-20}$ (cm ² molecule ⁻¹)	range (cm ⁻¹)	$\times 10^{-18}$ (cm molecule ⁻¹)
1,2-dihydroxybenzene	1619	(13.5 ± 0.24)	1653-1590	(3.56 ± 0.60)
	1517	(35.8 ± 0.90)	1537-1495	(8.50 ± 0.21)
	1325	(13.6 ± 0.31)	1340-1306	(2.02 ± 0.40)
	1092	(20.8 ± 0.70)	1112-1072	(3.45 ± 0.11)
1,2-dihydroxy-3-methylbenzene	3671	(20.2 ± 0.80)	3689-3648	(3.90 ± 0.15)
	3608	(25.9 ± 1.52)	3629-3583	(6.04 ± 0.35)
	1488	(20.6 ± 0.95)	1545-1467	(8.66 ± 0.40)
	1359	(7.83 ± 0.40)	1377-1343	(1.56 ± 0.10)
	1188	(20.6 ± 1.14)	1207-1136	(9.35 ± 0.52)
	759	(20.2 ± 0.80)	785-742	(2.93 ± 0.12)
1,2-dihydroxy-4-methylbenzene	3666	(11.3 ± 0.67)	3689-3648	(2.51 ± 0.15)
	3608	(18.9 ± 0.13)	3629-3583	(3.87 ± 0.27)
	1527	(22.2 ± 1.32)	1545-1467	(5.31 ± 0.22)
	1315	(5.41 ± 0.42)	1343-1377	(0.96 ± 0.75)
	1200	(4.85 ± 0.21)	1207-1185	(0.66 ± 0.52)
	1168	(12.3 ± 1.01)	1182-1153	(2.17 ± 0.18)
	1110	(14.5 ± 0.93)	1123-1090	(2.57 ± 0.10)
	790	(8.52 ± 0.52)	828-764	(2.80 ± 0.17)

Table V.2 FT-IR absorption cross sections of nitrophenol compounds

compound	absolute cross section		integrated cross section	
	wavenumber (cm ⁻¹)	(cm ² molecule ⁻¹)	region (cm ⁻¹)	(cm molecule ⁻¹)
2-nitrophenol	1627	$(3.10 \pm 0.34) \times 10^{-19}$	1654-1610	$(7.47 \pm 0.84) \times 10^{-18}$
	1343	$(4.21 \pm 0.47) \times 10^{-19}$	1367-1305	$(1.25 \pm 0.14) \times 10^{-17}$
3-methyl-2-nitrophenol	1609	$(4.46 \pm 0.38) \times 10^{-19}$	1643-1580	$(1.03 \pm 0.08) \times 10^{-17}$
	1351	$(2.23 \pm 0.20) \times 10^{-19}$	1373-1308	$(8.16 \pm 0.74) \times 10^{-18}$
5-methyl-2-nitrophenol	1634	$(3.58 \pm 0.13) \times 10^{-19}$	1652-1617	$(7.49 \pm 0.24) \times 10^{-18}$
	1603	$(3.46 \pm 0.12) \times 10^{-19}$	1615-1579	$(7.22 \pm 0.22) \times 10^{-18}$
	1335	$(4.35 \pm 0.13) \times 10^{-19}$	1362-1315	$(1.17 \pm 0.33) \times 10^{-17}$
	1203	$(2.48 \pm 0.07) \times 10^{-19}$	1221-1184	$(5.43 \pm 0.20) \times 10^{-18}$
4-methyl-2-nitrophenol	1639	$(1.51 \pm 0.05) \times 10^{-19}$	1668-1623	$(3.52 \pm 0.09) \times 10^{-18}$
	1335	$(3.78 \pm 0.16) \times 10^{-19}$	1364-1307	$(1.32 \pm 0.07) \times 10^{-17}$
	1191	$(2.75 \pm 0.02) \times 10^{-19}$	1209-1165	$(5.65 \pm 0.32) \times 10^{-18}$

Abbreviations

2NP	2-nitrophenol
3M2N	3-methyl-2-nitrophenol
3M4N	3-methyl-4-nitrophenol
4M2N	4-methyl-2-nitrophenol
5M2N	5-methyl-2-nitrophenol
6M2N	6-methyl-2-nitrophenol
BTX	Benzene, Toluene, Xylenes
CPC	Condensation Particle Counter
DFT	Density Functional Theory
DMA	Differential Mobility Analyzer
DOAS	Differential Optical Absorption Spectroscopy
EUPHORE	EUropean PHOto-REactor
FEP	fluorine-ethene-propene
FT-IR	Fourier Transform Infrared
GC-FID	Gas Chromatography - Flame Ionization Detector
GC-ECD	Gas Chromatography - Electron Capture Detector
GC-PID	Gas Chromatography - Photolionization Detector
GC-MS	Gas Chromatography - Mass Spectrometry
HC	Hydrocarbon compound
HONO	Nitrous acid
HPLC	High Performance Liquid Chromatography
LOPAP	LOng Path Absorption Photometer
MCT	mercury-cadmium- tellurium
NC	Nitrocresols
NMOCs	Non-Methane Organic Compounds
NO _x	(NO + NO ₂)
PAHs	Polycyclic Aromatic Hydrocarbons
PM	Particulate Matter

Appendix

ppmV	parts per million (1 ppmV = $2.46 \times 10^{13} \text{ cm}^{-3}$ at 1 atm and 298 K)
ppbV	parts per billion (1 ppbV = $2.46 \times 10^{10} \text{ cm}^{-3}$ at 1 atm and 298 K)
pptV	parts per trillion (1 pptV = $2.46 \times 10^7 \text{ cm}^{-3}$ at 1 atm and 298 K)
PTR-MS	Proton Transfer Reaction Mass Spectrometry
SAR	Structure-Activity Relationship
SMPS	Scanning Mobility Particle Sizer
SOA	Secondary Organic Aerosol
S/V	Surface/Volume ratio
TDL	Tuneable Diode Laser
UV/VIS	UltraViolet/VISible
VOC	Volatile Organic Compound

References

Acker, K., D. Möller, W. Wieprecht, F.X. Meixner, B. Bohn, S. Gilge, C. Plass-Dülmer, and H. Berresheim (2006)

Strong Daytime Production of OH from HNO₂ at a Rural Mountain Site,
Geophysical Research Letter, 33, L02809, doi:10.1029/2005GL024643, 1-4.

Aleksic, N., G. Boynton, G. Sistla, and J. Perry (2005)

Concentrations and Trends of Benzene in Ambient Air over New York State during 1990-2003,
Atmospheric Environment, 39, 40, 7894-7905.

Alicke, B., (2000)

The Role of Nitrous Acid in the Boundary Layer,
PhD thesis, University of Heidelberg, Heidelberg, Germany.

Alicke, B., U. Platt, and J. Stutz (2002)

Impact of Nitrous Acid Photolysis on the Total Hydroxyl Radical Budget during the Limitation of Oxidant Production/Pianura Padana Produzione di Ozono Study in Milan,
Journal of Geophysical Research-Atmosphere, 107, D22, No. 8196.

Alicke, B., A. Geyer, A. Hofzumahaus, F. Holland, S. Konrad, H.-W. Pätz, J. Schäfer, J. Stutz, A. Volz-Thomas, and U. Platt (2003)

OH Formation by HONO Photolysis during the BERLIOZ Experiment,
Journal of Geophysical Research-Atmosphere, 108 (D4), 8247-8252.

Alif, A., P. Boule, and J. Lemaire (1987)

Comportement Photochimique du Nitro-4 Phenol en Solution Aqueuse,
Chemosphere, 16, 10-12, 2213-2223.

Alif, A., P. Boule, and J. Lemaire (1990)

Photochemistry and Environment XII: Phototransformation of 3-Nitrophenol in Aqueous Solution,
Journal of Photochemistry and Photobiology A: Chemistry, 50, 331-342.

Alif, A., J.-F. Pilichowski, and P. Boule (1991)

Photochemistry and Environment XIII: Phototransformation of 2-Nitrophenol in Aqueous Solution,
Journal of Photochemistry and Photobiology A: Chemistry, 59, 209-219.

Altshuller, A.O.P., I.R. Cohen, S.F. Sleva, and S.L. Kopczynski (1962)

Air Pollution: Photooxidation of Aromatic Hydrocarbons,
Science, 138, 442-443.

Ammann, M., E. Roessler, R. Streckowski, and C. George (2005)

Nitrogen Dioxide Multiphase Chemistry: Uptake Kinetics on Aqueous Solutions Containing Phenolic Compounds,
Physical Chemistry Chemical Physics, 7, 2513-2518.

Andreae, M.O., and P.J. Crutzen (1997)

Atmospheric Aerosols: Biogeochemical Sources and Role in Atmospheric Chemistry,
Science, 276, 1052-1058.

Atkinson, R., W.P.L. Carter, C.N. Plum, A.M. Winer, and J.N. Pitts, Jr. (1984)

Kinetics of the Gas-Phase Reactions of NO₃ Radicals with a Series of Aromatics at 296 ± 2 K,
International Journal of Chemical Kinetics, 16, 887-898.

Atkinson, R., (1986)

Kinetics and Mechanisms of the Gas-Phase Reactions of the Hydroxyl Radical with Organic Compounds under Atmospheric Conditions,
Chemical Review, 86, 69-201.

Atkinson, R., (1987)

A Structure-Activity Relationship for the Estimation of the Rate Constants of OH Radicals with Organic Compounds,
International Journal of Chemical Kinetics, 19, 799-828.

Atkinson, R., S.M. Aschmann, and J.N. Pitts, Jr., (1988)

Rate Constants for Gas-Phase Reaction of the NO₃ Radical with a Series of Organic Compounds at 298 ± 2 K,
Journal of Physical Chemistry, 92, 3454-3457.

Atkinson, R., (1989)

Kinetics and Mechanisms of the Gas-Phase Reactions of the Hydroxyl Radical with Organic Compounds,
Journal of Physical Chemistry Reference Data, Monograph No. 1, 1-246.

- Atkinson, R., S.M. Aschmann, J. Arey, and W.P.L. Carter (1989)**
Formation of Ring-Retaining Products from the OH Radical-Initiated Reactions of Benzene and Toluene,
International Journal of Chemical Kinetics, 21, 801-827.
- Atkinson, R., (1991)**
Kinetics and Mechanisms of the Gas-Phase Reactions of the NO₃ Radical with Organic Compounds,
Journal of Physical Chemistry Reference Data, 20, 459-507.
- Atkinson, R., S.M. Aschmann, and J. Arey (1991)**
Formation of Ring-Retaining Products from the OH Radical-Initiated Reactions of o-, m-, and p-Xylene,
International Journal of Chemical Kinetics, 23, 77-97.
- Atkinson, R., S.M. Aschmann, and J. Arey (1992a)**
Reactions of OH and NO₃ Radicals with Phenol, Cresols, and 2-Nitrophenol at 296 ± 2 K,
Environmental Science & Technology, 26, 1397-1403.
- Atkinson, R., D.L. Baulch, R.A. Cox, R.F. Hampson, Jr., J.A. Kerr, and J. Troe (1992b)**
Evaluated Kinetic and Photochemical Data for Atmospheric Chemistry: Supplement IV.,
Journal of Physical Chemistry Reference Data, 21, 1125-1568.
- Atkinson, R., (1994)**
Gas-Phase Tropospheric Chemistry of Organic Compounds,
Journal of Physical Chemistry Reference Data, Monograph 2, 1-216.
- Atkinson, R., and S.M. Aschmann (1994)**
Products of the Gas-Phase Reactions of Aromatic Hydrocarbons: Effect of NO₂ Concentration,
International Journal of Chemical Kinetics, 26, 929-944.
- Atkinson, R., D.L. Baulch, R.A. Cox, R.F. Hampson, Jr., J.A. Kerr, M.J. Rossi, and J. Troe (1997)**
Evaluated Kinetic and Photochemical Data for Atmospheric Chemistry: Supplement VI. IUPAC Subcommittee on Gas Kinetic Data Evaluation for Atmospheric Chemistry,
Journal of Physical Chemistry Reference Data, 26, 1329-1499.
- Atkinson, R., (1998)**
Product Studies of Gas-Phase Reaction of Organic Compounds,
Pure & Applied Chemistry, 70, 7, 1335-1343.
- Atkinson, R., (2000)**
Atmospheric Chemistry of VOCs and NO_x,
Atmospheric Environment, 34, 2063-2101.

Atkinson, R., and J. Arey (2003)

Atmospheric Degradation of Volatile Organic Compounds,
Chemical Reviews, 103, 4605-4638.

Atkinson, R., D.L. Baulch, R.A. Cox, J.N. Crowley, R.F. Hampson, Jr., R.G. Hynes, M.E. Jenkin, J.A. Kerr, M.J. Rossi, and J. Troe (2005)

Summary of Evaluated Kinetic and Photochemical Data for Atmospheric Chemistry, IUPAC Subcommittee on Gas Kinetics Data Evaluation for Atmospheric Chemistry,
Web Version, www.iupac-kinetic.ch.cam.ac.uk, University of Cambridge, UK.

Baitinger, W.F., P.R. von Schleyer, T.S.S.R. Murty, and L. Robinson (1964)

Nitro Groups as Proton Acceptors in Hydrogen Bonding,
Tetrahedron, 20, 1635-1647.

Bandow, H., and N. Washida (1985)

Ring-Cleavage Reactions of Aromatic Hydrocarbon Studied by FT-IR Spectroscopy. I. Photooxidation of Toluene and Benzene in the NO_x – Air System,
Bulletin of Chemical Society of Japan, 58, 2531-2540.

Bardini, P., (2005)

Atmospheric Oxidation of Dimethylphenols and Nitrophenols,
PhD thesis, University of Cork, Cork, Ireland.

Barletta, B., R. Belloli, E. Bolzacchini, S. Meinardi, M. Orlandi, and B. Rindone (1998)

Toxic Nitrophenols from the Liquid Phase Nitration of Phenols,
Eurotrac-2 Symposium, Garmisch.

Barletta, B., R. Belloli, E. Bolzacchini, S. Meinardi, M. Orlandi, and B. Rindone (1999)

Determination of Toxic Nitrophenols in the Atmosphere by High Performance Liquid Chromatography,
Journal of Chromatography A, 846, 277-281.

Barnes, I., V. Bastian, K.H. Becker, E.H. Fink, and F. Zabel (1982)

Reactivity Studies of Organic Substances towards Hydroxyl Radicals under Atmospheric Conditions,
Atmospheric Environment, 16, 545-550.

Barnes, I., K.H. Becker, and N. Mihalopoulos (1994)

An FT-IR Product Study of the Photo-Oxidation of Dimethyl Disulfide,
Journal of Atmospheric Chemistry, 18, 267-289.

Barnes, I., and K.J. Brockmann (2001)

2nd EUPHORE Report 1998-1999,
Bergische Universität Wuppertal, Physikalische Chemie, FB 9, Germany.

Becker, K.H., (1996)

1st EUPHORE final report, EV5V-CT92-0059,
Bergische Universität Wuppertal, Physikalische Chemie , FB 9, Germany.

Behnke, W., B. Görlitz, W.U. Palm, and C. Zetzsch (1998)

Production, Sinks and Mutagenicity of Nitrophenols in the Atmosphere,
Proceedings of the EC Workshop „Chemical Mechanisms of Atmospheric Processes“ ed. K. H. Becker and G. Angeletti, Copenhagen, Denmark, 24-25 August.

Bejan, I., R.I. Olariu, I. Barnes., and K. Wirtz (2002)

FT-IR Investigations on the Gas-Phase Reaction of the NO₃ and OH Radicals with a Series of Benzenediol Compounds,
Proceedings of EUROTRAC Symposium, CMD-2002, Paris, France, 9-11 September, 37-42.

Bejan, I., I. Barnes, R. Olariu, and R. Mocanu (2004)

Secondary Organic Aerosol Formation from the Photolysis of Nitrophenols and Nitrocresols,
Proceeding of 1st General Assembly Conference, EGU, GRA, 6, 07566, Nice, France, 25 - 30 April.

Bejan, I., I. Barnes, R. Olariu, K.H. Becker, and R. Mocanu (2005)

New Results on the Atmospheric Chemistry of Oxygenated Aromatic Compounds,
Proceedings of General Assembly Conference, EGU, GRA, 7, 06143, Vienna, Austria, 24 - 29 April.

Bejan, I., I. Barnes, R. Olariu, K.H. Becker, and R. Mocanu (2005)

FT-IR Study of the Kinetic Gas-Phase Reactions of the OH Radical with a Series of Nitroaromatic Compounds,
Proceedings of the NATO Advanced Research Workshop, Environmental Simulation Chambers: Application to Atmospheric Chemical Processes, 2004, Zakopane, Poland, 01-04 October.

Bejan, I., Y. Abd El Aal, I. Barnes, Th. Benter, B. Bohn, P. Wiesen, and J. Kleffmann (2006)

The Photolysis of ortho-Nitrophenols: A new Gas Phase Source of HONO,
Physical Chemistry Chemical Physics, 8, 2028-2035.

Bejan, I., I. Barnes, Th. Benter, P. Wiesen, and J. Kleffmann (2007)

HONO Formation in the Photolysis of Methyl-Substituted Nitroaromatics,
to be published.

Belloli, R., B. Barletta, E. Bolzacchini, S. Meinardi, M. Orlandi, and B. Rindone (1999)

Determination of Toxic Nitrophenols in the Atmosphere by High-Performance Liquid Chromatography,
Journal of Chromatography A, 846, 277-281.

Berndt, T., and O. Böge (2003)

Gas Phase Reaction of OH Radicals with Phenol,
Physical Chemistry Chemical Physics, 5, 342-350.

Besemer, A.C., and H. Nieboer (1985)

The Wall as a Source of Hydroxyl Radicals in Smog Chambers,
Atmospheric Environment, 19, 507-513.

Bian, H., M.J. Prather, and T. Takemura (2003)

Tropospheric Aerosol Impacts on Trace Gas Budgets through Photolysis,
Journal of Geophysical Research, 108, D8, 4242,
DOI:10.1029/2002JD002743.

Bing, C., Y. Chun, and G.N. Khang (2005)

Direct Photolysis of Nitroaromatic Compounds in Aqueous Solutions,
Journal of Environmental Science (China), 17, 598–604.

Blake, D.R., T.W. Smith, T.-Y. Chen, W.J. Whipple, and F.S. Rowland (1994)

Effects of Biomass Burning on Summertime Nonmethane Hydrocarbon Concentration in the Canadian Wetlands,
Journal of Geophysical Research, 99, 1699–1719.

Bloss, C., V. Wagner, A. Bonzanini, M.E. Jenkin, K. Wirtz, M. Martin-Reviejo, and M.J. Pilling (2005a)

Evaluation of Detailed Aromatic Mechanisms (MCMv3 and MCMv3.1) against Environmental Chamber Data,
Atmospheric Chemistry and Physics, 5, 623–639.

Bloss, C., V. Wagner, M.E. Jenkin, R. Volkamer, W.J. Bloss, J.D. Lee, D.E. Heard, K. Wirtz, M. Martin-Reviejo, G. Rea, J.C. Wenger, and M.J. Pilling (2005b)

Development of a Detailed Chemical Mechanism (MCMv3.1) for the Atmospheric Oxidation of Aromatic Hydrocarbons,
Atmospheric Chemistry and Physics, 5, 641–664.

Böge, O., Y. Miao, A. Plewka, and H. Herrmann (2006)

Formation of Secondary Organic Particle Phase Compounds from Isoprene Gas-Phase Oxidation Products: An Aerosol Chamber and Field Study,
Atmospheric Environment, 40, 14, 2501-2509.

Bohn, B., (2005)

personal communication.

Bolzacchini, E., M. Bruschi, J. Hjorth, S. Meinardi, M. Orlandi, B. Rindone, and E. Rosenbohm (2001)

Gas-Phase Reaction of Phenol with NO₃,
Environmental Science & Technology, 35, 1791-1797.

Boocock, G., and R.J. Cvetanovič (1961)

Reaction of Oxygen Atoms with Benzene,
Canadian Journal of Chemistry, 39, 2436-2443.

Borisenko, K.B., C.W. Bock, and I. Hargittai (1994)

Intramolecular Hydrogen-Bonding and Molecular-Geometry of 2-Nitrophenol from a Joint Gas-Phase Electron-Diffraction and ab-Initio Molecular-Orbital Investigation,
Journal of Physical Chemistry, 98, 1442-1448.

Borisenko, K.B., and I. Hargittai (1996)

Barrier to Internal Rotation of the Nitro Group in Ortho-Nitrophenols from Gas-Phase Electron Diffraction,
Journal of Molecular Structure, 382, 171-176.

Bravo, H., R. Sosa, P. Sanchez, E. Bueno, and L. Gonzalez (2002)

Concentrations of Benzene and Toluene in the Atmosphere of the Southwestern Area at the Mexico City Metropolitan Zone,
Atmospheric Environment, 36, 3843-3849.

ten Brink, H.M., and H. Spolestra (1998)

The Dark Decay of HONO in Environmental (Smog) Chambers,
Atmospheric Environment, 32, 2, 247-251.

Brocco, D., R. Fratarcangeli, L. Lepore, M. Petricca, and I. Ventrone (1997)

Determination of Aromatic Hydrocarbons in Urban Air of Rome,
Atmospheric Environment, 31, 4, 557-566.

Calvert, J., R. Atkinson, K.H. Becker, R. Kamens, J. Seinfeld, T. Wallington, and G. Yarwood (2002)

The Mechanisms of the Atmospheric Oxidation of Aromatic Hydrocarbons,
Oxford University Press.

Carter, W.P.L., A.M. Winer, and J.N. Pitts, Jr., (1981)

Major Atmospheric Sink for Phenol and Cresols. Reaction with the Nitrate Radical,
Environmental Science & Technology, 15, 7, 829-831.

Chan, W.H., R.J. Nordstrom, J.G. Calvert, and J.H. Shaw (1976)

Kinetic Study of HONO Formation and Decay Reaction in Gaseous Mixtures of HONO, NO, NO₂, H₂O and N₂,
Environmental Science & Technology, 10, 674-682.

Chen, B., Y. Chun, and G.N. Khang (2005)

Direct Photolysis of Nitroaromatic Compounds in Aqueous Solutions,
Journal of Environmental Sciences - China, 17, 4, 598-604.

Chen, P.C., M. Lo, and S.C. Tzeng (1998)

Molecular Structures of Mononitrophenols and Their Thermal Decomposition Tautomerism,
Journal of Molecular Structure (Theochem.), 428, 257-266.

Chen, P.C., and Y.C. Chieh (2003)

Internal Rotation and Charge Transfer Study of 2-Nitrophenol,
Chemical Physics Letters, 372, 147–155.

Claeys, M., B. Graham, G. Vas, W. Wang, R. Vermeylen, V. Pashynska, J. Cafmeyer, P. Guyon, M.O. Andreae, P. Artaxo, and W. Maenhaut (2004)

Formation of Secondary Organic Aerosols through Photooxidation of Isoprene,
Science, 303, 5661, 1173-1176.

Cocheo, V., P. Sacco, C. Boaretto, E. DeSaeger, P.P. Ballesta, H. Skov, E. Goelen, N. Gonzalez, and A.B. Caracena (2000)

Urban Benzene and Population Exposure,
Nature, 404, 6774, 141-142.

Cocker, D.R., B.T. Mader, M. Kalberer, R.C. Flagan, and J.H. Seinfeld (2001)

The Effect of Water on Gas-Particle Partitioning of Secondary Organic Aerosol: II. m-Xylene and 1,3,5- Trimethylbenzene Photooxidation Systems,
Atmospheric Environment, 35, 6073-6085.

Crutzen, P.J., and P.H. Zimmermann (1991)

The Changing Photochemistry in the Troposphere,
Tellus, 43AB, 136-151.

Derwent, R.G., M.E. Jenkin, and S.M. Saunders (1996)

Photochemical Ozone Creation Potentials for a Large Number of Reactive Hydrocarbons under European Conditions,
Atmospheric Environment, 30, 181-199.

Derwent, R.G., M.E. Jenkin, S.M. Saunders, and M.J. Pilling (1998)

Photochemical Ozone Creation Potentials for Organic Compounds in Northwest Europe Calculated with a Master Chemical Mechanism,
Atmospheric Environment, 32, 2429-2441.

Docherty, K.S., and P.J. Ziemann (2003)

Effects of Stabilized Criegee Intermediate and OH Radical Scavengers on Aerosol Formation from Reactions of beta-Pinene with O₃,
Aerosol Science and Technology, 37, 11, 877-891.

Dubowski, Y., and M.R. Hoffmann (2000)

Photochemical Transformations in Ice: Implications for the Fate of Chemical Species,
Geophysical Research Letters, 27, 20, 3321-3324.

Dumdei, B.E., D.V. Kenny, P.B. Shepson, T.E. Kleindienst, C.M. Nero, L.T. Cupitt, and L.D. Claxton (1988)

MS/MS Analysis of the Products of Toluene Photooxidation and Measurement of Their Mutagenic Activity,
Environmental Science & Technology, 22, 1493-1498.

Eskinja, I., Z. Grabarič, and B.S. Grabarič (1995)

Monitoring of Pyrocatechol Indoor Air Pollution,
Atmospheric Environment, 29, 10, 1165-1170.

Eyde, L.A., and G.N. Richards (1991)

Analysis from Wood Smoke: Components Derived from Polysaccharides and Lignins,
Environmental Science & Technology, 25, 1133–1137.

Fantechi, G., N.R. Jensen, O. Saastad, J. Hjorth, and J. Peeters (1998)

Reaction of Cl Atoms with Selected VOCs: Kinetic, Products and Mechanisms,
Journal of Atmospheric Chemistry, 31, 247-267.

Fine, P.M., G.R. Cass, and B.R. Simoneit (2002)

Chemical Characterization of Fine Particle Emissions from the Fireplace Combustion of Woods Grown in the Southern United States,
Environmental Science & Technology, 36, 1442-1451.

Finlayson-Pitts, B.J., and J.N. Pitts, Jr., (1997)

Tropospheric Air Pollution: Ozone, Airborne Toxics, Polycyclic Aromatic Hydrocarbons and Particles,
Science, 276, 1045-1051.

Finlayson-Pitts, B.J., and J.N. Pitts, Jr., (2000)

Chemistry of the Upper and Lower Atmosphere: Theory, Experiments and Applications,
Academic Press, San Diego, CA; London, 1-969.

Finlayson-Pitts, B.J., L.M. Wingen, A.L. Sumner, D. Syomin, and K.A. Ramazan (2003)

The Heterogeneous Hydrolysis of NO₂ in Laboratory Systems and in Outdoor and Indoor Atmospheres: An Integrated Mechanism,
Physical Chemistry Chemical Physics, 5, 223–242.

Flickinger, C.W., (1976)

Benzenediols: Catechol, Resorcinol and Hydroquinone – A Review of the Industrial Toxicology and Current Industrial Exposure Limits,
American Industrial Hygiene Association Journal, 37, 596-606.

Forstner, H.J.L., R.C. Flagan, and J.H. Seinfeld (1997)

Secondary Organic Aerosol from the Photooxidation of Aromatic Hydrocarbons: Molecular Composition,

Environmental Science & Technology, 31, 1345-1358.

Geissler, A., and H.F. Schöler (1994)

Gas Chromatographic Determination of Phenol, Methylphenols, Chlorophenols, Nitrophenols and Nitroquinones in Water,
Water Research, 28, 2047–2053.

George, C., R.S. Strekowski, J. Kleffmann, K. Stemmler, and M. Ammann (2005)

Photoenhanced Uptake of Gaseous NO₂ on Solid Organic Compounds: A Photochemical Source of HONO,
Faraday Discussions, 130, 11, 1–16, DOI:10.1039/b417888m.

Geyer, A., B. Alicke, S. Konrad, T. Schmitz, J. Stutz, and U. Platt (2001)

Chemistry and Oxidation Capacity of the Nitrate Radical in the Continental Boundary Layer near Berlin,
Journal of Geophysical Research, 106, 8013-8025.

Grosjean, D., (1985)

Reactions of o-Cresol and Nitrocresol with NO_x in Sunlight and with Ozone-Nitrogen Dioxide Mixtures in the Dark,
Environmental Science & Technology, 19, 968-974.

Grosjean, D., (1991)

Atmospheric Fate of Toxic Aromatic Compounds,
Science of the Total Environment, 100, 367-414.

Gutzwiller, L., F. Arens, U. Baltensperger, H.W. Gaggeler, and M. Ammann (2002)

Significance of Semivolatile Diesel Exhaust Organics for Secondary HONO,
Environmental Science & Technology, 36, 677–682.

Harrison, M.A.J., J.N. Cape, and M.R. Heal (2002)

Experimentally Determined Henry's Law Coefficients of Phenol, 2-Methylphenol and 2-Nitrophenol in the Temperature Range 281-302 K,
Atmospheric Environment, 36, 1843-1851.

Harrison, M.A.J., S. Barra, D. Borghesi, D. Vione, C. Arsene, and R.I. Olariu (2005)

Nitrated Phenols in the Atmosphere: A Review,
Atmospheric Environment, 39, 231-248 and references therein.

Heiden, A.C., K. Kobel, M. Komenda, R. Koppmann, M. Shao, and J. Wildt (1999)

Toluene Emissions from Plants,
Geophysical Research Letters, 26, 1283–1286.

Heland, J., J. Kleffmann, R. Kurtenbach, and P. Wiesen (2001)

A New Instrument to Measure Gaseous Nitrous Acid (HONO) in the Atmosphere,
Environmental Science & Technology, 35, 15, 3207-3212.

Herterich, R. (1991)

Gas Chromatographic Determination of Nitrophenols in Atmospheric Liquid Water and Airborne Particulates,
Journal of Chromatography, 549, 313-324.

Hofzumahaus, A., A. Kraus, and M. Müller (1999)

Solar Actinic Flux Spectroradiometry: a Technique for Measuring Photolysis Frequencies in the Atmosphere,
Applied Optics, 38, 4443-4460.

Howe, G.E., L.L. Marking, T.D. Bills, J.J. Rach, and F.L. Mayer (1994)

Effects of Water Temperature and pH on Toxicity of Terbufos, Trichlorfon, 4-Nitrophenol and 2,4-Dinitrophenol to the Amphipod Gammarus-pseudolimnaeus and Rainbow-trout (Oncorhynchus-mykiss),
Environmental Toxicology and Chemistry, 13, 1, 51-66.

Howthorne, S.B., D.J. Miller, R.M. Barkley, and M.S. Krieger (1992)

Identification of Methoxylated Phenols as Candidate Tracer for Atmospheric Wood Smoke Pollution,
Environmental Science & Technology, 22, 1191-1196.

Hurley, M.D., O. Sokolov, T.J. Wallington, H. Takekawa, M. Karasawa, B. Klotz, I. Barnes, and K.H. Becker (2001)

Organic Aerosol Formation During the Atmospheric Degradation of Toluene,
Environmental Science & Technology, 35, 1358-1366.

Il'ichev, Y.V., and J. Wirz (2000)

Rearrangements of 2-Nitrobenzyl Compounds. 1. Potential Energy Surface of 2-Nitrotoluene and Its Isomers Explored with ab Initio and Density Functional Theory Methods,
Journal of Physical Chemistry A, 104, 7856–7870.

Isayev, O., B. Rasulev, L. Gorb, and J. Leszczynski (2006)

Structure-toxicity Relationships of Nitroaromatic Compounds,
Molecular Diversity, 10, 2, 233-245.

Ishag, M.I.O., and P.G.N. Moseley (1977)

Effects of UV Light on Dilute Aqueous Solutions of m- and p-Nitrophenol,
Tetrahedron, 33, 3141-3144.

Isidorov, V.A., I.G. Zenkevich, and B.V. Ioffe (1990)

Volatile Organic Compounds in Solfataric Gases,
Journal of Atmospheric Chemistry, 10, 329–340.

Izumi, K., and T. Fukuyama (1990)

Photochemical Aerosol Formation from Aromatic Hydrocarbons in the Presence of NO_x,
Atmospheric Environment, 24A, 1433-1441.

Jang, M., and R.M. Kamens (2001)

Characterization of Secondary Aerosol from the Photooxidation of Toluene in the Presence of NO_x and 1-Propene,
Environmental Science & Technology, 35, 3626-3639.

Jenkin, M.E., S.M. Saunders, V. Wagner, and M.J. Pilling (2003)

Protocol for the Development of the Master Chemical Mechanism, MCM v3 (Part B): Tropospheric Degradation of Aromatic Volatile Organic Compounds,
Atmospheric Chemistry and Physics, 3, 181–193.

Joeckel, P., C.A.M. Brenninkmeijer, and P.J. Crutzen (2003)

A Discussion on the Determination of Atmospheric OH and Its Trends,
Atmospheric Chemistry and Physics, 3, 107-118.

Johnson, D., M.E. Jenkin, K. Wirtz, and M. Martin-Reviejo (2005)

Simulating the Formation of Secondary Organic Aerosol from the Photooxidation of Aromatic Hydrocarbons,
Environmental Chemistry, 2, 1, 35-48.

Jones, G.R.H., and R.J. Cvetanovic (1961)

Reaction of Oxygen Atoms with Toluene,
Canadian Journal of Chemistry, 39, 2444-2451.

Juettner, F., and J.J. Henatsch (1986)

Anoxic Hypolimnion is a Significant Source of Biogenic Toluene,
Nature, 323, 30, 797–798.

Kanakidou, M., J.H. Seinfeld, S.N. Pandis, I. Barnes, F.J. Dentener, M.C. Facchini, R. Van Dingenen, B. Ervens, A. Nenes, C.J. Nielsen, E. Swietlicki, J.P. Putaud, Y. Balkanski, S. Fuzzi, J. Horth, G.K. Moortgat, R. Winterhalter, C.E.L. Myhre, K. Tsigaridis, E. Vignati, E.G. Stephanou, and J. Wilson (2005)

Organic Aerosol and Global Climate Modelling: A Review,
Atmospheric Chemistry and Physics, 5, 1053-1123.

Kawai, A., S. Goto, Y. Matsumoto, and H. Matsushita (1987)

Mutagenicity of Aliphatic and Aromatic Nitro Compounds, Industrial Materials and Related Compounds,
Japanese Journal of Industrial Health, 29, 34-54.

Kawamura, K., and I.R. Kaplan (1986)

Biogenic and Anthropogenic Organic Compounds in Rain and Snow Samples Collected in Southern California,
Atmospheric Environment, 20, 115–124.

Keywood, M.D., J.H. Kroll, V. Varutbangkul, R. Bahreini, R.C. Flagan, and J.H. Seinfeld (2004)

Secondary Organic Aerosol Formation from Cyclohexene Ozonolysis: Effect of OH Scavenger and the Role of Radical Chemistry,
Environmental Science & Technology, 38, 12, 3343-3350.

Kleffmann, J., R. Kurtenbach, and P. Wiesen (1994)

Surface Catalyzed Conversion of NO₂ into HONO and N₂O: A New Source of Atmospheric N₂O?,

In: Impact of Emissions from Aircraft and Spacecraft upon the Atmosphere, Proceedings of an International Scientific Colloquium, Cologne, Germany, 18-20 April, Porz-Wahnheide, 146-157.

Kleffmann, J., K.H. Becker, and P. Wiesen (1998)

Heterogeneous NO₂ Conversion Processes on Acid Surfaces: Possible Atmospheric Implications,
Atmospheric Environment, 32, 2721-2729.

Kleffmann, J., J. Heland, R. Kurtenbach, J. Lörzer, and P. Wiesen (2002)

A New Instrument (LOPAP) for the Detection of Nitrous Acid (HONO),
Environmental Science and Pollution Research, Sp. Iss. 4, 48-54.

Kleffmann, J., R. Kurtenbach, J.C. Lörzer, P. Wiesen, N. Kalthoff, B. Vogel, and H. Vogel (2003)

Measured and Simulated Vertical Profiles of Nitrous Acid - Part I: Field Measurements,
Atmospheric Environment, 37, 2949-2955.

Kleffmann, J., (2005)

personal communications.

Kleffmann, J., T. Gavriloaiei, A. Hofzumahaus, F. Holland, R. Koppmann, L. Rupp, E. Schlosser, M. Siese, and A. Wahner (2005)

Daytime Formation of Nitrous Acid: A Major Source of OH Radicals in a Forest,
Geophysical Research Letters, 32, L05818, DOI: 10.1029/2005GL022524.

Kleffmann, J., J.C. Lörzer, P. Wiesen, C. Kern, S. Trick, R. Volkamer, M. Rodenas, and K. Wirtz (2006)

Intercomparison of the DOAS and LOPAP techniques for the detection of nitrous acid (HONO),
Atmospheric Environment, 40, 20, 3640-3652.

Kleindienst, T.E., D.F. Smith, W. Li, E.O. Edney, D.J. Driscoll, R.E. Speer, and W.S. Weathers (1999)

Secondary Organic Aerosol Formation from the Oxidation of Aromatic Hydrocarbons in the Presence of Dry Submicron Ammonium Sulfate Aerosol,

Atmospheric Environment, 33, 3669-3681.

Kleindienst, T.E., T.S. Conver, C.D. McIver, and E.O. Edney (2004)

Determination of Secondary Organic Aerosol Products from the Photooxidation of Toluene and Their Implications in Ambient PM_{2.5},
Journal of Atmospheric Chemistry, 47, 79-100.

Klotz, B., I. Barnes, K.H. Becker, and B.T. Golding (1997)

Atmospheric Chemistry of Benzene Oxide/Oxepin,
Journal of the Chemical Society - Faraday Transactions. 93, 8, 1507-1516.

Klotz, B., S. Sørensen, I. Barnes, K.H. Becker, T. Etzkorn, R. Volkamer, U. Platt, K. Wirtz, and M. Martin-Reviejo (1998)

Atmospheric Oxidation of Toluene in a Large-volume Outdoor Photoreactor: In Situ Determination of Ring-Retaining Products Yields,
Journal of Physical Chemistry A, 102, 50, 10289-10299.

Kovács, A., V. Izvekov, G. Keresztury, and G. Pongor (1998)

Vibrational Analysis of 2-Nitrophenol. A Joint FT-IR, FT-Raman and Scaled Quantum Mechanical Study,
Chemical Physics, 238, 231-243.

Kovács, A., G. Keresztury, and V. Izvekov (2000)

Intramolecular Hydrogen-Bonding in 2-Nitroresorcinol. A Combined FT-IR, FT-Raman and Computational Study,
Chemical Physics, 253, 193-204.

Kroll, J.H., N.L. Ng, S.M. Murphy, R.C. Flagan, and J.H. Seinfeld (2006)

Secondary Organic Aerosol Formation from Isoprene Photooxidation,
Environmental Science & Technology, 40, 6, 1869-1877.

Kulmala, M., (2003)

How Particles Nucleate and Grow,
Science, 302 (5647), 1000-1001.

Kurtenbach, R., R. Ackermann, K.J. Brockmann, A. Geyer, J.A.G. Gomes, J.C. Lörzer, A. Niedojadlo, U. Platt, and K.H. Becker (1999)

VOC-Measurements in a Road Traffic Tunnel and in Urban Air of the City of Wuppertal,
TFS-LT3 Annual Report 1998, Edited by K. H. Becker, University of Wuppertal, Germany.

Kurtenbach, R., R. Ackermann, K.H. Becker, A. Geyer, J.A.G. Gomes, J.C. Lörzer, U. Platt, and P. Wiesen, (2002)

Verification of the Contribution of Vehicular Traffic to the Total NMVOC Emissions in Germany and the Importance of the NO₃ Chemistry in the City Air,
Journal of Atmospheric Chemistry, 42, 395-411.

Kurtenbach, R., (2005)

personal communication.

Leavell, S., and R.F. Curl, Jr., (1973)

Microwave-spectrum of 2-Nitrophenol – Structure of Hydrogen-Bond,
Journal of Molecular Spectroscopy, 45, 428–442.

Leone, J.A., R.C. Flagan, D. Grosjean, and J.H. Seinfeld (1985)

An Outdoor Smog Chamber and Modeling Study of Toluene-NO_x Photoxidation,
International Journal of Chemical Kinetics, 17, 177- 216.

Levy, H., (1971)

Normal Atmosphere: Large Radical and Formaldehyde Concentrations Predicted,
Science, 173, 141-142.

Leysens, G., F. Louis, and J-P Sawerysyn (2005)

Temperature Dependence of the Mass Accommodation Coefficients of 2-Nitrophenol, 2-Methylphenol, 3-Methylphenol, and 4-Methylphenol on Aqueous Surfaces,
Journal of Physical Chemistry A, 109, 1864-1872.

Li, Q., M.T. Aubrey, T. Christian, and B.M. Freed (1997)

Differential Inhibition of DNA Synthesis in Human T Cells by the Cigarette Tar Components Hydroquinone and Catechol,
Fundamental and Applied Toxicology, 38, 158-165.

Logan, J.A., (1985)

Tropospheric Ozone: Seasonal Behavior, Trends and Anthropogenic Influence,
Journal of Geophysical Research, 90, 10463-10482.

Lonnemann, W.A., T.A. Bellar, and A.P. Altshuller (1968)

Aromatic Hydrocarbons in the Atmosphere of the Los Angeles Basin,
Environmental Science & Technology, 2, 1017– 1020.

Lüttke, J., and K. Levsen (1997)

Phase Partitioning of Phenol and Nitrophenols in Clouds,
Atmospheric Environment, 31, 2649-2655.

Mackay, D., W.Y. Shiu, and K.C. Ma (1995)

Illustrated Handbook of Physical-Chemical Properties and Environmental Fate for Organic Chemicals,
Lewis Publishers, Boca Raton.

Martin-Reviejo, M., and K. Wirtz (2005)

Is Benzene a Precursor for Secondary Organic Aerosol?,
Environmental Science & Technology, 39, 4, 1045-1054.

McMurry, P.H., (2000)

A Review of Atmospheric Aerosol Measurements,
Atmospheric Environment, 34, 1959-1999.

Meylan, W.M., and P.H. Howard (1993)

Computer Estimation of the Atmospheric Gas-Phase Reaction Rate of Organic Compounds with Hydroxyl Radicals and Ozone,
Chemosphere, 26, 12, 2293-2299.

Monod, A., B.C. Sieve, P. Avino, T. Chen, D.R. Blake, and F.R. Rowland (2001)

Monoaromatic Compounds in Ambient Air of Various Cities: a Focus on Correlations between the Xylenes and Ethylbenzene,
Atmospheric Environment, 35, 135-149.

Nagaya, M., S. Kudoh, and M. Nakata (2006)

Infrared Spectrum and Structure of aci-nitro Form of 2-Nitrophenol in a Low-temperature Argon Matrix,
Chemical Physics Letters, 427, 67-71.

Neffel, A., A. Blatter, R. Hesterberg, and Th. Staffelbach (1996)

Measurements of Concentration Gradients of HNO₂ and HNO₃ over a Semi-Natural Ecosystem,
Atmospheric Environment, 30, 17, 3017–3025.

Nojima, K., K. Fukaya, S. Fukui, and S. Kanno (1975)

Studies on Photochemistry of Aromatic Hydrocarbons. II – The Formation of Nitrophenols and Nitrobenzene by the Photochemical Reaction of Benzene in the Presence of Nitrogen Monoxide,
Chemosphere, 2, 77-82.

Odum, J.R., T. Hoffmann, F. Bowman, D. Collins, R.C. Flagan, and J.H. Seinfeld (1996)

Gas/Particle Partitioning and Secondary Organic Aerosol Yields,
Environmental Science & Technology, 30, 2580-2585.

Odum, J.R., P.W. Jungkamp, R.J. Griffin, H.J.L. Forstner, R.C. Flagan, and J.H. Seinfeld (1997a)

Aromatics, Reformulated Gasoline, and Atmospheric Organic Aerosol Formation,
Environmental Science & Technology, 31, 1890-1897.

Odum, J.R., P.W. Jungkamp, R.J. Griffin, H.J.L. Forstner, R.C. Flagan, and J.H. Seinfeld (1997b)

The Atmospheric Aerosol-Forming Potential of Whole Gasoline Vapor,
Science, 276, 96-99.

Olariu, R.I., I. Barnes, K.H. Becker, and B. Klotz (2000)

References

Rate Coefficients for the Gas-Phase Reaction of OH Radicals with Selected Dihydroxybenzenes and Benzoquinones,
International Journal of Chemical Kinetics, 32, 696–702.

Olariu, R.I., (2001)

Atmospheric Oxidation of Selected Aromatic Hydrocarbons,
PhD thesis, University of Wuppertal, Germany.

Olariu, R.I., B. Klotz, I. Barnes, K.H. Becker, and R. Mocanu (2002)

FT-IR Study of the Ring-Retaining Products from the Reaction of OH Radicals with Phenol, o-, m- and p-Cresol,
Atmospheric Environment, 36, 3685-3697.

Olariu, R.I., I. Barnes, I. Bejan, C. Arsene, K.H. Becker, and K. Wirtz (2003)

Secondary Organic Aerosol Formation from the Atmospheric Oxidation of Phenols,
Proceeding of EGS-AGU-EUG Joint Assembly Conference, Geophys. Res. Abstr., 5, 11692, Nice, France, 06 - 11 April.

Olariu, R.I., A. Tomas, I. Barnes, I. Bejan, K.H. Becker, and K. Wirtz (2004)

Atmospheric Ozone Degradation Reaction of 1,2-Dihydroxybenzene: Aerosol Formation Study,
The European Photoreactor EUPHORE, 4th Report 2001, Ed. Ian Barnes, February 2004.

Olariu, R.I., I. Bejan, I. Barnes, B. Klotz, K.H. Becker, and K. Wirtz (2004)

Rate Coefficients for the Gas-Phase Reaction of NO₃ Radicals with Selected Dihydroxybenzenes,
International Journal of Chemical Kinetics, 36, 577–583.

Pankow, J.F., (1994a)

An Absorption Model of Gas/Particle Partitioning of Organic Compounds in the Atmosphere,
Atmospheric Environment, 28, 185-188.

Pankow, J.F., (1994b)

An Absorption Model of the Gas/Aerosol Partitioning Involved in the Formation of Secondary Organic Aerosol,
Atmospheric Environment, 28, 189-193.

Perner, D., and U. Platt (1979)

Detection of Nitrous Acid in the Atmosphere by Differential Optical Absorption,
Geophysical Research Letters, 6, 917-920.

Pilling, M.J., and P.W. Seakins (1995)

Reaction Kinetics,
Oxford University Press, Oxford, New York, United States, 1-305.

- Pitts, J.N., Jr., K.A. Vancauwenberghe, D. Grosjean, J.P. Schmid, D.R. Fitz, W.L. Belser, G.B. Knudson, and P.M. Hynds (1978)**
Atmospheric Reactions of Polycyclic Aromatic-Hydrocarbons - Facile Formation of Mutagenic Nitro-derivatives,
Science, 202, 4367, 515-519.
- Platt, U., D. Perner, G. Harris, A.M. Winer, and J.N. Pitts, Jr., (1980)**
Observation of Nitrous Acid in Urban Atmospheres by Differential Optical Absorption,
Nature, 285, 312-314.
- Platt, U., and F. Heintz (1994)**
Nitrate Radicals in Tropospheric Chemistry,
International Journal of Chemical Kinetics, 34, 289-300.
- Polášek, M., F. Tureček, P. Gerboux, and R. Flammang (2001)**
Nitrobenzene Isomers,
Journal of Physical Chemistry, 105, 995–1010.
- Prinn, R.G., R.F. Weiss, B.R. Miller, F.N. Huang, J. Alyea, D. Cunnold, P.J. Fraser, D.E. Hartley, and P.J. Simmonds (1995)**
Atmospheric Trends and Lifetime of CH₃CCl₃ and Global OH Concentrations,
Science, 269, 187-192.
- Ramazan, K.A., D. Syomin, and B.J. Finlayson-Pitts (2004)**
The Photochemical Production of HONO during the Heterogeneous Hydrolysis of NO₂,
Physical Chemistry Chemical Physics, 6, 3836–3843.
- Rappenglück, B., and P. Fabian (1999)**
Nonmethane Hydrocarbons (NMHC) in the Greater Munich Area / Germany,
Atmospheric Environment, 33, 3843-3857.
- Ravishankara, A.R., (1997)**
Heterogeneous and Multiphase Chemistry in the Troposphere,
Science, 276, 1058-1065.
- Ren, X., H. Harder, M. Martinez, R.L. Lesher, A. Oligier, J.B. Simpas, W.H. Brune, J.J. Schwab, K.L. Demerjian, Y. He, X. Zhou, and H. Gao (2003)**
OH and HO₂ Chemistry in the Urban Atmosphere of New York City,
Atmospheric Environment, 37, 3639–3651.
- Reuder, J., and H. Schwander (1999)**
Aerosol Effects on UV Radiation in Nonurban Regions,
Journal of Geophysical Research – Atmosphere, 104, D4, 4065-4077.
- Rippen, G., E. Zietz, R. Frank, T. Knacker, and W. Klöpffer (1987)**
Do Airborne Nitrophenols Contribute to Forest Decline?,

Environmental Technology Letters, 8, 475-482.

Rohrer, F., B. Bohn, T. Brauers, D. Bruning, F.J. Johnen, A. Wahner, and J. Kleffmann (2005)

Characterisation of the Photolytic HONO-Source in the Atmosphere Simulation Chamber SAPHIR,
Atmospheric Chemistry and Physics, 5, 2189–2201.

Schott, G., and N. Davidson (1958)

Shock Waves in Chemical Kinetics – The Decomposition of N₂O₅ at High Temperatures,
Journal of the American Chemical Society, 80, 8, 1841-1853.

Schreiber, W.M., (1989)

Some Effects of Intramolecular Hydrogen Bonding on Vibrational Spectra,
Journal of Molecular Structure, 197, 73-85.

Schüssler, W., and L. Nitschke (2001)

Nitrophenols in Precipitation,
Chemosphere, 42, 277-283.

Seinfeld, J.H., (1989)

Urban Air Pollution: State of the Science,
Science, 243, 745-752.

Seinfeld, J.H., and S.P. Pandis (1998)

Atmospheric Chemistry and Physics,
John Wiley and Sons, New York.

Seuwen, R., and P. Warneck (1996)

Oxidation of Toluene in NO_x Free Air: Product Distribution and Mechanism,
International Journal of Chemical Kinetics, 28, 315-332,

Shepson, P.B., T.E. Kleindienst, E.O. Edney, G.R. Namie, and J.H. Pittman (1985)

The Mutagenic Activity of Irradiated Toluene/NO_x/H₂O/Air Mixtures,
Environmental Science & Technology, 19, 249-255.

Silva, M.D., J. Gaspar, I.D. Silva, D. Leao, and J. Rueff (2003)

Induction of Chromosomal Aberrations by Phenolic Compounds: Possible Role of Reactive Oxygen Species,
Mutation Research-Genetic Toxicology and Environmental Mutagenesis, 540, 1, 29-42.

Silverstein, R.M., F.X. Webster, and D. Kiemle (2005)

Spectrometric Identification of Organic Compounds,
7th Edition, John Wiley & Sons, Hoboken, New York.

Smith, D.F., C.D. McIver, and T.E. Kleindienst (1998)

References

Primary Product Distribution from the Reaction of Hydroxyl Radicals with Toluene at ppb NO_x Mixing Ratios,
Journal of Atmospheric Chemistry, 30, 209-228.

Smith, D.F., T.E. Kleindienst, and C.D. McIver (1999)

Primary Product Distribution from the Reaction of OH with m-, p-Xylene, 1,2,4- and 1,3,5-Trimethylbenzene,
Journal of Atmospheric Chemistry, 34, 339-364.

Sommariva, R., (2000)

La Reattività del Fenolo con il Radicale Ossidrilico (The reactivity of Phenol with the Hydroxyl Radical),
Laurea Thesis, University of Milano-Bicocca, Milano, Italy.

Sorensen, M., M.D. Hurley, T.J. Wallington, T.S. Dibble, and O.J. Nielsen (2002)

Do Aerosols Act as Catalysts in the OH Radical Initiated Atmospheric Oxidation of Volatile Organic Compounds?,
Atmospheric Environment, 36, 39-40, 5947-5952.

Spittler, M., (2001)

Untersuchungen zur troposphärischen Oxidation von Limonen: Productanalysen, Aerosolbildung und Photolyse von Produkten,
PhD thesis, University of Wuppertal, Germany.

Staffelbach, T., A. Neftel, A. Blatter, A. Gut, M. Fahrni, J. Stahelin, A. Prevot, A. Hering, M. Lehning, B. Neininger, M. Baumle, G.L. Kok, J. Dommen, M. Hutterli, and M. Anklin (1997a)

Photochemical Oxidant Formation over Southern Switzerland .1. Results from Summer 1994,
Journal of Geophysical Research – Atmosphere, 102, D19, 23345-23362.

Staffelbach, T., A. Neftel, and L.W. Horowitz (1997b)

Photochemical Oxidant Formation over Southern Switzerland Model Results,
Journal of Geophysical Research – Atmosphere, 102, D19, 23363–23373.

Stemmler, K., M. Ammann, J. Kleffmann, and C. George (2005)

A New Source of Nitrous Acid: NO₂ Photochemistry on Various Organic Surfaces,
Geophysical Research Abstracts, 2005, 7, 07661, SRef-ID: 1607-7962/gra/.

Stemmler, K., M. Ammann, J. Kleffmann, and C. George (2006)

Photosensitized Reduction of Nitrogen Dioxide on Humic Acid as a Source of Nitrous Acid,
Nature, 440, 7081, 195–198.

Stern, J.E., R.C. Flagan, D. Grosjean, and J.H. Seinfeld (1987)

Aerosol Formation and Growth in Atmospheric Aromatic Hydrocarbon Photooxidation,
Environmental Science & Technology, 21, 1224-1231.

Stockwell, R.W., and J.G. Calvert (1978)

The Near Ultraviolet Absorption Spectrum of Gaseous HONO and N₂O₃,
Journal of Photochemistry, 8, 193 – 203.

Stohs, S.J., D. Bagchi, and M. Bagchi (1997)

Toxicity of Trace Elements in Tobacco Smoke,
Inhalation Toxicology, 9, 9, 867-890.

Surratt, J.D., S.M. Murphy, J.H. Kroll, N.L. Ng, L. Hildebrandt, A. Sorooshian, R. Szmigielski, R. Vermeylen, W. Maenhaut, M. Claeys, R.C. Flagan, and J.H. Seinfeld (2006)

Chemical Composition of Secondary Organic Aerosol Formed from the Photooxidation of Isoprene,
Journal of Physical Chemistry A, 110, 31, 9665-9690.

Taylor, W.D., T.D. Allston, M.J. Moscato, G.B. Fazekas, R. Kozlowski, and G.A. Takacs (1980)

Atmospheric Photo-dissociation Lifetimes for Nitromethane, Methyl Nitrite, and Methyl Nitrate,
International Journal of Chemical Kinetics, 12, 4, 231-240.

Tie, X.X., S. Madronich, S. Walters, D.P. Edwards, P. Ginoux, N. Mahowald, R.Y. Zhang, C. Lou, and G. Brasseur (2005)

Assessment of the Global Impact of Aerosols on Tropospheric Oxidants,
Journal of Geophysical Research – Atmosphere, 110, D3, D03204.

Tomas, A., R. Olariu, I. Barnes, and K.H. Becker (2003)

Kinetics of the Reaction of O₃ with Selected Benzenediols,
International Journal of Chemical Kinetics, 35, 223 - 230.

Tremp, J., P. Mattrel, S. Fingler, and W. Giger (1993)

Phenol and Nitrophenols as Tropospheric Pollutants: Emissions from Automobile Exhausts and Phase Transfer in the Atmosphere,
Water, Air & Soil Pollution, 68, 113-123.

Tsutsui, T., N. Hayashi, H. Maizumi, J. Huff, and J.C. Barrett (1997)

Benzene-, Catechol-, Hydroquinone- and Phenol-Induced Cell Transformation, Gene Mutations, Chromosome Aberrations, Aneuploidy, Sister Chromatid Exchanges and Unscheduled DNA Synthesis in Syrian Hamster Embryo Cells,
Mutation Research-Genetic Toxicology and Environmental Mutagenesis, 373, 1, 113-123.

Vogel, B., H. Vogel, J. Kleffmann, and R. Kurtenbach (2003)

References

Measured and Simulated Vertical Profiles of Nitrous Acid - Part II. Model Simulations and Indications for a Photolytic Source,
Atmospheric Environment, 37, 2957–2966.

Volkamer, R., B. Klotz, I. Barnes, T. Imamura, K. Wirtz, N. Washida, K.H. Becker, and U. Platt (2002)

OH-Initiated Oxidation of Benzene. Part I. Phenol Formation under Atmospheric Conditions,
Physical Chemistry Chemical Physics, 4, 1598-1610.

Voznakova, Z., J. Podehradská, and M. Kohlíčková (1996)

Determination of Nitrophenol in Soil,
Chemosphere, 33, 2, 285-291.

von Waltz, P., M. Häussermann, and A. Krull (1965)

Methoden der Quantitativen Bestimmung des Brenzcatechins im Cigarettenrauch,
Beiträge zur Tabakforschung, 3, 4, 263-277.

Wang, C.C., L.I. Davis, C.H. Wu, S. Japar, H. Niki, and B. Weinstock (1975)

Hydroxyl Radical Concentrations Measured in Ambient Air,
Science, 189, 797-800.

Warneck, P., (1988)

Chemistry of the Natural Atmosphere,
Academic Press, New York.

Wayne, R.P., I. Barnes, P. Biggs, J.P. Burrows, C.E. Canosa-Mas, J. Hjorth, G. Le Bras, G.K. Moortgat, D. Perner, G. Poulet, G. Restelli, and H. Sidebottom (1991)

The Nitrate Radical – Physics, Chemistry, and the Atmosphere,
Atmospheric Environment, 25A, 1, 1-203.

Weinstock, B., (1969)

Carbon Monoxide: Residence Time in the Atmosphere,
Science, 166, 224–225.

Winer, A.M., R. Atkinson, and J.N. Pitts, Jr., (1984)

Gaseous Nitrate Radical – Possible Nighttime Atmospheric Sink for Biogenic Organic-Compounds,
Science, 224, 4645, 156-159.

Winzor, F.L., (1935)

The Colouring Matters of Drosera Whittakeri. Part III. The Synthesis of Hydroxydroserone,
Journal of the Chemical Society – London, 336-338.

Zador, J., T. Turanyi, K. Wirtz, and M.J. Pilling (2006)

References

Measurement and Investigation of Chamber Radical Sources in the European Photoreactor (EUPHORE),
Journal of Atmospheric Chemistry, 55, 2, 147-166.

Ziemann, P.J., (2003)

Formation of Alkoxyhydroperoxy Aldehydes and Cyclic Peroxyhemiacetals from Reactions of Cyclic Alkenes with O₃ in the Presence of Alcohols,
Journal of Physical Chemistry A, 107, 12, 2048-2060.

Zhou, X.L., J. Beine, R.E. Honrath, J.D. Fuentes, W. Simpson, P.B. Shepson, and J.W. Bottenheim (2001)

Snowpack Photochemical Production of HONO: A Major Source of OH in the Arctic Boundary Layer in Springtime,
Geophysical Research Letters, 28, 4087–4090.

Zhou, X. L., K. Civerolo, H. Dai, G. Huang, J. Schwab, and K. Demerjian (2002a)

Summertime Nitrous Acid Chemistry in the Atmospheric Boundary Layer at a Rural Site in New York State,
Journal of Geophysical Research, 107, 4590.

Zhou, X., L. He, G. Huang, T.D. Thornberry, M.A. Carroll, and S.B. Bertman (2002b)

Photochemical Production of Nitrous Acid on Glass Sample Manifold Surface,
Geophysical Research Letters, 29, 14, 1681.

Zhou, X., L. Gao, Y. He, G. Huang, S.B. Bertman, K. Civerolo, and J. Schwab (2003)

Nitric Acid Photolysis on Surfaces in Low-NO_x Environments: Significant Atmospheric Implications,
Geophysical Research Letters, 30, 23, 2217.